DOI 10.1007/s10778-015-0710-x
International Applied Mechanics, Vol. 51, No. 5, September, 2015

SPATIAL PROBLEMS OF THE FRACTURE OF MATERIALS LOADED ALONG CRACKS (REVIEW)

V. L. Bogdanov[*], A. N. Guz[**], and V. M. Nazarenko[***]

The results of solving spatial problems of the fracture of cracked materials under loads acting along cracks are reviewed. A combined approach based on the three-dimensional linearized solid mechanics is used to analyze two nonclassical brittle-fracture mechanisms: (i) fracture of materials with initial stresses acting along cracks and (ii) fracture of materials compressed along parallel cracks. The results of solving nonaxisymmetric and axisymmetric problems for the most typical cases of arrangement of cracks relative to each other and to the boundaries of prestressed bodies are generalized. In the linearized theory, stresses and displacements are expressed in terms of harmonic potential functions. The Hankel transform is used to reduce problems for interacting cracks to the Fredholm equations of the second kind. This approach allows solving problems in a universal general form for compressible or incompressible, isotropic or transversely isotropic homogeneous elastic bodies with an arbitrary elastic potential using the theories of finite and small initial deformations and specifying the material model only at the stage of numerical solution of the general governing equations. New mechanical effects associated with the influence of the initial stresses and crack interaction on the asymptotic distribution of stresses and displacements near the crack tips are analyzed. Resonant effects occurring as the initial compressive stresses tend to the level at which local buckling of the material occurs near the crack are detected. This allows using the combined approach to determine the critical loads for bodies compressed along cracks. Conclusions on the behavior of the stress intensity factors and critical compressive loads with variation in the geometrical and material parameters are drawn

Keywords: initial (residual) stresses, compression along cracks, local buckling, Griffith–Irwin failure criteria, linearized solid mechanics, isolated cracks, interacting cracks, isotropic highly elastic materials, transversely isotropic elastic materials, mechanical effects

1. Introduction. Fracture mechanics is a division of solid mechanics that has been most intensively developed in the last decades. This is due to, on the one hand, the complexity of the fracture process, which requires the development of new and refined models and approaches to studying it at macro-, meso-, and micro-scales and the formulation of adequate failure criteria and, on the other hand, the great importance of fracture mechanics for the evaluation and prediction of strength, service life, and residual life of critical structures, machines, and mechanisms.

Despite the active development of classical fracture mechanics initiated by Griffith, Orowan, and Irwin [80, 129–131, 141], it fails to adequately treat certain theoretical and practical problems. Among them are the study of the effect of the initial (or residual) stresses acting in parallel to the crack plane on the stress–strain state of cracked bodies and the determination of the critical compressive loads acting in parallel to cracks. To solve these problems, it is necessary to develop new approaches and adequate failure criteria. It should be noted that the problem of the fracture of materials with initial stresses acting along cracks and the problem of the compression of materials along cracks are different in subject of study, but have a common feature: there

S. P. Timoshenko Institute of Mechanics, National Academy of Sciences of Ukraine, 3 Nesterova St., Kyiv, Ukraine 03057, e-mail: [*]bogdanov@nas.gov.ua, [**]guz@carier.kiev.ua, [***]nazvm1@gmail.com. Translated from Prikladnaya Mekhanika, Vol. 51, No. 5, pp. 3–89, September–October 2015. Original article submitted September 10, 2014.

are load components that are parallel to cracks. It is these loads whose effect cannot be described by classical fracture mechanics. This circumstance allows us to unite these problems into a group of problems of the fracture of materials loaded along cracks. The problems in this group are also related by the fact that they are solved using the three-dimensional linearized solid mechanics (TDLSM) [11, 12, 24, 97].

The present review generalizes and analyzes results on some classes of spatial axisymmetric and nonaxisymmetric problems for various cases of arrangement of cracks obtained with the combined approach based on TDLSM proposed in [63, 68, 69, 123].

The Introduction briefly addresses the results and approaches that are the subject of the present review, including classification of problems of fracture mechanics (classical and nonclassical problems), brief discussion of results on two nonclassical problems of fracture mechanics (fracture of materials with prestresses acting along cracks and fracture of bodies compressed in parallel to crack planes), and conceptualization of the combined approach to solving the two nonclassical problems using TDLSM.

The second section briefly describes TDLSM problem formulations, models of solids, methods for solving some problems of the fracture of materials loaded in parallel to cracks, and failure criteria for materials with prestresses acting along cracks and for bodies compressed along cracks.

The third section discusses results obtained with the combined approach to specific classes of spatial problems of the fracture of materials loaded along cracks. Results on nonaxisymmetric and axisymmetric problems for the most typical cases of arrangement of cracks relative to each other and to the boundaries of bodies will be discussed. Specific numerical results for compressible and incompressible isotropic hyperelastic materials and some types of composite materials (obtained with the continuum approach) will be presented. Mechanical effects due to the influence of prestresses, geometrical and material parameters on the stress intensity factors and critical compressive loads will be analyzed.

1.1. Classification of Problems of the Fracture of Cracked Bodies. The theory of propagation of cracks in materials under tensile and shear forces is a well-established division of fracture mechanics and is based on the following concepts and approaches: Griffith's fundamental theory of brittle fracture [80]; the Orowan–Irwin concept of quasibrittle fracture [129, 141], which made it possible to generalize Griffith's theory to inelastic structural materials; the energy failure criterion based on the concepts of elastic energy release rate and specific surface energy as a material constant [80, 130] or Irwin's stress-based failure criterion [131]; the concept of invariant (independent of the integration path) Eshelby–Cherepanov–Rice integral [53, 79, 144]; Leonov–Panasyuk–Wells criterion of critical crack opening displacement [42, 148]. These concepts and approaches were later generalized to combined stress states and compound bodies, nonstationary and cyclic loading, thermal and electromagnetic fields, viscoelastic, composite, and other materials [53, 59, 74, 78, 133, 134]). Currently, most studies on fracture mechanics are based on the five approaches mentioned above. In this connection, problems solved with these approaches can be regarded as classical problems of fracture mechanics.

However, a number of problems in this field are yet to be analyzed to the full. Among them are study of new failure mechanisms that cannot be described with the five concepts and approaches, formulation of new failure criteria corresponding to these mechanisms, and study of classes of problems for materials and structural members subject to new failure mechanisms. These problems can be regarded as nonclassical problems of fracture mechanics.

Note that Guz was the first to propose this classification of problems of fracture mechanics (into classical and nonclassical) in the introduction to the multivolume monograph [46]. Such a classification is obviously conventional and not always unambiguous. However, this classification allows a relatively accurate evaluation of the novelty of studies on fracture mechanics and the adequacy of models and approaches they use to analyze new failure mechanisms. For example, this classification was used in [29, 30, 70, 73, 92, 98, 108, 109, 112, 118, 133] to generalize and analyze new results on some nonclassical problems of fracture mechanics.

Nonclassical problems of fracture mechanics include:

– fracture initiated in the microstructure of composites (failure of composites compressed along reinforcement initiated by microbuckling of the material, end crushing of compressed composites due to local buckling near their ends, and shredding of composites with curved internal structure under tension or compression);

– brittle fracture of cracked materials with initial (residual) stresses;

– brittle and ductile fracture of materials compressed along parallel cracks initiated by local buckling near cracks;

– fracture of thin-walled cracked bodies initiated by preliminary buckling under tension;

– crack propagation in materials with initial (residual) stresses;

– brittle fracture of materials with cracks with interacting faces under dynamic loads;

– delayed fracture of viscoelastic bodies caused by subcritical growth of cracks.

The number of results on these nonclassical problems of fracture mechanics is much less than the number of results obtained using classical approaches, which are usually based on essentially approximate models. For example, approximate models were widely used, beginning with [49], to analyze failure in the microstructure of composites (see [30, Sec. 0.4 of introduction] for a detailed review of such studies) and fracture of homogeneous and composite materials compressed along cracks [112] (see Sec. 1.3 below for a brief description of the design models used). Using approximate models introduces substantial quantitative errors to the results and leads in many cases to qualitative disagreement with experimental data [112]. Hence, with approximate models, it is rather difficult to carry out a reliable analysis of nonclassical problems and fracture mechanisms.

It is therefore significant to use rigorous problem formulations, mathematical models, and methods to study nonclassical problems of fracture mechanics and failure mechanisms. Such studies were conducted in [23, 24, 27, 28, 31, 32, 34, 36, 37, 46, 58, 90, 98, 99, 107, 114, 122] using the most rigorous and exact problem formulations in solid mechanics. For example, fracture initiated by local buckling was studied using the three-dimensional linearized theory of stability of deformable bodies [11, 12, 24, 97] or the two-dimensional linearized theory of stability of thin-walled structural members [32], and the stress–strain state was analyzed using the three-dimensional equations of the statics of deformable bodies.

In what follows, we will briefly review studies on two theoretically and practically important nonclassical problems of fracture mechanics: (i) fracture of materials with initial (residual) stresses and (ii) fracture of bodies compressed along cracks.

1.2. Problems of the Brittle Fracture of Materials with Initial (Residual) Stresses Acting along Cracks. Initial (or residual, process-induced) stresses occur due to the inhomogeneity of linear or bulk strains in adjacent regions of the material. Such stresses are almost always induced in real structural materials and structural members by the manufacturing process (which is especially typical of composites [54, 55, 77] and polymers), joining (by, for instance, welding [43]), surface machining [44, 76], and operation and have a strong effect on the fracture behavior of bodies with cracks. Such problems are also quite typical for biomechanics (modeling of blood vessels and living tissues), geophysics, seismology, and other research areas, either fundamental or applied.

Of special interest are problems in which the initial (residual) stresses act along cracks (in Fig. 1 and below, S_0^{11} are the initial or residual stresses acting along a crack, Q'_{22} are additional (effective or operating) stresses (normal stresses are assumed as an example)). Problems of the brittle fracture of cracked materials with initial (residual) stresses acting in parallel to cracks are considered nonclassical because when the linear theory of elasticity (see, e.g., [135]) is used, the prestresses S_0^{11} acting along cracks do not appear in the expressions for the stress intensity factors and crack opening displacement (COD) and, hence, in the classical criteria such as Griffith–Irwin, critical COD, or their generalizations. Note that the effect of the prestresses can be incorporated into the specific surface energy γ. However, this approach is impractical because γ must depend on both the prestresses and the class of problems under consideration.

In his papers [13–15, 19, 22, 23, 28, 81, 89] published since 1980, Guz used the three-dimensional linearized solid mechanics (see [11, 24, 97, 99, 101, 110] for its principles and state of the art) to solve problems of fracture mechanics of prestressed materials. In these studies, he developed methods for solving plane, antiplane, and spatial problems of the fracture of cracked bodies with prestresses that are considerably higher than the additional stress and strain fields, which allows using linearized relations. Such a problem formulation is quite obvious and logical for, for example, composites with one preferred reinforcement direction and cracks located along reinforcement [54]. For such composites, prestresses S_0^{11} acting along the reinforcement can be an order of magnitude higher than the ultimate strength Q'_{22} (Fig. 1). Also, brittle fracture criteria for materials with initial (residual) stresses were formulated in [87, 88]. They are analogs of the classical Griffith–Irwin failure criteria and go over into them as the prestresses tend to zero (see Sec. 2.5 below for more details on failure criteria for prestressed materials with cracks). A key justification for this approach is that the use of linearized relations to solve this class of problems of fracture mechanics, unlike classical fracture mechanics, allows describing the basic phenomenon associated with the effect of the load components acting along cracks on the fracture behavior of materials.

This approach is universal and allows analysis in general terms for compressible and incompressible, isotropic and orthotropic (in the plane and antiplane cases) or transversely isotropic (in the three-dimensional case) elastic materials with arbitrary elastic potential for the theory of finite (large) initial deformations and the first and second theories of small initial deformations. The model of a material is specified (for example, the elastic potential is assigned one form or another) only at the

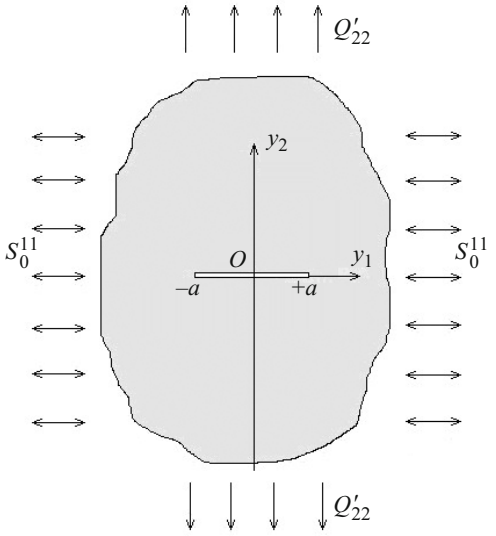

Fig. 1

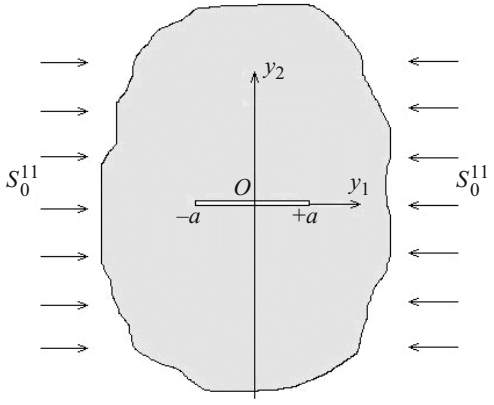

Fig. 2

final stage, i.e., during the numerical analysis of the general characteristic equations, governing integral equations, etc., derived at the previous stage. This general approach to problems of the brittle fracture of materials with prestresses can be generalized to inelastic materials. It should be taken into account that the additional (to the prestresses) stress and strain fields applied to elastoplastic materials disturb the stress–strain state and, hence, change the unloading zones, which considerably complicates the analysis.

This general approach made it possible to find solutions to some classes of static plane problems for isolated mode I, II, III cracks and a wedged crack in the form of an infinite strip [16–18, 23, 28, 81, 89]. Spatial axisymmetric problems for isolated internal and external mode I, II, III penny-shaped cracks in an unbounded material with prestresses and a general spatial problem for an internal penny-shaped crack are addressed in [19–21, 23, 28, 40, 82]. Spatial problems for unbounded prestressed bodies with elliptic mode I, II, III cracks were analyzed in [28, 35].

New mechanical effects associated with the initial (residual) stresses were detected there. For example, it was shown that the stresses near the tip of an isolated "free" crack (i.e., a crack with only stresses specified on its faces) do not depend on the prestresses and are equal to those observed in the mechanics of brittle fracture of materials without prestresses. The opening of the crack faces is strongly dependent on the prestresses. In plane wedging problems and in the general spatial shear problem for "free" cracks, the stress intensity factors are strongly dependent on the prestresses and are not equal to those in the mechanics of brittle fracture of materials without prestresses. It was also revealed that as the prestresses tend to the critical level that causes surface instability of a half-plane or a half-space, the basic variables change resonantly: the stresses and displacements at the crack tip tend to infinity and the critical loads in the linearized theory tend to zero (see Sec. 1.4 for more details on this mechanical effect).

The above results for plane and spatial static problems for one crack in materials with initial (residual) stresses are conclusive within the framework of the general formulation (for various material models) and were generalized in the monographs [23, 27 (Ch. 6, Sec. 1), 28, 30 (Vol 2, Ch. 7)] and the references therein. In [23, 25–28, 91], it was proved that the order of singularity at the crack tip in the fracture mechanics of materials with initial (residual) stresses acting along cracks is the same as the order of singularity (square-root singularity) at the crack tip in classical linear fracture mechanics.

Later, this general formulation was also used to solve a number of problems of the fracture of prestressed materials with interacting cracks. For example, some spatial problems for penny-shaped cracks in a half-space and in a layer with prestresses and for arrays of parallel cracks in unbounded prestressed bodies were addressed in [2, 4–6, 38, 48, 60–62, 70, 72, 139]. The effect of prestresses and the interaction of cracks with each other and with the boundaries of bodies on the stress intensity factors near the cracks was analyzed. For example, it was shown that unlike problems for isolated "free" cracks, the distribution of stresses and displacements near the crack tip in problems for interacting "free" cracks is strongly dependent on the prestresses. Studies on prestressed materials with interacting cracks were reviewed in detail in [114, 122].

Some classes of problems of crack propagation in materials with initial (residual) stresses acting along cracks were considered in [23, 28, 85, 93–96, 100]. The effect of the prestresses on the motion of an interface crack between two materials with initial (residual) stresses was analyzed in [102–105]. Possible critical phenomena accompanying the growth of cracks in prestressed materials (including in the interface) were analyzed. It was shown that as crack growth rate in a prestressed material tends to the speed of a Rayleigh wave in this material, the stresses and displacements near cracks abruptly increase to infinity, which are resonant phenomena. We will not dwell on such studies here because they were detailed in the review [110] and in the monograph [30, Ch. 10].

The static and dynamic problems of the fracture of materials with initial (residual) stresses acting along cracks have a universal general form for all models and problem formulations, according to the approach mentioned in the first part of the present section. Researchers often follow another approach by using a specific model (for example, for a material with specific elastic potential) from the very beginning of the study on three-dimensional linearized solid mechanics. Examples of such studies are [1, 51, 75, 127, 136, 137, 143, 145]. A fundamental shortcoming of this approach is the necessity to repeat the entire analysis to solve the same problem for a different model, which may lead to repetition of results, including those obtained using the universal approach for different models. Examples are given and analyzed in [106, 110, 116]. A review of such studies is beyond the scope of the present paper.

1.3. Problems of the Fracture of Materials Compressed along Cracks. The need for resolving practical issues and engineering problems in some fields of science and technology necessitates studying the fracture of bodies with cracks under compression. For example, the mechanics of composites (especially laminates) and the mechanics of materials with coating (heat insulation, anticorrosion, etc.) often deal with near-surface bulging (separation) near delaminations under compressive stresses of various nature. Many engineering problems involving design of products with structural defects are reduced to design models where compressive forces act along crack-like defects. Such problems arise in geomechanics in modeling tectonic forces in highlands (fractured stratified rock mass), construction (design of various supports), etc.

Problems of the fracture of bodies compressed along cracks are considered nonclassical because uniform compression strictly along cracks (Fig. 2) in isotropic and orthotropic materials (in orthotropic bodies, cracks are assumed to be located in planes parallel to one of the planes of material symmetry) induces a homogeneous stress–strain state, no matter what viscoelastoplastic model is, which means that the corresponding solutions have no singularities at the crack tips. Hence, with this type of loading, the stress intensity factors and crack opening displacement are equal to zero; therefore, approaches based on the classical Griffith–Irwin theory, critical COD criterion, or their generalizations are inapplicable.

In the problem under consideration, fracture is most probably begins, as in the problem of the compression of structural members along axes of symmetry, with local buckling of the material around the crack [27, 30, 33, 112]. There can be two situations with this failure mechanism, depending on the configuration of the specimen and the arrangement of cracks in it [112].

One situation is when the initial stage of fracture (local buckling of the material near cracks) coincides with the main stage fracture of the entire specimen, i.e., after buckling, the material no longer takes the load because the material surrounding the region that has lost stability does not provide sufficient support for it. This situation is observed in materials with cracks located in parallel planes and forming a periodic (in the direction perpendicular to the line of action of the compressive load) array of cracks penetrating the whole specimen. This is because buckling of the material around a periodic array of parallel coaxial cracks gives rise to a phenomenon similar to a plastic hinge going through the thickness of a beam in bending.

The other situation is where local buckling does not lead to fracture, but causes the material to change over to an adjacent equilibrium mode near cracks. With further increase in the external load, no failure occurs due to the "supporting" action of the surrounding material.

In the former case, the study of fracture is completed by determining the critical load that causes local buckling of the material around the cracks. In the latter case, the study of fracture should be continued, proceeding from the distribution of stresses and strains in the adjacent equilibrium mode of the material near cracks. In the adjacent equilibrium state, the configuration of cracks is different and not all stress intensity factors are equal to zero because there are bending stresses due to asymmetry and the material is now compressed not only along cracks, but also in other directions. Because of this, local buckling can be accompanied by other failure mechanisms described, for example, by the Griffith–Irwin failure criteria.

According to the classification introduced in [112], the local buckling of the material around a crack that initiates fracture is addressed by the first basic problem of the fracture of bodies compressed along cracks. The second basic problem of the fracture of bodies compressed along cracks is concerned with the postcritical deformation of a material with cracks with

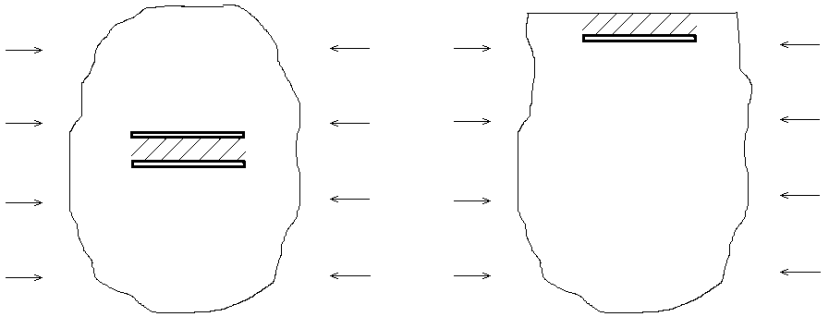

a *b*

Fig. 3

allowance for the changed configuration of the body after local buckling. The present paper reviews studies related to the first basic problem.

Thus, what both failure mechanisms for bodies compressed along cracks have in common is the local buckling of the material near cracks as the initial stage of fracture. The approaches to studying this stage of the fracture of bodies compressed along cracks and approaches to determining the corresponding critical loads can be classified as follows [112].

One approach is to model the portion of the material (hatched region in Fig. 3*a*, *b*) between parallel cracks or between a crack and the boundary by a beam (plane problem) or by a plate or a shell (spatial problem). This approach, which has been widely applied beginning with [140], is called the beam approximation. Such beams, plated, and shells are analyzed using various applied theories of stability of thin-walled structures (Bernoulli, Kirchhoff–Love, Timoshenko hypotheses, etc.), setting various boundary conditions for these thin-walled elements such as clamping or hinging (though these are elastic restraints in reality).

The beam approximation was widely developed in [10, 45, 47, 73, 128, 147]. Despite possible usefulness for engineering applications and relative simplicity, the beam approximation has essential shortcomings. For example, this approach is not applicable to all geometries and systems of forces. For example, if there is one crack in an unbounded material, it is difficult to justify the thickness of the beam. Also, applied theories of stability of thin-walled systems cannot be used when cracks are spaced far from each other. Finally, the beam approximation introduces an irreducible error to the results because the substantial change in energy at the crack tip is determined by the type of singularity in the stress distribution near this tip. Applied theories used to describe the deformation of isolated beams, plates, or shells do not allow evaluating the order of this singularity corresponding to the exact (three-dimensional) description. Studies employing the beam approximation were reviewed in [112], indicating the shortcomings inherent in these approach and irreducible errors that it introduces.

Therefore, it is necessary to use more rigorous approaches that would adequately describe the phenomena involved. Such rigorous approaches employ the three-dimensional linearized theory of stability of deformable bodies to analyze the fracture of compressed materials with local buckling near the crack [11, 12, 24, 97]. For example, in [83] for two-dimensional problems and in [84] for three-dimensional problems, Guz proposed a failure criterion expressed as a critical load causing local buckling near cracks and found by solving the appropriate eigenvalue problems in the three-dimensional linearized theory of stability of deformable bodies. Problem statements, basic equations, and results are presented in a universal general form for compressible and incompressible, isotropic and orthotropic (in plane cases) or transversely isotropic (in three-dimensional case) materials with arbitrary elastic potential and elastoplastic materials for the theory of finite (large) initial deformations and the first and second theories of small initial deformations. For elastoplastic materials, the generalized concept of increasing load [24, 97] is additionally used, thus neglecting the change in the unloading zones during loss of stability. This approach introduces no essential errors typical for the beam approximation and ensures accuracy typical for solid mechanics.

This general approach was used in [23, 33, 83, 84, 86] to find the exact solutions to plane and spatial problems for homogeneous and composite materials (continuum problem formulation) compressed along isolated cracks and along an arbitrary number of complanar cracks. It was shown that the critical loads that cause local buckling of the material near cracks in this case are equal to the critical compressive loads causing surface instability of a half-space without cracks.

Later, the linearized approach was used to solve plane and spatial problems for elastic and elastoplastic homogeneous bodies compressed along arrays of interacting parallel cracks (see, e.g., [9, 67, 71, 119–121, 124, 138]). It was shown that the

interaction of cracks with each other and with the free surface of the specimen substantially (by an order of magnitude and more) reduces the critical compressive stresses compared with those for an unbounded material compressed along an isolated crack or an array of complanar cracks. Such studies are reviewed in detail in [30, 33, 36, 37, 109, 112, 114, 122]. The passages to the limit as the distances between parallel coaxial cracks or between a crack and the boundary of the half-space tends to zero (see, e.g., [113]) have been recently analyzed to assess the limits of applicability of the beam approximation.

Piecewise-homogeneous material models helped to obtain results on the mechanics of brittle and ductile fracture of materials compressed along plane micro- and macrocracks located at the interface between dissimilar materials [30, 39, 115, 117, 125, 126, 149]. Problems of the viscoelastic fracture of composites and structural members compressed along cracks solved using the TLTSDB are generalized in [56, 57].

This completes the brief discussion of studies on the fracture of elastic, elastoplastic, and viscoelastic materials compressed along cracks. The foundations of the fracture mechanics of materials compressed along cracks, including associated concepts, approaches, and specific problems, and new mechanical effects revealed in solving them are discussed in [112].

1.4. Combined Approach to Problems of the Fracture of Materials under Loads Acting along Cracks. Earlier, the two nonclassical problems of fracture mechanics, namely, fracture of bodies with initial (residual) stresses acting along a crack and fracture of materials compressed along parallel cracks were analyzed separately. This was due to the logic of development of these (different in subject of study) groups of nonclassical problems and the complexity of mathematical methods used to solve them.

It should be noted that even the pioneering studies on the brittle fracture of prestressed unbounded materials with isolated cracks [13, 14, 19, 22, 23] revealed a new mechanical effect: the stress and strain fields near a crack and, hence, the critical loads depend on the prestresses. For example, it was shown that as the initial (residual) stresses tend to the stress levels that cause the surface instability of a half-plane (for plane problems) or a half-space (for spatial problems), the stresses and displacements at the crack tip predicted by the linearized theory abruptly increase to infinity, which are resonant phenomena. As the initial (residual) compressive stresses in bodies with a "free" crack tend to the critical level that causes the surface instability of a half-plane or a half-space, the ultimate loads in the linearized theory tend to zero.

As an illustration, we will discuss results for a compressible isotropic body with a disk-shaped crack of radius a located in the plane $y_3 = 0$; the body has equal tensile (or compressive) prestresses $S_0^{11} = S_0^{22}$ acting along the Oy_1- and Oy_2-axes and characterized by coefficients of elongation (or shortening) along the coordinate axes $\lambda_1 = \lambda_2$ ($\lambda_1 > 1$correspond to initial tension, $\lambda_1 < 1$ to initial compression, and $\lambda_1 = 1$ to zero prestresses). Let us consider the general case of shear where uniform shear stresses of intensity q are applied to the lower and upper faces of the crack at an angle β to the Oy_1-axis (Fig. 4). The exact solution [23, 28] indicates that the mode II and III stress intensity factors are nonzero in this case:

$$K_{II} = K^{(II)} \cdot K_{II}^0, \quad K_{III} = K^{(III)} \cdot K_{III}^0,$$

where K_{II} and K_{III} are the mode I and II stress intensity factors in a material with prestresses $S_0^{11} = S_0^{22}$ under a given external shear load; K_{II}^0 and K_{III}^0 are the mode II and III stress intensity factors in the same material without prestresses under the same external load; $K^{(II)}$ and $K^{(III)}$ are the dimensionless mode I and mode II stress intensity factors that characterize the effect of the prestresses.

Figure 5 shows the factors $K^{(II)}$ (curves *1*, *2*, *3*) and $K^{(III)}$ (curves *1′*, *2′*, *3′*) as functions of the coefficient of elongation (shortening) λ_1 for a compressible isotropic material with a harmonic elastic potential [132] and Poisson's ratio ν = 0.2, 0.3, 0.5 (curves *1*, *2*, *3*, respectively). As can be seen, there are vertical asymptotes representing the surface instability of the half-space, the corresponding shortening coefficient $\lambda_1 = (1+\nu)/2$. Thus, as the prestresses tend to the critical level causing surface instability of the half-space, resonant phenomena occur.

On the other hand, as noted in Sec. 1.3, in studying the fracture of unbounded materials compressed along an isolated crack that is initiated by local buckling near the crack, it was found out [23, 33] that the critical compressive loads acting along a crack are equal to the critical loads causing surface instability of a half-space. The local buckling of the material near the crack is similar to surface instability.

The above two mechanical effects suggest that the phenomenon of surface instability is fundamental for both the mechanics of brittle fracture of materials with prestresses acting along cracks and the mechanics of fracture of materials compressed along cracks. This situation can be explained by invoking the following physical considerations. When the initial

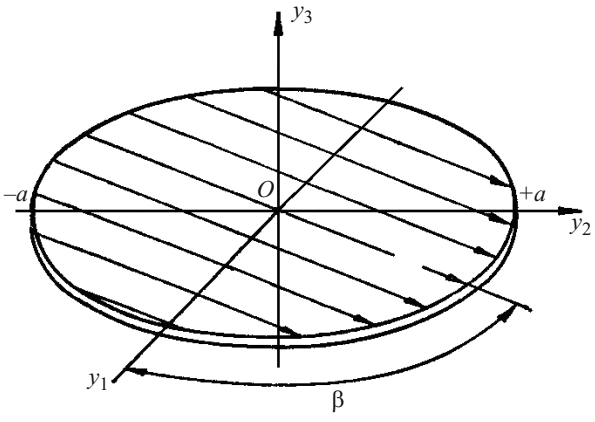

Fig. 4

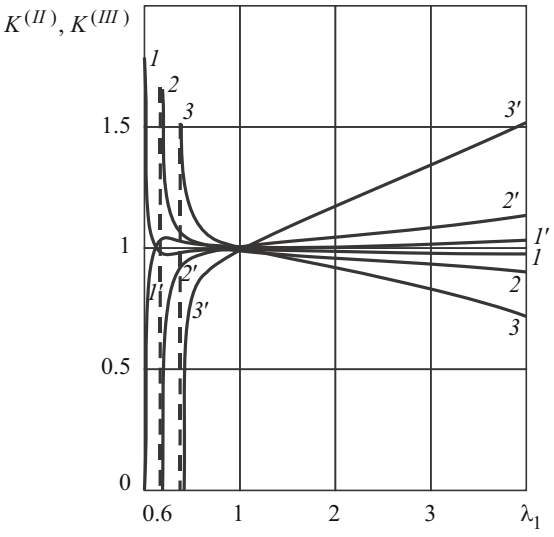

Fig. 5

stresses acting along cracks reach the critical level at which surface instability of a half-space occurs, the state at the crack tip is neutral equilibrium. A minor increase in the external load is sufficient to disturb the neutral equilibrium and to initiate the fracture process characterized by local buckling of the material near the crack.

Considering this physical interpretation, we may expect similar "resonant" phenomena (abrupt increase in the stresses and displacements near cracks) to occur in prestressed materials with other geometrical arrangements of cracks when the initial compressive stresses tend to the stresses causing local buckling of the material compressed along parallel cracks. This assumption was validated in [139] for a prestressed semibounded body with a near-surface crack. Figures 6*a* and 6*b* show the ratios K_{II} / K_{II}^{∞} and K_I / K_{II}^{∞} (where K_I and K_{II} are the stress intensity factors for a near-surface crack in a prestressed half-space; K_{II}^{∞} is the SIF for an isolated crack in an unbounded material without prestresses) for an incompressible highly elastic material with Treloar potential [146] containing a near-surface mode II crack parallel to the free surface of the material as functions of λ_1 for different values of the distance between the crack and the free surface divided by the radius of the crack. It can be seen that K_{II} / K_{II}^{∞} and K_I / K_{II}^{∞} tend to infinity (vertical asymptotes) as the initial compressive stresses tend to the critical level causing local buckling of the material compressed along the near-surface crack (see, e.g., [36, 120]).

It should be noted that both nonclassical problems mentioned above are solved using related mathematics of TDLSM. The linearized equilibrium equations and the equations of state are identical for both classes of problems, and so are the configurations of the bodies and the arrangements of defects. The essential difference in statement and solution between problems of the brittle fracture of materials with initial stresses acting along cracks and problems of the brittle and ductile fracture of materials compressed along an array of cracks located in parallel planes is that we deal with boundary-value problems (with nonzero boundary conditions on the crack faces), as in the linear mechanics of brittle fracture, in the former case and with eigenvalue problems (with zero boundary conditions on the crack faces) in the latter case.

Therefore, it appears reasonable to combine problems of the fracture of prestressed materials and problems of the fracture of materials compressed along cracks to be solved using TDLSM. This will help to substantially reduce awkward mathematical calculations and allow a more adequate description and correct interpretation of all mechanical effects associated with the action of loads along cracks.

A combined approach based on TDLSM to studying the fracture of prestressed materials and the fracture of cracked materials compressed along cracks was proposed in [68, 69, 63, 123]. This approach made it possible to develop a simpler and effective method for determining the critical loads for materials compressed along cracks without the need to solve eigenvalue problems using the three-dimensional linearized theory of stability of deformable bodies. The critical loads are found by solving boundary-value problems of the fracture of prestressed materials. The load parameters are changed continuously to find initial compressive stresses at which the amplitudes (of stresses and displacements) at the crack tips change resonantly. These initial

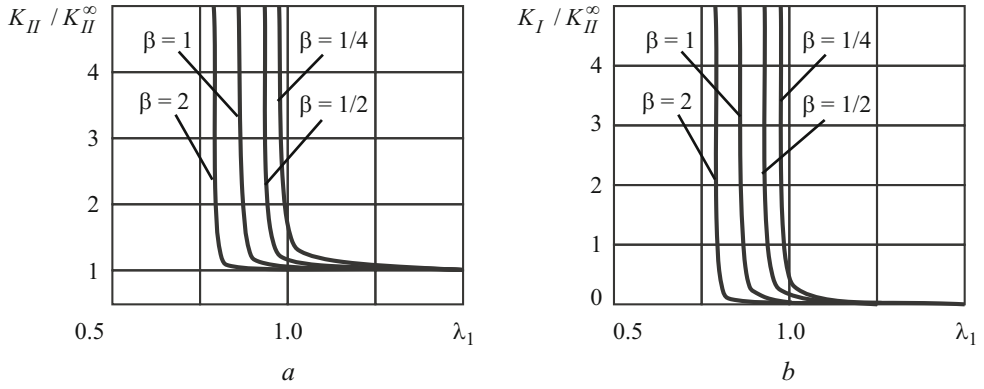

a *b*

Fig. 6

stresses are the eigenvalues of the eigenvalue problem for bodies compressed along cracks. It is obvious that the compressive prestresses in problems of the fracture of prestressed materials must not exceed the critical values at which local buckling of the material occurs near the cracks.

Note that a mathematically similar approach is used in some other divisions of mechanics. For example, as the frequency of an external load that forces a linear mechanical system to undergo vibrations tends to the natural frequency of the system, the amplitude of vibrations changes resonantly. This phenomenon underlies one of the approaches widely used to determine the natural frequencies (modes) of linear systems.

1.5. On Classes of Problems of the Fracture of Materials under Loads Acting along Cracks. The present review addresses two groups of nonclassical problems of fracture mechanics: (i) brittle fracture of materials with initial (residual) stresses acting in parallel to crack planes and (ii) fracture of bodies compressed along parallel cracks, both initiated by local buckling of the material near the cracks. Studies that employed the combined approach (see Sec. 1.4) to solving these problems are reviewed here.

We will consider spatial problems solved using the TDLSM approach [11, 24, 97], which allows formulating and solving problems in a universal general form for compressible and incompressible elastic bodies with an arbitrary elastic potential for the theory of finite (large) initial deformations and the first and second theories of small initial deformations. The results to be discussed were obtained for homogeneous isotropic hyperelastic materials and composite materials with elastic components. Composites were modeled by a transversely isotropic body with reduced (effective) characteristics and planes of isotropy parallel to the crack planes [30, 41, 52, 77], which is a well-known continuum model.

The problems of the fracture of homogeneous and composite materials with cracks under loads acting along cracks can be divided into three classes, depending on the arrangement of defects.

First class: cracks are located in several (finite number of) parallel planes that are far from the edges, i.e., the effect of the free (or reinforced) surface can be neglected (Fig. 7*a*). Second class: cracks are located in parallel planes and form a periodic (along the axis perpendicular to the line of action of the load) array, i.e., actually, penetrate the entire specimen (Fig. 7*b*). Third class: cracks are located in parallel planes near the edge of the material, i.e., the effect of the free (or reinforced) surface must be taken into account (Fig. 7*c*). In this case, we deal with near-surface fracture of a material.

Due to the complexity and inadequate development of the nonclassical problems of fracture mechanics under consideration, this review addresses the following characteristic (reference) arrangements of cracks:

(a) an isolated internal crack in an unbounded body;

(b) a near-surface crack parallel to the boundary of the half-space;

(c) two internal parallel coaxial (i.e., with coinciding projections, not shifted relative to each other) cracks in an unbounded body;

(d) a periodic array of parallel coaxial cracks in an unbounded body.

Results are presented for circular (penny-shaped) cracks because this configuration is the most typical for brittle materials [135].

Formulating and solving problems for such arrangements of defects allow us to separate out, into a pure form, and analyze the basic laws of interaction of cracks with each other and with the edges of bodies under loads acting along cracks. An

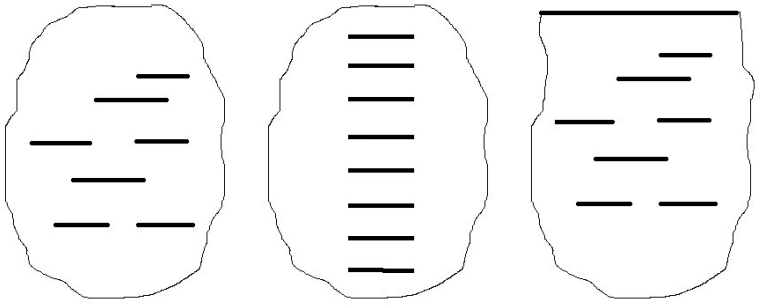

a *b* *c*

Fig. 7

isolated crack is the limiting case because all the other cases of arrangement of interacting cracks are reduced to it as the distances between cracks or between the crack and the surface of the material tend to infinity. Thus, the results obtained for an isolated crack can be used to test results for long distances between cracks. Solving the problem for a near-surface crack parallel to the surface of the material, we can estimate the effect of the interaction between the crack and the boundary of the body on its fracture behavior. Solving problems for two parallel coaxial cracks and a periodic array of coaxial parallel cracks, we can estimate the effect of the interaction of cracks with each other on the fracture behavior and are limiting cases for problems of the fracture of materials with an arbitrary finite number of coaxial parallel cracks. Mathematically, the problem for a body with a periodic array of coaxial parallel cracks is reduced to the problem for a layer with one crack parallel to the edges of the layer; therefore, the method for solving it can be used to solve problems for a crack in a prestressed layer with free or reinforced edges.

For each of the arrangement of cracks, we will discuss results obtained for different systems of forces acting on the faces of mode I, II, and III cracks. Also, we will discuss the critical loads causing local buckling found using the combined approach to problems of the fracture of materials with prestresses acting along cracks and cracked bodies compressed along cracks.

2. General Formulation of Linearized Spatial Problems of the Fracture of Materials under Loads Acting along Cracks. In this section, we will briefly discuss formulations of TDLSM problems, linearized equilibrium equations, representation of their solutions in terms of potential functions, material models, methods for solving some problems of the fracture of materials under loads acting along cracks, failure criteria for materials with prestresses acting along cracks and for bodies compressed along cracks. We will mainly use the terminology and notation adopted in the monographs [23, 28, 30].

2.1. Basic Equations of Three-Dimensional Linearized Solid Mechanics. As indicated in the Introduction, problems of the fracture of materials under forces acting along cracks are solved using the combined approach based on TDLSM. Historically, TDLSM evolved within the framework of the three-dimensional linearized theory of stability of deformable bodies and the theory of wave propagation in materials with initial (residual) stresses (see [99, 101, 111] for a detailed historical sketch of their development). The most general equations of TDLSM are derived by rigorous and consistent linearization of the equations of nonlinear elasticity. Therefore, we will briefly discuss some equations of nonlinear elasticity, the general principles of their linearization, and the linearized equilibrium equations, boundary conditions, and expressions for the Green strain tensor.

The deformed configuration of a body will be described in Lagrangian coordinates $x_j \equiv x^j$ $(j = \overline{1,3})$, which coincide with the Cartesian coordinates with unit vectors $\vec{g}_j$ in the natural (undeformed) configuration because the covariant, $\vec{g}_j$, and contravariant, $\vec{g}^{\,j}$, basis vectors coincide for Cartesian coordinates.

The metric tensor is given by

$$g_{mn} \equiv g^{nm} \equiv g_m^n = \delta_m^n = \delta_{nm},$$

$$g = \det||g_{rs}|| \equiv g^{-1} = \det||g^{rs}|| = 1. \tag{2.1}$$

Each point (particle) of the material is associated with three parameters x^m, the one-to-one correspondence holding at any instant τ. We introduce the following notation: $\vec{r}$ is the position vector of a point before deformation (in the natural configuration); $\vec{r}\,*$ is the position vector of the same point after deformation; $\vec{u}$ is the displacement vector of the point; the

coordinates $x_n \equiv x^n$ are considered frozen in the body; the asterisk refers to the deformed configuration. We can now write the following expressions:

$$\vec{r}^*(x_m, \tau) = \vec{r}(x_m) + \vec{u}(x_m, \tau),$$

$$\vec{r} = \vec{g}_n x_n, \qquad \vec{u} = \vec{g}_n u_n. \tag{2.2}$$

If $\vec{g}^*_m$ and $\vec{g}^m_*$ are the covariant and contravariant basis vectors in the deformed configuration and g^*_{nm}, g^{nm}_*, and $g^n_{*m} = \delta^n_m$ are the covariant, contravariant, and mixed components of the metric tensor in the deformed configuration, then the expressions below follow from (2.2):

$$d\vec{r}^* = \frac{\partial \vec{r}^*}{\partial x^m} dx^m = \vec{g}^*_m dx^m,$$

$$\vec{g}^*_m = \frac{\partial \vec{r}^*}{\partial x^m} = \vec{g}_m + \vec{g}_n \frac{\partial u_n}{\partial x^m}.$$

Forming the difference of squared arc elements in the deformed and undeformed configurations and performing transformations, we get

$$ds^{*2} - ds^2 = d\vec{r}^* \cdot d\vec{r}^* - d\vec{r} \cdot d\vec{r} = (g^*_{nm} - g_{nm})\, dx^n dx^m,$$

$$g^*_{nm} = \delta_{nm} + 2\varepsilon_{nm}, \tag{2.3}$$

where ε_{nm} are the components of the Green strain tensor,

$$2\varepsilon_{nm} = \frac{\partial u_n}{\partial x_m} + \frac{\partial u_m}{\partial x_n} + \frac{\partial u_k}{\partial x_n}\frac{\partial u_k}{\partial x_m} \qquad (n, m, k = \overline{1,3}). \tag{2.4}$$

These formulas allow determining changes in geometrical objects during deformation, such as

change in the length of a line element (coefficient of elongation) aligned with the coordinate axis x_n,

$$\lambda_{(n)} = \frac{ds^*_n}{ds_n} = \sqrt{1 + 2\varepsilon_{nn}}, \tag{2.5}$$

change in the angle ($\tilde{\psi}_{nm} = \psi_{nm} - \psi^*_{nm}$, ψ^*_{nm} is the angle after deformation) between the coordinate lines x_n and x_m,

$$\sin\tilde{\psi}_{nm} = \frac{(\delta_{nm} + 2\varepsilon_{nm})\sqrt{1-\delta_{nm}}}{\sqrt{(1+2\varepsilon_{nn})(1+2\varepsilon_{mm})}} - \delta_{nm}\sqrt{1 - \frac{(\delta_{nm} + 2\varepsilon_{nm})^2}{(1+2\varepsilon_{nn})(1+2\varepsilon_{mm})}}, \tag{2.6}$$

change in an area element of the surface $x_n = \text{const}$,

$$\frac{dS^*_n}{dS_n} = \sqrt{(1+2\varepsilon_{mm})(1+2\varepsilon_{kk}) - (\delta_{mk} + 2\varepsilon_{mk})^2},$$

$$n \neq m \neq k \neq n, \tag{2.7}$$

change in a volume element formed by the coordinate surfaces,

$$\frac{dV^*}{dV} = \sqrt{\det||\delta_{rs} + 2\varepsilon_{rs}||}. \tag{2.8}$$

It follows from (2.4) that the Green strain tensor is a symmetric tensor of the second rank whose algebraic invariants are

$$A_1 = \varepsilon_{nn}, \quad A_2 = \varepsilon_{nm}\varepsilon_{mn}, \quad A_3 = \varepsilon_{nm}\varepsilon_{mk}\varepsilon_{kn}. \tag{2.9}$$

It is possible to form other systems of invariants for the Green strain tensor that are expressed in terms of algebraic invariants (2.9). For example, the following system of invariants is often used [12]:

$$I_1 = 3 + 2\varepsilon_{nn} = 3 + 2A_1,$$

$$I_2 = 3 + 4\varepsilon_{nn} + 2(\varepsilon_{nn}\varepsilon_{mm} - \varepsilon_{nm}\varepsilon_{mn}) = 3 + 4A_1 + 2(A_1^2 - A_2),$$

$$I_3 = \det||\delta_{rs} + 2\varepsilon_{rs}|| = 1 + 2A_1 + 2(A_1^2 - A_2) + \frac{4}{3}(2A_3 - 3A_1A_2 + A_1^3). \tag{2.10}$$

If the elastic body is incompressible, then $I_3 = 1$ follows from the last expression in (2.10) and from (2.8).

Let us consider the principal values ε_1, ε_2, and ε_3 of the Green strain tensor. Moreover, let the coordinate lines x_n be aligned with the principal directions of the Green strain tensor. Denoting the coefficients of elongation (2.5) by λ_n and introducing relative coefficients of elongation δ_n, we get

$$\lambda_n = \sqrt{1 + 2\varepsilon_n}, \quad \delta_n = \lambda_n - 1 = \sqrt{1 + 2\varepsilon_n} - 1, \quad 2\varepsilon_n = \lambda_n^2 - 1, \quad 2\varepsilon_n = (\delta_n + 1)^2 - 1. \tag{2.11}$$

In this case, it is possible to introduce another system of invariants:

$$s_1 = (\lambda_1 - 1) + (\lambda_2 - 1) + (\lambda_3 - 1) \equiv \delta_1 + \delta_2 + \delta_3,$$

$$s_2 = (\lambda_1 - 1)^2 + (\lambda_2 - 1)^2 + (\lambda_3 - 1)^2 \equiv \delta_1^2 + \delta_2^2 + \delta_3^2,$$

$$s_3 = (\lambda_1 - 1)^3 + (\lambda_2 - 1)^3 + (\lambda_3 - 1)^3 \equiv \delta_1^3 + \delta_2^3 + \delta_3^3. \tag{2.12}$$

Also, the expressions below follow from (2.9):

$$A_1 = \varepsilon_1 + \varepsilon_2 + \varepsilon_3,$$

$$A_2 = \varepsilon_1^2 + \varepsilon_2^2 + \varepsilon_3^2,$$

$$A_3 = \varepsilon_1^3 + \varepsilon_2^3 + \varepsilon_3^3. \tag{2.13}$$

To characterize the stress state, the finite-deformation theory uses various stress tensors (see [12, 97] for more details). For example, when the stress vector $\vec{t}^{\,(i)}$ applied to an area $x_i = \text{const}$ in the deformed configuration and measured per unit area in the undeformed configuration is considered, the symmetric stress tensor $\widetilde{S}$ and the asymmetrical Piola–Kirchhoff stress tensor $\widetilde{t}$ are introduced:

$$\vec{t}^{\,(i)} = t^{ij}\vec{g}_j = S^{ij}\vec{g}_j^{\,*}. \tag{2.14}$$

The relationship between the tensors $\widetilde{S}$ and $\widetilde{t}$ follows from the second expression in (2.3) and (2.14):

$$t^{ij} = S^{in}\left(\delta_{nj} + \frac{\partial u_j}{\partial x_n}\right). \tag{2.15}$$

From (2.1) and (2.14) we get

$$\vec{t}^{\,(i)} = t^{ij}\vec{g}_j \equiv t_{ij}\vec{g}^{\,j}, \quad \vec{g}_j \equiv \vec{g}^{\,j}. \tag{2.16}$$

Let us now formulate the equilibrium equations (body forces being absent), boundary conditions for stresses on a portion S_1 of the surface, and boundary conditions for the displacements on a portion S_2 of the surface [24] in the form of components for the covariant basis vectors $\vec{g}_j$ in the undeformed configuration:

$$\frac{\partial}{\partial x_i} t_{ij} = \frac{\partial}{\partial x_i}\left[S^{in}\left(\delta_{jn} + \frac{\partial u_j}{\partial x_n} \right)\right] = 0,$$

$$N_i t_{ij}\big|_{S_1} = N_i \left[S^{in}\left(\delta_{jn} + \frac{\partial u_j}{\partial x_n} \right)\right]\Bigg|_{S_1} = Q_j\big|_{S_1} = P_j,$$

$$Q_j \equiv N_i \left[S^{in}\left(\delta_{jn} + \frac{\partial u_j}{\partial x_n} \right)\right], \qquad u_j\big|_{S_2} = f_j, \tag{2.17}$$

where P_j are the components (for $\vec{g}_j$) of the external load vector fixed to the surface of the body in the deformed configuration, but measured per unit area in the undeformed configuration; N_i are the components of the unit normal vector to the surface of the body in the undeformed configuration; f_j are the components of the right-hand sides of the boundary conditions for displacements.

The system of geometrically nonlinear equations (2.17) should be supplemented with constitutive equations, which will be presented in Sec. 2.2 for some material models.

We will now briefly outline the main principles of deriving the linearized equations. We will consider three equilibrium states of an elastic body:

(i) natural (undeformed) state in which stresses and strains are zero;

(ii) initial (or residual) stress–strain state or, differently, unperturbed state, denoted by index "0" (in problems of the fracture of prestressed materials, this state is induced by the initial (residual) stresses acting along cracks);

(iii) perturbed stress–strain state (represented as the sum of the second state and perturbations). The stress–strain state of prestressed materials is perturbed by additional loads applied to the crack faces.

The perturbations are considered small compared with the unperturbed (second) state. We will use no index to refer to the perturbations. Therefore, it can be assumed that the second and third states are described by the same equations of nonlinear elasticity. Thus, we will only consider initial or residual stress–strain states resulting from elastic deformation. It should be noted that "elastic" initial or residual stresses in one part of a solid can be induced by "inelastic" deformation of complex physical nature in its another part.

To derive the basic equations of the TDLSM, we will use the principle of linearization. The foregoing can be illustrated by a simple example. Let the following relation in nonlinear elasticity hold:

$$y = f(x), \tag{2.18}$$

where the natural (undeformed, first) state is the beginning of the process. Formula (2.18) can be written for the initial and perturbed states as

$$y_0 = f(x_0),$$

$$y_0 + y = f(x_0 + x), \tag{2.19}$$

where x and y are perturbations. Since the perturbations are small ($|x| << |x_0|$), we can linearize relation (2.19):

$$y_0 + y \approx f(x_0) + x\left(\frac{df}{dx}\right)\Big|_{x=x_0}. \tag{2.20}$$

Subtracting expression (2.19) for the second (initial) state from the linearized relation (2.20) for the third state, we obtain

$$y \approx x\left(\frac{df}{dx}\right)\Big|_{x=x_0}. \tag{2.21}$$

Let us now consider the linearized theory of elasticity for bodies with initial (residual) stresses. Its basic equations (2.21) relate the perturbations.

For example, linearizing the nonlinear kinematic equations (2.2), (2.4), (2.5), (2.7), (2.8) (see [24, 97] for more details), we obtain linearized expressions:

for the covariant basis vectors in the deformed state:

$$\vec{g}^{\,*}_m = \vec{g}_n \frac{\partial u_n}{\partial x_m}, \tag{2.22}$$

for the Green strain tensor:

$$2\varepsilon_{nm} = \left[\left(\delta_{mj} + \frac{\partial u^0_j}{\partial x_m}\right)\frac{\partial}{\partial x_n} + \left(\delta_{nj} + \frac{\partial u^0_j}{\partial x_n}\right)\frac{\partial}{\partial x_m}\right]u_j,$$

$$g^{\,*}_{nm} = 2\varepsilon_{nm}, \tag{2.23}$$

for other geometrical objects:

$$\lambda_{(n)} = (1+2\varepsilon^0_{nn})^{-1/2}\left(\delta_{jn} + \frac{\partial u^0_j}{\partial x_n}\right)\frac{\partial u_j}{\partial x_n}, \tag{2.24}$$

$$\frac{dS^{\,*}_n}{dS_n} = \sqrt{\frac{g^{\,*}_0}{g^{nn}_{*0}}}\left(g^{nn}_{*0}g^{mk}_{*0} - g^{nm}_{*0}g^{nk}_{*0}\right)\left(\delta_{mj} + \frac{\partial u^0_j}{\partial x_m}\right)\frac{\partial u_j}{\partial x_k},$$

$$n \neq m \neq k \neq n, \tag{2.25}$$

$$\frac{dV^*}{dV} = \sqrt{g^{\,*}_0}\,g^{nm}_{*0}\left(\delta_{jm} + \frac{\partial u^0_j}{\partial x_m}\right)\frac{\partial u_j}{\partial x_n}. \tag{2.26}$$

From (2.9), (2.10), (2.23), we get linearized relations for determining the invariants of the Green strain tensor:

$$A_1 = \left(\delta_{jn} + \frac{\partial u^0_j}{\partial x_n}\right)\frac{\partial u_j}{\partial x_n}, \quad A_2 = 2\varepsilon^0_{nm}\left(\delta_{jm} + \frac{\partial u^0_j}{\partial x_m}\right)\frac{\partial u_j}{\partial x_n}, \quad A_3 = 3\varepsilon^0_{im}\varepsilon^0_{ni}\left(\delta_{jm} + \frac{\partial u^0_j}{\partial x_{mn}}\right)\frac{\partial u_j}{\partial x_n}, \tag{2.27}$$

$$I_1 = 2\left(\delta_{jn} + \frac{\partial u^0_j}{\partial x_n}\right)\frac{\partial u_j}{\partial x_n}, \quad I_2 = 4(\delta_{nm} + \delta_{nm}\varepsilon^0_{ii} - \varepsilon^0_{nm})\left(\delta_{jm} + \frac{\partial u^0_j}{\partial x_m}\right)\frac{\partial u_j}{\partial x_n}. \tag{2.28}$$

The incompressibility condition is

$$g^{nm}_{*0}\varepsilon_{nm} \equiv g^{nm}_{*0}\left(\delta_{im} + \frac{\partial u^0_j}{\partial x_m}\right)\frac{\partial u_j}{\partial x_n} = 0. \tag{2.29}$$

According to (2.17), we obtain the following linearized equilibrium equations and boundary conditions:

the equilibrium equations

$$\frac{\partial}{\partial x_i}\left[\left(\delta_{nj}+\frac{\partial u_j^0}{\partial x_n}\right)S^{in}+S_0^{in}\frac{\partial u_j}{\partial x_n}\right]=0, \tag{2.30}$$

where the stress tensors $\widetilde{t}$ and $\widetilde{S}$ are related by

$$t_{ij}=\left(\delta_{nj}+\frac{\partial u_j^0}{\partial x_n}\right)S^{in}+S_0^{in}\frac{\partial u_j}{\partial x_n}, \tag{2.31}$$

the boundary conditions

$$N_i\, t_{ij}\big|_{S_1}=\left\{\left(\delta_{nj}+\frac{\partial u_j^0}{\partial x_n}\right)S^{in}+S_0^{in}\frac{\partial u_j}{\partial x_n}\right\}\Bigg|_{S_1}=P_j,$$

$$u^i\big|_{S_2}=f_j, \tag{2.32}$$

where P_j are the components (with respect to $\vec{g}_i$) of the perturbations of the right-hand sides of the boundary conditions for stresses; f_j are the perturbations of the right-hand sides of the boundary conditions for displacements; N_i are the components of the unit normal vector to the surface of the body in the undeformed state.

The above basic linearized equations are for the theory of finite (large) initial deformations. These equations can also be reformulated for two theories of small initial deformations (see [24, 97, 99] for more details).

For example, the first theory of small initial deformations is based on the assumption that the elongations and shears are small and can be neglected compared with unity. Its basic equations include

the equilibrium equations

$$\frac{\partial}{\partial x_i}\left[\left(\delta_{nj}+\frac{\partial u_j^0}{\partial x_n}\right)\sigma^{in}+\sigma_0^{in}\frac{\partial u_j}{\partial x_n}\right]=0, \tag{2.33}$$

where the components of the asymmetric Piola–Kirchhoff stress tensor $\widetilde{t}$ and the components of the usually used symmetric stress tensor $\widetilde{\sigma}$ are related by

$$t_{ij}=\left(\delta_{nj}+\frac{\partial u_j^0}{\partial x_n}\right)\sigma^{in}+\sigma_0^{in}\frac{\partial u_j}{\partial x_n}, \tag{2.34}$$

the boundary conditions have the form (2.32), (2.34), and the incompressibility condition is

$$g^{nm}\left(\delta_{im}+\frac{\partial u_j^0}{\partial x_m}\right)\frac{\partial u_j}{\partial x_n}=0. \tag{2.35}$$

In addition to the assumption made in the first theory of small initial deformations, the second theory of small initial deformations assumes that the initial state can be determined using the geometrically linear theory. In this case, the components of the Green strain tensor for the initial state are given by

$$2\varepsilon_{nm}^0=\frac{\partial u_n^0}{\partial x_m}+\frac{\partial u_m^0}{\partial x_n}. \tag{2.36}$$

The basic equations of the second theory include

the equilibrium equations

$$\frac{\partial}{\partial x_i}\left[\sigma^{ij} + \sigma_0^{in}\frac{\partial u_j}{\partial x_n}\right] = 0, \tag{2.37}$$

where the components of the asymmetric Piola–Kirchhoff stress tensor $\widetilde{t}$ and the components of the usually used symmetric stress tensor $\widetilde{\sigma}$ are related by

$$t_{ij} = \sigma^{ij} + \sigma_0^{in}\frac{\partial u_j}{\partial x_n}, \tag{2.38}$$

the boundary conditions have the form (2.32), (2.37), and the incompressibility condition is

$$g^{nj}\frac{\partial u_j}{\partial x_n} = 0. \tag{2.39}$$

2.2. On Models of Solids. Here we will briefly discuss the basic equations of the nonlinear and linearized theories for elastic compressible and incompressible bodies, which will be used below.

For hyperelastic bodies, it is assumed that there exists an elastic potential function characterizing the elastic strain energy [24, 97, 99]:

$$\delta\Phi = S^{ij}\delta\varepsilon_{ij}. \tag{2.40}$$

For the theory of finite (large) deformations, from (2.40) we obtain general expressions for the components of the stress tensor:

$$S^{ij} = \frac{1}{2}\left(\frac{\partial}{\partial\varepsilon_{ij}} + \frac{\partial}{\partial\varepsilon_{ji}}\right)\Phi \tag{2.41}$$

for compressible bodies and

$$S^{ij} = \frac{1}{2}\left(\frac{\partial}{\partial\varepsilon_{ij}} + \frac{\partial}{\partial\varepsilon_{ji}}\right)\Phi + pg_*^{ij} \tag{2.42}$$

for incompressible bodies, where p is a scalar function related to hydrostatic pressure.

We will further consider the most typical and theoretically and practically important models: isotropic hyperelastic materials with different elastic potentials and composites as popular structural materials.

Isotropic Hyperelastic Materials. For compressible hyperelastic materials, it is convenient to use elastic potentials derived from the basis algebraic invariants (2.9), (2.27) of the Green strain tensor (2.4), (2.23):

$$\Phi = \sum_{i,j,k} c_{ijk} A_1^i A_2^j A_3^k, \quad c_{ijk} = \text{const}. \tag{2.43}$$

With a difference finite number of terms retained in (2.43), we have different elastic potentials. For example, keeping terms up to the second order, we obtain the following elastic potential [23]:

$$\Phi = \frac{1}{2}\lambda A_1^2 + \mu A_2 \tag{2.44}$$

which becomes linear in changing over to the classical theory of linear elasticity, the parameters λ and μ being the Lamé constants.

Retaining terms up the third order in (2.43), we get the Murnaghan potential [23]:

$$\Phi = \frac{1}{2}\lambda A_1^2 + \mu A_2 + \frac{a}{3}A_1^3 + bA_1A_2 + \frac{c}{3}A_3. \tag{2.45}$$

Using the invariants of the Green strain tensor s_1, s_2, s_3 in the form (2.12), representing the elastic potential for compressible materials in terms of these invariants in a form similar to (2.43),

$$\Phi^s = \sum_{i,j,k} c^s_{ijk} s_1^i s_2^j s_3^k, \qquad c^s_{ijk} = \text{const}, \tag{2.46}$$

and retaining a finite number of terms in (2.46), we obtain elastic potentials in terms of the basis invariants. For example, keeping two terms in (2.46) and introducing new notation for the constants, we obtain a harmonic elastic potential [132]:

$$\Phi^s = \frac{1}{2}\lambda s_1^2 + \mu s_2. \tag{2.47}$$

Elastic potentials for incompressible hyperelastic materials are constructed in a similar way. For example, using the system of invariants (2.12) and retaining one term in series (2.46), we obtain the simplest elastic potential for an incompressible material (Bartenev–Khazanovich potential) [3]:

$$\Phi^s = 2\mu s_1, \qquad \mu = \text{const}. \tag{2.48}$$

Using the system of invariants I_1, I_2, I_3 (2.10), (2.28) and retaining a finite number of terms in the series, we can obtain the Treloar potential [146]:

$$\Phi = c_{10}(I_1 - 3), \qquad c_{10} = \text{const}. \tag{2.49}$$

Note that an elastic incompressible isotropic material described by the Treloar potential is called a neo-hookean material.

More details on other elastic potentials can be found in [24, 97].

Composite Materials. In studying composite materials, we will assume that cracks are much larger than structural elements of composites (i.e., macrocracks) and will consider only fracture processes in which composites do not manifest themselves as piecewise-homogeneous materials (interface fracture, etc.). With such assumptions, following [30, 41, 52, 77], we will model a composite by an anisotropic continuum with effective characteristics (for example, a transversely isotropic body with planes of isotropy parallel to the crack planes $x_3 = \text{const}$).

The elastic potential for an anisotropic compressible body can be represented in the following general form [30]:

$$\Phi = E^{ijnm}\varepsilon_{ij}\varepsilon_{nm} + E^{ijnmpq}\varepsilon_{ij}\varepsilon_{nm}\varepsilon_{pq} + \dots. \tag{2.50}$$

Keeping terms up to the second order in (2.50) and using the second theory of small deformations (for which $S^{ij} \equiv \sigma_{ij}$), we obtain the following constitutive equations:

$$\sigma_{ij} = A_{ijnm}\varepsilon_{nm}, \qquad \varepsilon_{nm} = a_{nmij}\sigma_{ij}. \tag{2.51}$$

For example, for a transversely isotropic body with Ox_3 as an axis of isotropy, we have

$$\begin{gathered}
\sigma_{11} = A_{11}\varepsilon_{11} + A_{12}\varepsilon_{22} + A_{13}\varepsilon_{33}, \qquad \sigma_{12} = (A_{11} - A_{12})\varepsilon_{12}, \\
\sigma_{22} = A_{12}\varepsilon_{11} + A_{11}\varepsilon_{22} + A_{13}\varepsilon_{33}, \qquad \sigma_{13} = 2A_{44}\varepsilon_{13}, \\
\sigma_{23} = 2A_{44}\varepsilon_{23}, \qquad \sigma_{33} = A_{13}\varepsilon_{11} + A_{13}\varepsilon_{22} + A_{33}\varepsilon_{33}.
\end{gathered} \tag{2.52}$$

Using five independent technical constants (elastic moduli E_j, shear moduli G_{ij}, and Poisson's ratios ν_{ij}), we can rearrange the constitutive equations (2.52) as

$$\varepsilon_{11} = \frac{1}{E_1}\sigma_{11} - \frac{\nu_{12}}{E_1}\sigma_{22} - \frac{\nu_{31}}{E_3}\sigma_{33}, \quad \varepsilon_{12} = \frac{1}{2G_{12}}\sigma_{12},$$

$$\varepsilon_{22} = -\frac{\nu_{12}}{E_1}\sigma_{11} + \frac{1}{E_1}\sigma_{22} - \frac{\nu_{31}}{E_3}\sigma_{33}, \quad \varepsilon_{13} = \frac{1}{2G_{13}}\sigma_{13},$$

$$\varepsilon_{23} = \frac{1}{2G_{13}}\sigma_{23}, \quad \varepsilon_{33} = -\frac{\nu_{31}}{E_3}\sigma_{11} - \frac{\nu_{31}}{E_3}\sigma_{22} + \frac{1}{E_3}\sigma_{33}, \tag{2.53}$$

$$G_{12} = \frac{E_1}{2(1+\nu_{12})}.$$

Transversely isotropic materials with effective macrocharacteristics model will be used to model laminated composites with isotropic plies and fibrous composites reinforced with random short ellipsoidal fibers in the plane $x_3 = \text{const}$ [52]. The effective macrocharacteristics of these composites are determined by the elastic characteristics and volume fraction of their components. For example, the macrocharacteristics of a composite laminate with isotropic plies are as follows [52]:

$$E_1^* = \frac{4\Delta G_{12}^*}{2G_{12}^*\lambda_{33}^* + \Delta}, \quad E_3^* = \frac{\Delta}{\lambda_{11}^* + \lambda_{12}^*}, \quad \nu_{31}^* = \frac{\lambda_{13}^*}{\lambda_{11}^* + \lambda_{12}^*}, \quad \nu_{12}^* = \frac{E_1^*}{2G_{12}^*} - 1,$$

$$G_{13}^* = \lambda_{44}^*, \quad G_{12}^* = \lambda_{66}^*, \quad \Delta = \lambda_{33}^*(\lambda_{11}^* + \lambda_{12}^*) - 2\lambda_{13}^{*2},$$

$$\lambda_{13}^* = \langle\lambda\rangle - c_1c_2(\lambda_1 - \lambda_2)(\lambda_1 + 2\mu_1 - \lambda_2 - 2\mu_2)z,$$

$$\frac{1}{2}(\lambda_{11}^* + \lambda_{12}^*) = \langle\lambda + \mu\rangle - c_1c_2(\lambda_1 - \lambda_2)^2 z,$$

$$\lambda_{33}^* = \langle\lambda + 2\mu\rangle - c_1c_2(\lambda_1 - \lambda_2 + 2\mu_1 - 2\mu_2)z,$$

$$\lambda_{44}^* = \mu_1\mu_2\mu_4^{-1}, \quad \lambda_{66}^* = \langle\mu\rangle, \quad z = (\lambda_4 + 2\mu_4)^{-1},$$

$$\lambda_4 = c_1\lambda_2 + c_2\lambda_1, \quad \mu_4 = c_1\mu_2 + c_2\mu_1, \quad \langle\kappa\rangle \equiv c_1\kappa_1 + c_2\kappa_2 \tag{2.54}$$

the plies are laid up in the plane x_1x_2; λ_ν and μ_ν are the Lamé constants of the νth ply ($\nu = 1, 2$); c_ν is the volume fraction of plies with elastic characteristics λ_ν and μ_ν. For example, the Lamé constants appearing in (2.54) have the following values for a composite with aluminoborosilicate-glass plies in composition with maleic epoxy resin plies [52]:

$$\lambda_1 = 1.94\cdot10^4 \text{ MPa}, \quad \mu_1 = 2.92\cdot10^4 \text{ MPa} \quad \text{for the glass and}$$

$$\lambda_2 = 3.69\cdot10^3 \text{ MPa}, \quad \mu_2 = 1.14\cdot10^3 \text{ MPa} \quad \text{for the resin.}$$

The effective macrocharacteristics of a composite reinforced with random ellipsoidal short carbon fibers (with a volume fraction of 0.7) in the isotropy plane $x_3 = \text{const}$ are the following [52]:

$$E_1 = 1\cdot10^4 \text{ MPa}, \quad E_3 = 3\cdot10^4 \text{ MPa}, \quad G_{13} = 1\cdot10^4 \text{ MPa}, \quad \nu_{12} = 0.125, \quad \nu_{31} = 0.09.$$

Using the general approach to the linearization of nonlinear equations, we obtain the following linearized constitutive equations [24, 97]:

$$t_{ij} = \omega_{ij\alpha\beta} \frac{\partial u_\alpha}{\partial x_\beta}, \qquad S^{in} = \lambda_{in\alpha\beta} \frac{\partial u_\alpha}{\partial x_\beta} \tag{2.55}$$

for compressible bodies, where the components of the tensors $\widetilde{\lambda}$ and $\widetilde{\omega}$ are defined by

$$\lambda_{ij\alpha\beta} = \frac{1}{4}\left(\delta_{m\alpha} + \frac{\partial u^0_\alpha}{\partial x_m}\right)\left(\frac{\partial}{\partial \varepsilon^0_{m\beta}} + \frac{\partial}{\partial \varepsilon^0_{\beta m}}\right)\left(\frac{\partial}{\partial \varepsilon^0_{in}} + \frac{\partial}{\partial \varepsilon^0_{ni}}\right)\Phi^0,$$

$$\omega_{ij\alpha\beta} = \frac{1}{4}\left(\delta_{nj} + \frac{\partial u^0_j}{\partial x_n}\right)\left(\delta_{m\alpha} + \frac{\partial u^0_\alpha}{\partial x_m}\right)\left(\frac{\partial}{\partial \varepsilon^0_{m\beta}} + \frac{\partial}{\partial \varepsilon^0_{\beta m}}\right)\left(\frac{\partial}{\partial \varepsilon^0_{in}} + \frac{\partial}{\partial \varepsilon^0_{ni}}\right)\Phi^0 + \delta_{\alpha j} S_0^{i\beta},$$

$$S_0^{i\beta} = \frac{1}{2}\left(\frac{\partial}{\partial \varepsilon^0_{i\beta}} + \frac{\partial}{\partial \varepsilon^0_{\beta i}}\right)\Phi^0, \qquad \Phi^0 = \Phi(\varepsilon^0_{11}, \ldots, \varepsilon^0_{33}), \tag{2.56}$$

$$t_{ij} = \kappa_{ij\alpha\beta} \frac{\partial u_\alpha}{\partial x_\beta} + q^{ij} p, \qquad S^{in} = \mu_{in\alpha\beta} \frac{\partial u_\alpha}{\partial x_\beta} + g^{in}_{*0} p \tag{2.57}$$

for incompressible bodies, where the components of the tensors $\widetilde{\kappa}$, $\widetilde{\mu}$, $\widetilde{q}$ are defined by

$$\kappa_{ij\alpha\beta} = \left(\delta_{nj} + \frac{\partial u^0_j}{\partial x_n}\right)\left(\delta_{m\alpha} + \frac{\partial u^0_\alpha}{\partial x_m}\right)\left[\frac{1}{4}\left(\frac{\partial}{\partial \varepsilon^0_{m\beta}} + \frac{\partial}{\partial \varepsilon^0_{\beta m}}\right)\left(\frac{\partial}{\partial \varepsilon^0_{in}} + \frac{\partial}{\partial \varepsilon^0_{ni}}\right)\Phi^0 - p^0 (g^{i\beta}_{*0} g^{mn}_{*0} + g^{im}_{*0} g^{\beta n}_{*0})\right] + \delta_{\alpha j} S_0^{i\beta},$$

$$\mu_{ij\alpha\beta} = \left(\delta_{m\alpha} + \frac{\partial u^0_\alpha}{\partial x_m}\right)\left[\frac{1}{4}\left(\frac{\partial}{\partial \varepsilon^0_{m\beta}} + \frac{\partial}{\partial \varepsilon^0_{\beta m}}\right)\left(\frac{\partial}{\partial \varepsilon^0_{in}} + \frac{\partial}{\partial \varepsilon^0_{ni}}\right)\Phi^0 - p^0 (g^{i\beta}_{*0} g^{mn}_{*0} + g^{im}_{*0} g^{\beta n}_{*0})\right],$$

$$q^{ij} = g^{im}_{*0}\left(\delta_{mj} + \frac{\partial u^0_j}{\partial x_m}\right), \qquad S_0^{i\beta} = p^0 g^{i\beta}_{*0} + \frac{1}{2}\left(\frac{\partial}{\partial \varepsilon^0_{i\beta}} + \frac{\partial}{\partial \varepsilon^0_{\beta i}}\right)\Phi^0, \tag{2.58}$$

where q^{ij}_{*0} are the contravariant components of the metric tensor in the initial stress state. Moreover, the tensors $\widetilde{\lambda}$ and $\widetilde{\omega}$, $\widetilde{\kappa}$ and $\widetilde{\mu}$ are related by

$$\omega_{ij\alpha\beta} = \left(\delta_{nj} + \frac{\partial u^0_j}{\partial x_n}\right)\lambda_{in\alpha\beta} + \delta_{\alpha j} S_0^{i\beta},$$

$$\kappa_{ij\alpha\beta} = \left(\delta_{nj} + \frac{\partial u^0_j}{\partial x_n}\right)\mu_{in\alpha\beta} + \delta_{\alpha j} S_0^{i\beta}. \tag{2.59}$$

For a compressible anisotropic (in particular, transversely isotropic) material for the second theory of small initial deformations, we have

$$\omega_{ij\alpha\beta} = \lambda_{ij\alpha\beta} + \delta_{\alpha j} S_0^{i\beta},$$

$$\lambda_{ij\alpha\beta} = \delta_{ij}\delta_{\alpha\beta} A_{i\beta} + (1-\delta_{ij}) G_{ij} (\delta_{i\beta}\delta_{j\alpha} + \delta_{i\alpha}\delta_{j\beta}),$$

$$S_0^{i\beta} = \delta_{i\chi} \sum_{k=1}^{3} A_{ik} \varepsilon^0_{kk} + 2(1-\delta_{i\beta}) G_{i\beta} \varepsilon^0_{i\beta}. \tag{2.60}$$

2.3. General Solutions of the Linearized Equations for Homogeneous Initial States. Here we will briefly discuss the basic equations of TDLSM for compressible and incompressible solids with homogeneous initial stress–strain states and general solutions of the linearized equilibrium equations expressed in terms of potential functions.

To solve problems of the fracture of materials with prestresses acting along cracks and the fracture of materials compressed along parallel cracks, it is convenient to use the coordinates of the initial (second) state. Therefore, along with the Lagrangian coordinates $x_j \equiv x^j$, which coincide with the Cartesian coordinates in the natural (undeformed) state, we will use the Cartesian coordinates $y_j \equiv y^j$ $(j = \overline{1,3})$ of the initial (second) stress–strain state. The coordinates x_j and y_j of the same material point of a body are related by

$$y_j = \lambda_j x_j, \qquad \lambda_j = \text{const}, \qquad j = \overline{1,3}, \tag{2.61}$$

where λ_j are the coefficients of elongation (or shortening) along the coordinate axes Oy_j (Ox_j) associated with the prestresses.

Loads acting strictly along cracks induce a homogeneous initial (second) stress–strain state characterized by the following relations for the components of the displacement vector:

$$u_m^0 = \lambda_m^{-1}(\lambda_m - 1) y_m . \tag{2.62}$$

Let us also introduce the following notation and use the prime to refer to the initial (second) state: Q'_{ij} are the components of an asymmetric stress tensor per unit area in the initial state; P'_j are the components of the surface load vector on an area with unit normal vector $\vec{N}$. We obtain the following relations [24, 97]:

$$Q'_{ij} = \frac{\lambda_i}{\lambda_1\lambda_2\lambda_3} t_{ij}, \qquad P'_j = \frac{\lambda_i N_i^{-1}}{\lambda_1\lambda_2\lambda_3} P_j . \tag{2.63}$$

If the initial stress–strain state defined by (2.62) is homogeneous, the constitutive equations (2.55), (2.57), (2.63) become:

$$Q'_{ij} = \omega'_{ij\alpha\beta} \frac{\partial u_\alpha}{\partial y_\beta} \tag{2.64}$$

for compressible bodies and

$$Q'_{ij} = \kappa'_{ij\alpha\beta} \frac{\partial u_\alpha}{\partial y_\beta} + \delta_{ij} p' \tag{2.65}$$

for incompressible bodies

$$\left(\omega'_{ij\alpha\beta} = \frac{\lambda_i\lambda_\beta}{\lambda_1\lambda_2\lambda_3} \omega_{ij\alpha\beta} = \frac{\lambda_i\lambda_j\lambda_\alpha\lambda_\beta}{\lambda_1\lambda_2\lambda_3} \left[\delta_{ij}\delta_{\alpha\beta} A_{i\beta} + (1-\delta_{ij})(\delta_{i\alpha}\delta_{j\beta} + \delta_{i\beta}\delta_{j\alpha})\mu_{ij} \right] + \frac{\lambda_i\lambda_\beta}{\lambda_1\lambda_2\lambda_3} S_0^{\beta\beta}, \right.$$

$$\left. \kappa'_{ij\alpha\beta} = \lambda_i\lambda_\beta\kappa_{ij\alpha\beta} = \lambda_i\lambda_j\lambda_\alpha\lambda_\beta \left[\delta_{ij}\delta_{\alpha\beta} A_{i\beta} + (1-\delta_{ij})(\delta_{i\alpha}\delta_{j\beta} + \delta_{i\beta}\delta_{j\alpha})\mu_{ij} \right] + \lambda_i\lambda_\beta\delta_{i\beta}\delta_{j\alpha} S_0^{\beta\beta} \right),$$

and $A_{i\beta}, \mu_{ij}, S_0^{\beta\beta}$ are determined by the material model (in particular, elastic potential) chosen.

The linearized equilibrium equations (2.30), (2.31) take the following form in the coordinates y_j:

$$\frac{\partial}{\partial y_j} Q'_{ij} = 0. \tag{2.66}$$

With (2.64), (2.65), these equilibrium equations can be written for displacements:

$$L'_{m\alpha}u_\alpha = 0, \quad L'_{m\alpha} = \omega'_{ij\alpha\beta}\frac{\partial^2}{\partial y_i \partial y_\beta} \quad (m, \alpha, i, \beta = \overline{1,3}) \tag{2.67}$$

for compressible bodies and

$$N'_{m\alpha}u_\alpha = 0, \quad u_4 \equiv p', \tag{2.68}$$

for incompressible bodies, where $N'_{m\alpha} = \kappa'_{im\alpha\beta}\frac{\partial^2}{\partial y_i \partial y_\beta}(1-\delta_{m4})(1-\delta_{\alpha 4}) + \delta_{\alpha 4}(1-\delta_{m4})\frac{\partial}{\partial y_m} + \delta_{m4}(1-\delta_{\alpha 4})\frac{\partial}{\partial y_\alpha}$, $(m, \alpha, i, \beta = \overline{1,3})$.

As can be seen, if the initial state (2.62) is homogeneous, the linearized equilibrium equations for displacements (2.67), (2.68) constitute systems of partial differential equations with constant coefficients. In [24, 97] the operator method was used to find general solutions to these equations in one of the following forms (or their linear combination):

$$u_i^{(j)} = \left[\frac{\partial(\det||L'_{rs}||)}{\partial(L'_{m\alpha})}\right]\Phi'^{(j)}, \quad [\det||L'_{rs}||]\Phi'^{(j)} = 0 \quad (j = \overline{1,3}) \tag{2.69}$$

for compressible bodies and

$$u_\alpha^{(m)} = \frac{\partial(\det||N'_{rs}||)}{\partial(N'_{m\alpha})}\Phi'^{(m)}, \quad \det||N'_{rs}||\Phi'^{(m)} = 0 \quad (m = \overline{1,4}) \tag{2.70}$$

for incompressible bodies.

It is possible to further simplify the general solutions of the linearized equilibrium equations for spatial problems in the special case of homogeneous initial state where the prestresses acting along the Oy_1- and Oy_2-axes are equal. We will assume that if the initial state (2.62) is homogeneous, the following conditions for isotropic and transversely isotropic bodies with axis of isotropy Oy_3 are also satisfied:

$$S_0^{11} = S_0^{22} \neq 0, \quad S_0^{33} = 0, \quad \lambda_1 = \lambda_2 \neq \lambda_3, \quad \varepsilon_{11}^0 = \varepsilon_{22}^0. \tag{2.71}$$

Let us consider an arbitrary cylindrical coordinate system with axis aligned with Oy_3 and an arbitrary curve (in the initial deformed state) with unit normal $\vec{N}$ and tangent $\vec{S}$ vectors in the plane y_1Oy_2; N_1 and N_2 are the projections of the unit vector $\vec{N}$ onto the Oy_1- and Oy_2-axes. If the initial stress–strain state is given by (2.62), (2.71), then the components u_N and u_S of the displacement vector can be expressed in terms of two potential functions Ψ and χ as follows [24, 97]:

$$u_N = \frac{\partial}{\partial S}\Psi - \frac{\partial^2}{\partial N\,\partial y_3}\chi, \quad u_S = -\frac{\partial}{\partial N}\Psi - \frac{\partial^2}{\partial S\,\partial y_3}\chi,$$

$$u_3 = \frac{\omega'_{1111}}{\omega'_{1133} + \omega'_{1313}}\left(\Delta_1 + \frac{\omega'_{3113}}{\omega'_{1111}}\frac{\partial^2}{\partial y_3^2}\right)\chi \tag{2.72}$$

for compressible bodies and

$$u_N = \frac{\partial}{\partial S}\Psi - \frac{\partial^2}{\partial N\,\partial y_3}\chi, \quad u_S = -\frac{\partial}{\partial N}\Psi - \frac{\partial^2}{\partial S\,\partial y_3}\chi, \quad u_3 = \lambda_1 q_1 \lambda_3^{-1} q_3^{-1}\Delta_1\chi,$$

$$p = \lambda_1^{-1}q_1^{-1}\left\{\left[\kappa'_{1111} - \lambda_1 q_1 \lambda_3^{-1} q_3^{-1}(\kappa'_{1133} + \kappa'_{1313})\right]\Delta_1 + \kappa'_{3113}\frac{\partial^2}{\partial y_3^2}\right\}\frac{\partial}{\partial y_3}\kappa' \tag{2.73}$$

for incompressible bodies, where $\Delta_1 \equiv \frac{\partial^2}{\partial y_1^2} + \frac{\partial^2}{\partial y_2^2}$; $\frac{\partial}{\partial N}$ and $\frac{\partial}{\partial S}$ are normal and tangent derivatives, respectively.

The potential functions Ψ and χ satisfy the equations

$$\left(\Delta_1 + n_3 \frac{\partial^2}{\partial y_3^2}\right)\Psi = 0,$$

$$\left(\Delta_1 + n_1 \frac{\partial^2}{\partial y_3^2}\right)\left(\Delta_1 + n_2 \frac{\partial^2}{\partial y_3^2}\right)\chi = 0, \tag{2.74}$$

where n_j, $j = \overline{1,3}$, are the roots of the algebraic (characteristic) equations corresponding to the differential equations (2.74),

$$n_{1,2} = c' \pm (c'^2 - \omega'_{3113}\omega'_{3333}\omega'^{-1}_{1331}\omega'^{-1}_{1111})^{-1/2}, \quad n_3 = \omega'_{3113}\omega'^{-1}_{3113},$$

$$2c'\omega'_{1111}\omega'_{1331} = \omega'_{1331}\omega'_{3113} + \omega'_{1111}\omega'_{3333} - (\omega'_{1133} + \omega'_{1313})^2 \tag{2.75}$$

for compressible bodies and

$$n_{1,2} = c' \pm (c'^2 - q_{33}^2 q_{11}^{-2}\kappa'_{3113}\kappa'^{-1}_{1331})^{-1/2}, \quad n_3 = \kappa'_{3113}\kappa'^{-1}_{3113},$$

$$2c'\kappa'_{1331} = \kappa'_{3333} + q_{11}^{-2}q_{33}^{-2}\kappa'_{1111} - 2q_{11}^{-1}q_{33}(\kappa'_{1133} + \kappa'_{1313}) \tag{2.76}$$

for incompressible bodies.

The general solutions can further be simplified by defining a function χ satisfying the fourth-order equation (2.74) in terms of two functions satisfying second-order equations [24, 97].

For example, if the roots of the characteristic equation ($n_1 \neq n_2$) are unequal, then introducing new functions $\Psi = -\varphi_3$ and $\partial\chi / \partial y_3 = -(\varphi_1 + \varphi_2)$ satisfying the equations $(\Delta_1 + \partial^2 / (\partial z_3^2))\varphi_j = 0$, $z_j = n_j^{-1/2} y_3$ ($j = \overline{1,3}$), we obtain the following expressions for the displacements:

$$u_N = \frac{\partial}{\partial N}(\varphi_1 + \varphi_2) - \frac{\partial \varphi_3}{\partial S}, \quad u_S = \frac{\partial}{\partial S}(\varphi_1 + \varphi_2) + \frac{\partial \varphi_3}{\partial N},$$

$$u_3 = m_1 n_1^{-1/2}\frac{\partial \varphi_1}{\partial z_1} + m_2 n_2^{-1/2}\frac{\partial \varphi_1}{\partial z_2}.$$

For incompressible bodies, we have the following expression for the scalar p':

$$p = \lambda_1^{-1}q_1^{-1}\left\{\left[\kappa'_{1111} - \lambda_1 q_1 \lambda_3^{-1} q_3^{-1}(\kappa'_{1133} + \kappa'_{1313})\right]\Delta_1 + \kappa'_{3113}\frac{\partial^2}{\partial y_3^2}\right\}(\varphi_1 + \varphi_2).$$

If the roots of the characteristic equation are equal ($n_1 = n_2$), then introducing new functions $\Psi = -\varphi_3$, $\chi = \chi_{(2)} + y_3\chi_{(3)}$, $\partial\chi_{(2)} / \partial y_3 = -\varphi_1$, $\chi_{(3)} = -\varphi_2$, $\varphi = -(\varphi_1 + \varphi_2)$: $F = -\partial\varphi_2 / \partial z_1$, $\Phi \equiv \partial\varphi / \partial z_1$, we obtain the following expressions for the displacements:

$$u_N = -\frac{\partial \varphi}{\partial N} - z_1\frac{\partial F}{\partial N} - \frac{\partial \varphi_3}{\partial S}, \quad u_S = -\frac{\partial \varphi}{\partial S} - z_1\frac{\partial F}{\partial S} + \frac{\partial \varphi_3}{\partial N},$$

$$u_3 = n_1^{-1/2}(m_1 - m_2 + 1)F - m_1 n_1^{-1/2}\frac{\partial \varphi}{\partial z_1} - m_1 n_1^{-1/2} z_1\frac{\partial F}{\partial z_1}$$

where φ, F, Φ, φ_3 are harmonic functions.

In a circular cylindrical coordinate system r, θ, y_3, the general solutions for unequal roots of the characteristic equation are represented as

$$u_r = \frac{\partial(\varphi_1+\varphi_2)}{\partial r} - \frac{1}{r}\frac{\partial\varphi_3}{\partial\theta}, \qquad u_\theta = \frac{1}{r}\frac{\partial(\varphi_1+\varphi_2)}{\partial\theta} + \frac{\partial\varphi_3}{\partial r}, \qquad u_3 = \frac{m_2}{\sqrt{n_1}}\frac{\partial\varphi_1}{\partial z_1} + \frac{m_2}{\sqrt{n_2}}\frac{\partial\varphi_2}{\partial z_2},$$

$$Q'_{33} = C_{44}\left[d_1 l_1 \frac{\partial^2}{\partial z_1^2}\varphi_1 + d_2 l_2 \frac{\partial^2}{\partial z_2^2}\varphi_2\right],$$

$$Q'_{3r} = C_{44}\left\{d_1 n_1^{-1/2}\frac{\partial^2}{\partial r\partial z_1}\varphi_1 + d_2 n_2^{-1/2}\frac{\partial^2}{\partial r\partial z_2}\varphi_2 - n_3^{-1/2}\frac{1}{r}\frac{\partial^2}{\partial\theta\partial z_3}\varphi_3\right\},$$

$$Q'_{3\theta} = C_{44}\left\{d_1 n_1^{-1/2}\frac{1}{r}\frac{\partial^2}{\partial\theta\partial z_1}\varphi_1 + d_2 n_2^{-1/2}\frac{1}{r}\frac{\partial^2}{\partial\theta\partial z_2}\varphi_2 + n_3^{-1/2}\frac{\partial^2}{\partial r\partial z_3}\varphi_3\right\}. \tag{2.77}$$

The parameters appearing in (2.77) are defined by

$$C_{44} = \omega'_{1313}, \qquad m_j = (\omega'_{1111}n_j - \omega'_{3113})(\omega'_{1133} + \omega'_{1313})^{-1},$$

$$d_j = 1 + m_j, \qquad l_j = (\omega'_{3333}m_j - \omega'_{1133}n_j)n_j^{-1}(1+m_j)^{-1}\omega'_{1313}, \qquad j = 1, 2, \tag{2.78}$$

for compressible bodies and

$$C_{44} = \kappa'_{1313}, \qquad m_j = \lambda_1 q_1 \lambda_3^{-1} q_3^{-1} n_j, \qquad d_j = 1 + m_j,$$

$$l_j = \kappa'^{-1}_{1313} n_j^{-1}(1+m_j)^{-1}[\kappa'_{3333}m_j + n_j(\lambda_1^{-1}q_1^{-1}\lambda_3 q_3 \kappa'_{1111} - \kappa'_{1313} - 2\kappa'_{1133}) - \lambda_1^{-1}q_1^{-1}\lambda_3 q_3 \kappa'_{3113}],$$

$$j = 1, 2, \tag{2.79}$$

for incompressible bodies.

For equal roots of the characteristic equation, the general solutions have the form

$$u_r = -\frac{\partial\varphi}{\partial r} - z_1\frac{\partial F}{\partial r} - \frac{1}{r}\frac{\partial\varphi_3}{\partial\theta}, \qquad u_\theta = -\frac{1}{r}\frac{\partial\varphi}{\partial\theta} - z_1\frac{1}{r}\frac{\partial F}{\partial\theta} + \frac{\partial\varphi_3}{\partial r},$$

$$u_3 = (m_1 - m_2 + 1)n_1^{-1/2}F - m_1 n_1^{-1/2}\Phi - m_1 n_1^{-1/2}\frac{\partial F}{\partial z_1},$$

$$Q'_{33} = C_{44}\left\{(d_1 l_1 - d_2 l_2)\frac{\partial F}{\partial z_1} - d_1 l_1 \frac{\partial\Phi}{\partial z_1} - d_1 l_1 z_1 \frac{\partial^2 F}{\partial z_1^2}\right\},$$

$$Q'_{3r} = C_{44}\left\{n_1^{-1/2}\frac{\partial}{\partial r}\left[(d_1 - d_2)F - d_1\Phi\right] - n_1^{-1/2}d_1 z_1 \frac{\partial^2 F}{\partial r\partial z_1} - n_3^{-1/2}\frac{1}{r}\frac{\partial^2\varphi_3}{\partial\theta\partial z_3}\right\},$$

$$Q'_{3\theta} = C_{44}\left\{n_1^{-1/2}\frac{1}{r}\frac{\partial}{\partial\theta}\left[(d_1 - d_2)F - d_1\Phi\right] - n_1^{-1/2}d_1 z_1 \frac{1}{r}\frac{\partial^2 F}{\partial\theta\partial z_1} + n_3^{-1/2}\frac{\partial^2\varphi_3}{\partial r\partial z_3}\right\}, \tag{2.80}$$

where C_{44}, m_1, l_1, d_j, $j = 1, 2$, are parameters determined from (2.78) and (2.79) for compressible and incompressible bodies, respectively; m_2 and l_2 are parameters given by

$$m_2 = (\omega'_{1133} - \omega'_{1313})(\omega'_{1133} + \omega'_{1313})^{-1},$$

$$l_2 = \left[\omega'_{3333}(m_1 + m_2 - 1) - \omega'_{1133} n_1\right] n_1^{-1}(1 + m_2)^{-1}\omega'^{-1}_{1313} \tag{2.81}$$

for compressible bodies and

$$m_2 = 1,$$

$$l_2 = (2n_1\kappa'_{1313})^{-1}[\kappa'_{3333} m_1 + n_1(\lambda_1^{-1} q_1^{-1}\lambda_3 q_3 \kappa'_{1111} - \kappa'_{1313} - 2\kappa'_{1133}) - 3\lambda_1^{-1} q_1^{-1}\lambda_3 q_3 \kappa'_{3113}] \tag{2.82}$$

for incompressible bodies.

The values of the parameters in (2.77) and (2.80) for some materials are given below:

a material with harmonic potential (2.47) (compressible body; equal roots):

$$\lambda_3 = 1 - 2\nu(1-\nu)^{-1}, \quad n_1 = n_2 = \lambda_3^2 / \lambda_1^2, \quad n_3 = 2\lambda_3^2 (2\lambda_1 - \lambda_3)^{-1}(\lambda_1 + \lambda_3)^{-1},$$

$$m_1 = \lambda_3 / \lambda_1, \quad m_2 = \frac{\nu\lambda_1 + (3\nu - 1)\lambda_3}{\nu\lambda_1 + (1-\nu)\lambda_3}, \quad l_1 = \frac{\lambda_1}{\lambda_3}, \quad l_2 = \frac{1 + \nu + (\nu - 2)\lambda_1}{2\nu\lambda_3},$$

$$d_1 = 1 + \frac{\lambda_3}{\lambda_1}, \quad d_2 = \frac{2\nu(\lambda_1 + \lambda_3)}{\nu\lambda_1 + (1-\nu)\lambda_3}, \quad C_{44} = \frac{2\mu\lambda_3}{\lambda_1(\lambda_1 + \lambda_3)}, \tag{2.83}$$

where $\nu = \lambda / (2(\lambda + \mu))$ is Poisson's ratio;

a material with Bartenev–Khazanovich potential (2.48) (incompressible body; equal roots):

$$\lambda_3 = \lambda_1^{-2}, \quad n_1 = n_2 = \lambda_1^{-3}, \quad n_3 = 2\lambda_1^{-6}(\lambda_1^{-3} + 1)^{-1}, \quad m_1 = \lambda_1^{-3}, \quad m_2 = 1,$$

$$l_1 = \lambda_1^3, \quad l_2 = (1 - \lambda_1^3)/2, \quad d_1 = \lambda_1^{-3} + 1, \quad d_2 = 1, \quad C_{44} = 2\mu\lambda_1^{-2}(1 + \lambda_1^3)^{-1}, \tag{2.84}$$

a material with Treloar potential (2.49) (incompressible body; unequal roots):

$$\lambda_3 = \lambda_1^{-2}, \quad n_1 = \lambda_1^{-6}, \quad n_2 = 1, \quad n_3 = \lambda_1^{-6}, \quad m_1 = \lambda_1^{-6}, \quad m_2 = 1,$$

$$l_1 = \frac{2\lambda_1^6}{1 + \lambda_1^6}, \quad l_2 = \frac{1}{2}(1 + \lambda_1^6), \quad d_1 = 1 + \lambda_1^{-6}, \quad d_2 = 2, \quad C_{44} = 2c_{10}\lambda_1^{-4}, \tag{2.85}$$

a composite material modeled by a transversely isotropic body, (2.52)–(2.54):

$$n_{1,2} = \frac{1}{2}(\mu_{13} + \sigma_{11}^0)^{-1}(A_{11} + \sigma_{11}^0)^{-1}\Big\{(A_{11}A_{33} + \sigma_{11}^0 A_{33} + \sigma_{11}^0\mu_{13} - 2A_{13}\mu_{13} - A_{13}^2)$$

$$\pm\sqrt{(A_{11}A_{33} + \sigma_{11}^0 A_{33} + \sigma_{11}^0\mu_{13} - 2A_{13}\mu_{13} - A_{13}^2)^2 - 4(A_{11} + \sigma_{11}^0)(\mu_{13} + \sigma_{11}^0)\mu_{13}A_{33}}\Big\},$$

$$n_3 = \mu_{13}(\mu_{12} + \sigma_{11}^0)^{-1}, \quad m_j = [(A_{11} + \sigma_{11}^0)n_j - \mu_{13}](A_{13} + \mu_{13})^{-1}, \quad d_j = 1 + m_j,$$

$$l_j = [n_j(A_{11}A_{33} + \sigma_{11}^0 A_{33} - A_{13}^2 - A_{13}\mu_{13}) - A_{33}\mu_{13}][n_j(A_{11} + \sigma_{11}^0) + A_{13}]^{-1} n_j^{-1}\mu_{13}^{-1},$$

$$C_{44} = \mu_{13} \quad (j = 1, 2) \tag{2.86}$$

$$\Big(A_{11} = E_1(1 - \nu_{13}\nu_{31})A^{-1}, \quad A_{13} = E_1\nu_{31}(1 + \nu_{12})A^{-1}, \quad A_{33} = E_3(1 - \nu_{12}^2)A^{-1}, \quad \mu_{12} = G_{12},$$

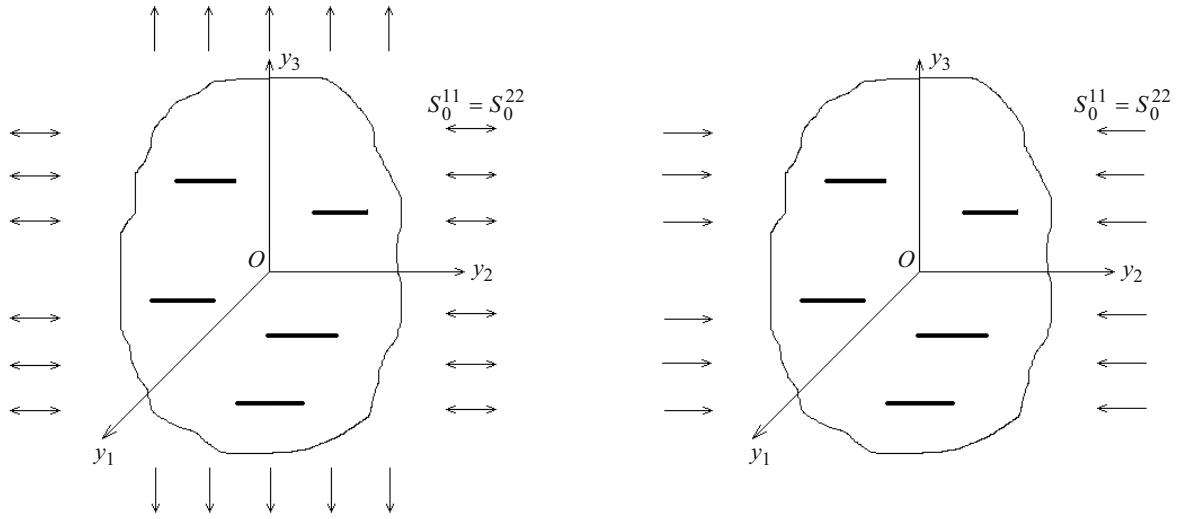

a *b*

Fig. 8

$$\mu_{13} = G_{13}, \quad A = 1 - \nu_{12}^2 - 2\nu_{13}\nu_{31} - 2\nu_{12}\nu_{13}\nu_{31}, \quad \sigma_{11}^0 = E_1(\lambda_1 - 1)(1 - \nu_{12})^{-1} G_{13}^{-1} \Big).$$

2.4. Formulation of Spatial Linearized Problems of the Fracture of Materials under Loads Acting along Cracks and General Methods to Solve Them. To formulate problems, we will use coordinates of the initial stress–strain state y_j, $j = \overline{1, 3}$, which are related by (2.61) to the Cartesian coordinates of the undeformed state. Cracks are modeled by mathematical cuts of zero thickness, as in classical fracture mechanics [135].

Two classes of problems are considered:

(i) determination and analysis of the stress–strain state of a cracked elastic body with prestresses $S_0^{11} = S_0^{22}$ acting in parallel to crack planes (Fig. 8*a*) and

(ii) determination of the critical loads for a cracked material compressed along parallel cracks (Fig. 8*b*).

The general problem formulation is as follows. Consider elastic isotropic materials with arbitrary elastic potential or composite materials with elastic components containing cracks in parallel planes $y_3 = \text{const}$. The cracks in the composite materials are assumed much larger than their structural elements, and only fracture processes are studied in which composites do not manifest themselves as piecewise-homogeneous materials. With such assumptions, it is possible to model a composite by a transversely isotropic continuum with effective characteristics and isotropy planes parallel to the crack planes (see Sec. 2.2).

The initial normal stresses act along the planes in which cracks are located; the prestresses are zero on these planes. In this case, the initial stress–strain state is homogeneous and defined by (2.62) and (2.71). The perturbations of the initial stress–strain state that are generated by additional (to the initial stresses) loads (the normal stresses Q'_{33} are presented in Fig. 8*a* as an example) are assumed much smaller than the initial stress–strain state, which allows using TDLSM.

Thus, it is necessary to find the exact solution to the linearized equilibrium equations for displacements (2.67), (2.68). In the general case, the boundary conditions on the crack faces are

$$Q'_{3j} = P'_j, \quad y_k \in S_1, \tag{2.87}$$

where S_1 denotes the domains occupied by the cracks. For problems of compression along cracks, it is necessary to set $P'_j \equiv 0$ in the boundary conditions (2.87). These conditions should be supplemented with the boundary conditions for the stresses and/or displacements on the surface of the material (for finite bodies) and the conditions of regularity (decay) of the stress and displacement fields at infinity (for infinite bodies). The above general problem formulation is specified for each system of forces and arrangement of cracks.

We will use the following procedure to solve the spatial linearized problems formulated. The general solutions (2.77), (2.80) of the linearized equilibrium equations are used to reduce the boundary conditions for problems originally formulated for

stresses and displacements to boundary-value problems for unknown harmonic potential functions ($\varphi_1, \varphi_2, \varphi_3$ for unequal roots and $\varphi, F, \Phi, \varphi_3$ for equal roots of the characteristic equation). Next, the unknown harmonic potential functions are expanded into Fourier series in the circumferential coordinate with coefficients in the form of Hankel transforms in the radial coordinate of the order corresponding to the harmonic for nonaxisymmetric problems and in the form of Hankel transforms in the radial coordinate of zero order for axisymmetric problems. The boundary conditions on the plane $y_3 = \text{const}$ allow reducing the number of unknown functions in the Hankel transforms by the number of conditions. The remaining boundary conditions lead to a system of dual integral equations for the unknown functions appearing in the Hankel transforms.

The next stage is to solve the system of dual integral equations by reducing them to Schlomilch's integral equations by the substitution method [50]. Solving the Schlomilch equations, we obtain a closed-form solution of the problem in terms of potential functions (for isolated cracks in an infinite body) or governing inhomogeneous Fredholm equations of the second kind (for interacting cracks). This procedure is applied separately to the cases of equal and unequal roots of the characteristic equation.

Using the solutions for the harmonic potential functions, we can find the distribution of stresses and displacements in the material and derive the expressions for the stress intensity factors and crack opening displacements by analyzing the asymptotic stress distribution near the crack. The stress intensity factors, as in classical fracture mechanics without prestresses [135], are the coefficients of the singularities in the distribution of stresses near the crack.

$$K_I = \lim_{r_1 \to 0} \sqrt{2\pi r_1}\, Q'_{33},$$

$$K_{II} = \lim_{r_1 \to 0} \sqrt{2\pi r_1}\, Q'_{3r},$$

$$K_{III} = \lim_{r_1 \to 0} \sqrt{2\pi r_1}\, Q'_{3\theta}, \tag{2.88}$$

where r_1 is the distance from the crack tip.

According to the combined approach described in Sec. 1.4, the critical compressive loads that cause local buckling of the material near the crack are determined by numerically solving the above-mentioned inhomogeneous linearized problems of the fracture of prestressed bodies to find the initial compressive stresses at which the stress–strain state and the stress intensity factors change abruptly (resonantly) near the crack. There is no need to additionally solve eigenvalue problems using the three-dimensional linearized theory of stability.

The generality of the above formulation of linearized problems for different material models is determined by the following aspects [24, 28]. The initial stress–strain state is statically determinate and homogeneous. The general solutions of the linearized equilibrium equations (2.77), (2.80) for homogeneous initial states are formally represented in a universal form for different material models (compressible and incompressible hyperelastic materials with arbitrary elastic potential, composite materials). The coefficients appearing in the general solutions depend on the material model. The chosen model is specified at the final stage at which the governing equations obtained in general form are solved. We will use the theory of finite (higher) initial deformations to study hyperelastic bodies and the second theory of small initial deformations to study composite materials, determining their initial stress–strain state with the geometrically linear theory.

Thus, a single general approach can be used to solve linearized boundary-value problems of the fracture of materials with initial (residual) stresses acting in parallel to crack planes and the fracture of bodies compressed along cracks, for various material models.

2.5. Failure Criteria for Materials under Loads Acting along Cracks. Following [23, 28, 34], we will briefly discuss brittle-fracture criteria that allow for the effect of initial (residual) stresses acting along cracks on the critical loads and generalize the Griffith and Irwin criteria and discuss a failure criterion for bodies compressed along cracks.

Failure Criteria for Bodies with Prestresses Acting along Cracks. To determine the critical loads for prestressed bodies, it was proposed in [23, 28, 87, 88] to use an energy failure corresponding to the Griffith–Irwin criterion [80, 130] for materials without prestresses and a stress-based criterion corresponding to the Irwin criterion [131] for materials without prestresses.

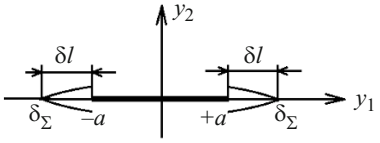

Fig. 9

Consider a crack located in the plane y_1Oy_3 (y_j, $j=\overline{1,3}$, are the Cartesian coordinates of the initial state induced by the prestresses) and occupying the domain ($|y_1|<a$, $y_2=0$, $-\infty<y_3<+\infty$) (Fig. 9). According to the energy criterion [80], fracture begins when

$$\delta U_0+\delta A^{(e)}_{\delta\Sigma}=0, \tag{2.89}$$

where $\delta\Sigma=2\delta l$ is the change in the surface area of the crack per unit length of the Oy_3-axis; U_0 is the internal energy determined by the surface energy; $\delta A^{(e)}_{\delta\Sigma}$ is the energy flow to the crack tip related to the decrease in the strain energy with increase in the crack length by δl (U_0 and $\delta A^{(e)}_{\delta\Sigma}$ are normalized to length along the Oy_3-axis).

The change of the surface energy is expressed as

$$\delta U_0=\gamma d\Sigma=2\delta l,$$

where γ is the surface energy density. In the classical fracture mechanics of materials without prestresses, it is usually assumed that $\gamma=\text{const}$ [53, 80]. In the mechanics of brittle fracture of prestressed materials, it is, apparently, necessary to assume that, generally, γ depends on the prestresses.

The energy flow to the crack tip $\delta A^{(e)}_{\delta\Sigma}$ is determined by the stresses applied along the imaginary continuation of the crack. For example, in the case of uniaxial tension, we have the following energy flow at infinity of the Oy_2-axis [23, 28]:

$$\delta A^{(e)}_{\delta\Sigma}=-\int_0^{\delta l}(Q'_{22}u_2+Q'_{21}u_1+Q'_{23}u_3)\,dx,$$

where Q'_{ij} and u_j are determined by the initial and additional loads resulting from the solution of linearized problems. On the crack line, we have

$$Q'_{22}=\frac{1}{\sqrt{2\pi r_1}}K_I,$$

$$Q'_{21}=\frac{1}{\sqrt{2\pi r_1}}K_{II},$$

$$Q'_{23}=\frac{1}{\sqrt{2\pi r_1}}K_{III}, \tag{2.90}$$

where r_1 is the distance from the crack tip; K_I, K_{II}, and K_{III} are the stress intensity factors resulting from the solution of linearized problems. Thus, criterion (2.89) is related to the factors K_I, K_{II}, K_{III} and the surface energy density γ. Taking (2.90) into account, we will consider criterion expressions (2.89) for some materials in the problem formulation under consideration.

Material with Bartenev–Khazanovich potential (incompressible body; the parameters are determined from (2.48), (2.84)). For this material, the failure criterion follows from (2.89), (2.90) [23, 28]:

$$(K_I^2+\lambda_1^2K_{II}^2)\frac{\lambda_1^2}{3\lambda_1^2-1}+K_{III}^2\,\frac{1+\lambda_1}{2\lambda_1}=4\mu\gamma. \tag{2.91}$$

If there are no prestresses ($\lambda_1 = 1$), expression (2.91) becomes

$$K_I^2 + K_{II}^2 + 2K_{III}^2 = 8\mu\gamma, \tag{2.92}$$

which coincides with the classical Griffith–Irwin criterion for materials without prestresses [53] if $\mu = E/3$ and $\nu = 1/2$ for incompressible bodies.

Material with Treloar potential (incompressible body; the parameters are determined from (2.49), (2.85)). For this material, the failure criterion is as follows [23, 28]:

$$(K_I^2 + \lambda_1^2 K_{II}^2)\frac{\lambda_1^2(\lambda_1^2+1)}{\lambda_1^6 + \lambda_1^4 + 3\lambda_1^2 - 1} + K_{III}^2 = 8c_{10}\gamma, \tag{2.93}$$

which coincides with the classical criterion (2.92) if $2c_{10} = \mu = E/3$.

For different types of cracks in prestressed materials, simplest stress-based failure criteria can be represented as follows [23, 28]:

$$K_I = K_{Ic}, \quad K_{II} = K_{IIc}, \quad K_{III} = K_{IIIc}, \tag{2.94}$$

where $K_{Ic}, K_{IIc}, K_{IIIc}$ are the critical stress intensity factors for prestressed materials, which are determined experimentally and, in the general case, depend on the prestresses.

Failure Criterion for Materials Compressed along Cracks. The classical Griffith–Irwin failure criteria are inapplicable to bodies compressed along cracks (see Sec. 1.3). According to the criterion proposed in [23, 33, 83, 84] based on the three-dimensional linearized theory of stability of deformable bodies, fracture of a body with cracks begins with local buckling of the material near the cracks.

In this connection, the theoretical ultimate compressive strength for the fracture mechanism under consideration is the stresses (or the shortening along the coordinate axes) induced by the critical compressive load causing local buckling around cracks [112].

3. Results for Specific Classes of Spatial Problems. Here we will discuss results obtained with the combined approach applied to nonaxisymmetric and axisymmetric spatial problems of the fracture of materials loaded along cracks for the following arrangements of cracks: isolated internal crack in an unbounded body; an internal near-surface crack parallel to the boundary of the half-space; two parallel internal cracks in an unbounded body; a periodic array of internal parallel coaxial cracks in an unbounded body.

The solutions found were used to analyze the asymptotic stress distribution near crack tips and to derive expressions for the stress intensity factors for such material models as hyperelastic materials with Bartenev–Khazanovich, Treloar, or harmonic potential and composite materials (composite laminates with isotropic plies and composites reinforced with short ellipsoidal fibers). The combined approach described in Sec. 1.4 was used to determine, for these materials, the critical compressive loads that cause local buckling near cracks. The effect of the initial stresses, geometrical parameters (the crack radius and the distance between cracks or between the crack and the surface of the material), and material characteristics on the stress intensity factors and critical compressive loads was analyzed.

3.1. Isolated Penny-Shaped Crack in an Unbounded Material. We will discuss spatial problems for an unbounded material containing a penny-shaped crack of radius a. Equal initial (residual) stresses $S_0^{11} = S_0^{22}$ act along the Oy_1- and Oy_2-axes (Fig. 10) and induce a homogeneous initial stress–strain state ((2.62), (2.71) (hereafter, we use the Lagrangian coordinates y_j, $j = \overline{1,3}$, of the initial stress–strain states and the circular cylindrical coordinates r, θ, y_3 or r, θ, z_j, where $z_j = n_j^{-1/2} y_3$, $j = \overline{1,3}$, derived from them).

We will separately consider nonaxisymmetric and axisymmetric problems for mode I cracks and for mode II and III cracks. As an example, we will detail the procedure for solving a nonaxisymmetric problem for a mode I crack. The other problems are solved in a similar way.

3.1.1. Nonaxisymmetric Problem for a Mode I Crack. A mode I crack, as in the fracture mechanics of materials without prestresses [53, 135], is a crack to which a normal load $\sigma(r, \theta)$ is applied symmetrically about the plane $y_3 = 0$. Since the

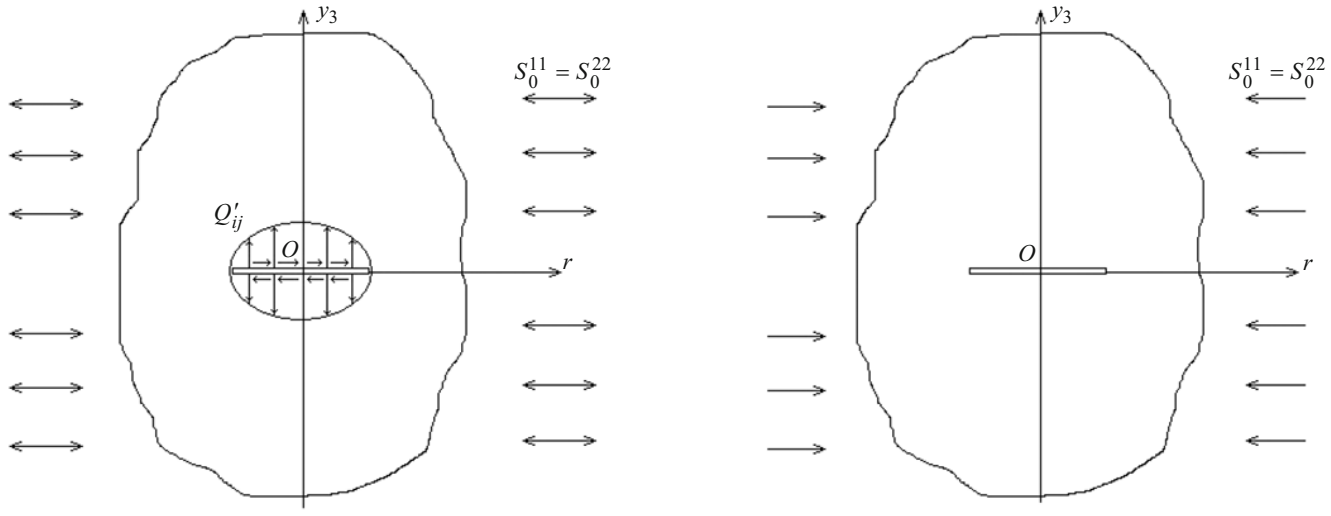

a *b*

Fig. 10

geometry and system of forces of the problem are symmetric, we have the following boundary conditions on the boundary $y_3 = 0$ of the upper half-space $y_3 \geq 0$:

$$Q'_{33}(r, \theta, 0) = -\sigma(r, \theta), \quad Q'_{3r}(r, \theta, 0) = Q'_{3\theta}(r, \theta, 0) = 0 \quad (0 \leq r \leq a),$$
$$u_3(r, \theta, 0) = 0, \quad Q'_{3r}(r, \theta, 0) = Q'_{3\theta}(r, \theta, 0) = 0 \quad (a < r < \infty), \tag{3.1}$$

(hereafter $0 \leq \theta \leq 2\pi$).

If an unbounded body is compressed along an internal penny-shaped crack (Fig. 10*b*), the boundary conditions on the crack faces are the following (the first row in (3.1)):

$$Q'_{33}(r, \theta, 0) = 0, \quad Q'_{3r}(r, \theta, 0) = Q'_{3\theta}(r, \theta, 0) = 0 \quad (0 \leq r \leq a).$$

We will separately consider the cases of equal and unequal roots of the characteristic equation (see Sec. 2.3) in common form for compressible and incompressible bodies. Using the general solutions (2.77), (2.80) of the linearized equilibrium equations, we represent the boundary conditions (3.1) in terms of potential functions. According to (3.1), the components Q'_{3r} and $Q'_{3\theta}$ of the stress tensor are equal to zero on the plane $y_3 = 0 (z_j = 0, j = \overline{1,3})$. We have

$$C_{44}\left(d_1 l_1 \frac{\partial^2 \varphi_1}{\partial z_1^2} + d_2 l_2 \frac{\partial^2 \varphi_2}{\partial z_2^2} \right) = -\sigma(r, \theta) \quad (r \leq a),$$

$$C_{44}\left(d_1 n_1^{-1/2} \frac{\partial^2 \varphi_1}{\partial r \partial z_1} + d_2 n_2^{-1/2} \frac{\partial^2 \varphi_2}{\partial r \partial z_2} - n_3^{-1/2} \frac{1}{r} \frac{\partial^2 \varphi_3}{\partial r \partial z_3} \right) = 0 \quad (0 \leq r < \infty),$$

$$C_{44}\left(d_1 n_1^{-1/2} \frac{1}{r} \frac{\partial^2 \varphi_1}{\partial \theta \partial z_1} + d_2 n_2^{-1/2} \frac{1}{r} \frac{\partial^2 \varphi_2}{\partial \theta \partial z_2} + n_3^{-1/2} \frac{\partial^2 \varphi_3}{\partial r \partial z_3} \right) = 0 \quad (0 \leq r < \infty),$$

$$m_1 n_1^{-1/2} \frac{\partial \varphi_1}{\partial z_1} + m_2 n_2^{-1/2} \frac{\partial \varphi_1}{\partial z_2} = 0 \quad (r > a) \tag{3.2}$$

for unequal roots and

$$C_{44}\left[(d_1 l_1 - d_2 l_2)\frac{\partial F}{\partial z_1} - d_1 l_1 \frac{\partial \Phi}{\partial z_2}\right] = -\sigma(r,\theta) \qquad (r \le a),$$

$$C_{44}\left\{n_1^{-1/2}\frac{\partial}{\partial r}\left[(d_1 - d_2)F - d_1\Phi\right] - n_3^{-1/2}\frac{1}{r}\frac{\partial^2 \varphi_3}{\partial\theta\partial z_3}\right\} = 0 \qquad (0 \le r < \infty),$$

$$C_{44}\left\{n_1^{-1/2}\frac{1}{r}\frac{\partial}{\partial\theta}\left[(d_1 - d_2)F - d_1\Phi\right] + n_3^{-1/2}\frac{1}{r}\frac{\partial^2 \varphi_3}{\partial r\partial z_3}\right\} = 0 \qquad (0 \le r < \infty),$$

$$(m_1 - m_2 + 1)n_1^{-1/2}F - m_1 n_1^{-1/2}\Phi = 0 \qquad (r > a) \tag{3.3}$$

for equal roots.

Next, we will consider only the case of unequal roots because the derivations for equal roots are similar.

The normal load on the crack faces $\sigma(r,\theta)$ is expanded into a Fourier series in the circumferential coordinate θ:

$$\sigma(r,\theta) = \sum_{n=0}^{\infty} \sigma_1^{(n)}(r)\cos n\theta,$$

$$\sigma_1^{(0)}(r) = \frac{1}{\pi}\int_0^{\pi} \sigma(r,\theta)d\theta,$$

$$\sigma_1^{(n)}(r) = \frac{2}{\pi}\int_0^{\pi} \sigma(r,\theta)\cos n\theta\, d\theta. \tag{3.4}$$

Expressions (3.4) represent the case where the function $\sigma(r,\theta)$ is even in θ. If this function is odd in the circumferential coordinate, expression (3.4) should be replaced by

$$\sigma(r,\theta) = \sum_{n=1}^{\infty} \sigma_2^{(n)}(r)\sin n\theta,$$

$$\sigma_2^{(n)}(r) = \frac{2}{\pi}\int_0^{\pi} \sigma(r,\theta)\sin n\theta\, d\theta. \tag{3.5}$$

All the other derivations are similar. In the general case, it is necessary to use a superposition of (3.4) and (3.5).

The harmonic potential functions φ_j, $j = \overline{1,3}$, appearing in (3.2) are also expanded into Fourier series in the coordinate θ with coefficients in the form of Hankel transforms in the radial coordinate r of order equal to the order of the circumferential harmonic:

$$\varphi_1(r,\theta,z_1) = \sum_{n=0}^{\infty}\cos n\theta\int_0^{\infty} A_n(\lambda)e^{-\lambda z_1}J_n(\lambda r)\frac{d\lambda}{\lambda},$$

$$\varphi_2(r,\theta,z_2) = \sum_{n=0}^{\infty}\cos n\theta\int_0^{\infty} B_n(\lambda)e^{-\lambda z_2}J_n(\lambda r)\frac{d\lambda}{\lambda},$$

$$\varphi_3(r,\theta,z_3) = \sum_{n=0}^{\infty}\sin n\theta\int_0^{\infty} C_n(\lambda)e^{-\lambda z_3}J_n(\lambda r)\frac{d\lambda}{\lambda}, \tag{3.6}$$

where the perturbations of stresses and displacements decay with distance from the crack.

Substituting (3.6) into the second and third equations in (3.2) defined on the plane $y_3 = 0$, we obtain

$$A_n = -\frac{d_2 n_2^{-1/2}}{d_1 n_1^{-1/2}} B_n, \quad C_n = 0. \tag{3.7}$$

Substituting (3.7) into the first and fourth equations in (3.2), we get

$$\sum_{n=0}^{\infty} \cos n\theta \left[D^{(1)} \int_0^{\infty} B_n(\lambda) J_n(\lambda r) \lambda d\lambda - \sigma_1^{(n)}(r) \right] = 0, \qquad r \le a,$$

$$\sum_{n=0}^{\infty} \cos n\theta \, D^{(2)} \int_0^{\infty} B_n(\lambda) J_n(\lambda r) \lambda d\lambda = 0, \qquad r > a \tag{3.8}$$

$$\left(D^{(1)} = C_{44} k d_2 \sqrt{n_1}, \quad D^{(2)} = d_2 n_2^{-1/2} (m_1 d_1^{-1} - m_2 d_2^{-1}), \right.$$

$$\left. k = k_1 - k_2, \quad k_1 = l_1 n_2^{-1/2}, \quad k_2 = l_2 n_1^{-1/2} \right). \tag{3.9}$$

As the coefficients of the harmonics $\cos n\theta$ are equated to zero, Eqs. (3.8) decompose into dual integral equations for each nth harmonic in θ:

$$D^{(1)} \int_0^{\infty} B_n(\lambda) J_n(\lambda r) \lambda d\lambda = \sigma_1^{(n)}(r), \qquad r \le a, \qquad n = 0, 1, 2, \ldots,$$

$$D^{(2)} \int_0^{\infty} B_n(\lambda) J_n(\lambda r) \lambda d\lambda = 0, \qquad r > a, \qquad n = 0, 1, 2, \ldots. \tag{3.10}$$

It is expedient to solve the system of dual integral equations (3.10) by the substitution method [50], representing the unknown functions $B_n(\lambda)$ $(n = 0, 1, 2, \ldots)$ in the form

$$B_n(\lambda) = \sqrt{\pi\lambda / 2} \int_0^a \sqrt{t} \, \omega_n(t) J_{n+1/2}(\lambda t) dt, \tag{3.11}$$

where $\omega_n(t)$ $(n = 0, 1, 2, \ldots)$ are unknown functions continuous together with their first derivatives on the interval $[0, a]$.

Using the expression of the discontinuous Weber–Schafheitlin integral

$$\int_0^{\infty} \sqrt{\lambda} J_n(\lambda r) J_{n+1/2}(\lambda t) d\lambda = \begin{cases} 0, & 0 \le t < r, \\ \dfrac{\sqrt{2} r^n}{\sqrt{\pi} t^{n+1/2} \sqrt{t^2 - r^2}}, & 0 \le r < t \end{cases} \tag{3.12}$$

we see that the second equation in (3.10) (valid for $r > a$) holds identically.

Next, substituting expression (3.11) into the first equation (3.10) and using the formulas

$$\lambda J_n(\lambda r) = r^{-n-1} \frac{d}{dr} \left[r^{n+1} J_{n+1}(\lambda r) \right],$$

$$\int_0^{\infty} \sqrt{\lambda} J_{n+1}(\lambda r) J_{n+1/2}(\lambda t) d\lambda = \begin{cases} 0, & 0 \le r < t, \\ \dfrac{\sqrt{2} t^{n+1/2}}{\sqrt{\pi} r^{n+1} \sqrt{r^2 - t^2}}, & 0 \le t < r \end{cases} \tag{3.13}$$

we obtain

$$\frac{d}{dr}\int_0^r \frac{t^{n+1}}{\sqrt{r^2-t^2}}\,\omega_n(t)dt = r^{n+1}\,\frac{\sigma_1^{(n)}(r)}{D^{(1)}}.$$

Integrating the last equation over r from 0 to r and substituting $t = r\sin\theta$ into it, we arrive at the Schlomilch equation

$$\int_0^{\pi/2} r^{n+1}(\sin\theta)^{n+1}\,\omega_n(r\sin\theta)d\theta = \frac{1}{D^{(1)}}\int_0^r \rho^{n+1}\sigma_1^{(n)}(\rho)d\rho,$$

which has the following solution [50]:

$$\omega_n(x) = \frac{2x}{\pi D^{(1)}}\int_0^{\pi/2}(\sin\theta)^{n+1}\,\sigma_1^{(n)}(x\sin\theta)d\theta. \tag{3.14}$$

Substituting (3.14) into (3.11) and taking (3.7) into account, we obtain the following expressions for the functions A_n, B_n, C_n in (3.6):

$$A_n(\lambda) = -\sqrt{\frac{2}{\pi}}\,\frac{\sqrt{\lambda}}{C_{44}kd_1\sqrt{n_2}}\int_0^a J_{n+1/2}(\lambda t)\frac{dt}{t^{n-1/2}}\int_0^t \frac{x^{n+1}\sigma_1^{(n)}(x)dx}{\sqrt{t^2-x^2}},$$

$$B_n(\lambda) = \sqrt{\frac{2}{\pi}}\,\frac{\sqrt{\lambda}}{C_{44}kd_2\sqrt{n_1}}\int_0^a J_{n+1/2}(\lambda t)\frac{dt}{t^{n-1/2}}\int_0^t \frac{x^{n+1}\sigma_1^{(n)}(x)dx}{\sqrt{t^2-x^2}},$$

$$C_n(\lambda) = 0. \tag{3.15}$$

Using expressions (3.15), we can determine the potential harmonic functions φ_j, $j = \overline{1,3}$, from (3.6) and the distribution of stresses and displacements from (2.77). For example, in the plane $y_3 = 0$ we have

$$Q'_{33}(r,\theta,0) = -\sqrt{\frac{2}{\pi}}\sum_{n=0}^{\infty}\cos n\theta\int_0^{\infty}\left\{\int_0^a\left[\int_0^t \frac{x^{n+1}}{\sqrt{t^2-x^2}}\,\sigma_1^{(n)}(x)dx\right]t^{-n+1/2}J_{n+1/2}(\lambda t)dt\right\}\lambda^{3/2}J_n(\lambda r)d\lambda,$$

$$Q'_{3r}(r,\theta,0) = 0, \qquad Q'_{3\theta}(r,\theta,0) = 0, \tag{3.16}$$

$$u_3(r,\theta,0) = \sqrt{\frac{2}{\pi}}\,\frac{n_1^{-\frac{1}{2}}n_2^{-\frac{1}{2}}(m_1-m_2)}{C_{44}d_1d_2k}\sum_{n=0}^{\infty}\cos n\theta\int_0^{\infty}\left\{\int_0^a\left[\int_0^t \frac{x^{n+1}}{\sqrt{t^2-x^2}}\,\sigma_1^{(n)}(x)dx\right]t^{-n+\frac{1}{2}}J_{n+\frac{1}{2}}(\lambda t)dt\right\}\lambda^{\frac{1}{2}}J_n(\lambda r)d\lambda,$$

$$u_r(r,\theta,0) = \sqrt{\frac{2}{\pi}}\,\frac{d_1n_1^{-\frac{1}{2}} - d_2n_2^{-\frac{1}{2}}}{C_{44}d_1d_2k}\,\frac{\partial}{\partial r}\sum_{n=0}^{\infty}\cos n\theta\int_0^{\infty}\left\{\int_0^a\left[\int_0^t \frac{x^{n+1}}{\sqrt{t^2-x^2}}\,\sigma_1^{(n)}(x)dx\right]t^{-n+\frac{1}{2}}J_{n+\frac{1}{2}}(\lambda t)dt\right\}\lambda^{-\frac{1}{2}}J_n(\lambda r)d\lambda,$$

$$u_\theta(r,\theta,0) = -\sqrt{\frac{2}{\pi}}\,\frac{d_1n_1^{-\frac{1}{2}} - d_2n_2^{-\frac{1}{2}}}{C_{44}d_1d_2k}\sum_{n=0}^{\infty}\sin n\theta\,\frac{n}{r}\int_0^{\infty}\left\{\int_0^a\left[\int_0^t \frac{x^{n+1}}{\sqrt{t^2-x^2}}\,\sigma_1^{(n)}(x)dx\right]t^{-n+\frac{1}{2}}J_{n+\frac{1}{2}}(\lambda t)dt\right\}\lambda^{-\frac{1}{2}}J_n(\lambda r)d\lambda.$$

Performing similar derivations for the case of equal roots, we obtain the components of the stress tensor and the displacement vector in the plane $y_3 = 0$:

$$Q'_{33}(r,\theta,0)=-\sqrt{\frac{2}{\pi}}\sum_{n=0}^{\infty}\cos n\theta\int_0^{\infty}\left\{\int_0^a\left[\int_0^t\frac{x^{n+1}}{\sqrt{t^2-x^2}}\sigma_1^{(n)}(x)dx\right]t^{-n+1/2}J_{n+1/2}(\lambda t)dt\right\}\lambda^{3/2}J_n(\lambda r)d\lambda,$$

$$Q'_{3r}(r,\theta,0)=0,\qquad Q'_{3\theta}(r,\theta,0)=0, \tag{3.17}$$

$$u_3(r,\theta,0)=\sqrt{\frac{2}{\pi}}\frac{n_1^{-\frac{1}{2}}(2m_1-m_2+1)}{C_{44}d_1d_2(l_1-l_2)}\sum_{n=0}^{\infty}\cos n\theta\int_0^{\infty}\left\{\int_0^a\left[\int_0^t\frac{x^{n+1}}{\sqrt{t^2-x^2}}\sigma_1^{(n)}(x)dx\right]t^{-n+\frac{1}{2}}J_{n+\frac{1}{2}}(\lambda t)dt\right\}\lambda^{\frac{1}{2}}J_n(\lambda r)d\lambda,$$

$$u_r(r,\theta,0)=\sqrt{\frac{2}{\pi}}\frac{m_1-m_2}{C_{44}d_1d_2(l_1-l_2)}\frac{\partial}{\partial r}\sum_{n=0}^{\infty}\cos n\theta\int_0^{\infty}\left\{\int_0^a\left[\int_0^t\frac{x^{n+1}}{\sqrt{t^2-x^2}}\sigma_1^{(n)}(x)dx\right]t^{-n+\frac{1}{2}}J_{n+\frac{1}{2}}(\lambda t)dt\right\}\lambda^{-\frac{1}{2}}J_n(\lambda r)d\lambda,$$

$$u_\theta(r,\theta,0)=-\sqrt{\frac{2}{\pi}}\frac{m_1-m_2}{C_{44}d_1d_2(l_1-l_2)}\sum_{n=0}^{\infty}\sin n\theta\frac{n}{r}\int_0^{\infty}\left\{\int_0^a\left[\int_0^t\frac{x^{n+1}}{\sqrt{t^2-x^2}}\sigma_1^{(n)}(x)dx\right]t^{-n+\frac{1}{2}}J_{n+\frac{1}{2}}(\lambda t)dt\right\}\lambda^{-\frac{1}{2}}J_n(\lambda r)d\lambda.$$

As can be seen from (3.16) and (3.17), the components of the tress tensor in the crack plane are the same in the cases of unequal and equal roots and do not depend on the prestresses. The components of the displacement vector are different in the cases of unequal and equal roots and depend on the prestresses because the material parameters C_{44}, k, d_i, l_i, n_i $(i=1,2)$ depend on the coefficient of initial elongation (shortening) λ_1.

Comparing the expressions for the components of the displacement vector in (3.16), (3.17) with the respective expressions in [135, pp. 10–11] for a linear elastic body without prestresses, we can represent these components for $y_3=0$ as

$$u_3(r,\theta,0)=K^{(3)}u_3^{(0)}(r,\theta,0),$$

$$u_r(r,\theta,0)=K^{(r)}u_r^{(0)}(r,\theta,0),$$

$$u_\theta(r,\theta,0)=K^{(\theta)}u_\theta^{(0)}(r,\theta,0), \tag{3.18}$$

where $u_3(r,\theta,0)$, $u_r(r,\theta,0)$, $u_\theta(r,\theta,0)$ are the components of the displacement vector in a prestressed elastic body; $u_3^{(0)}(r,\theta,0), u_r^{(0)}(r,\theta,0), u_\theta^{(0)}(r,\theta,0)$ are the components of the displacement vector in a linear elastic body without prestresses; $K^{(3)}, K^{(r)}, K^{(\theta)}$ are coefficients describing the effect of the prestresses. We have

$$K^{(3)}=2\mu\frac{\lambda+\mu}{\lambda+2\mu}\frac{d_1-d_2}{C_{44}d_1d_2(l_1\sqrt{n_1}-l_2\sqrt{n_2})},$$

$$K^{(r)}=K^{(\theta)}=2(\lambda+\mu)\frac{d_1\sqrt{n_2}-d_2\sqrt{n_1}}{C_{44}d_1d_2(l_1\sqrt{n_1}-l_2\sqrt{n_2})} \tag{3.19}$$

for unequal roots and

$$K^{(3)}=2\mu\frac{\lambda+\mu}{\lambda+2\mu}\frac{2d_1-d_2}{C_{44}d_1d_2\sqrt{n_1}(l_1-l_2)},$$

$$K^{(r)}=K^{(\theta)}=2(\lambda+\mu)\frac{d_1-d_2}{C_{44}d_1d_2(l_1-l_2)} \tag{3.20}$$

for equal roots.

Consider the asymptotic distribution of stresses and displacements near the tip of the crack in its plane $y_3 = 0$. We introduce the following notation:

$$r = a + r_1, \quad r_1 > 0, \quad r_1 << a,$$
$$r = a - r_2, \quad r_2 > 0, \quad r_2 << a. \tag{3.21}$$

Using the first relation in (3.16) and the formula $\lambda J_{n+1/2}(\lambda t) = -t^{n-1/2} \frac{d}{dt}[t^{-n+1/2} J_{n-1/2}(\lambda t)]$, integrating the discontinuous integral (3.13) by parts, and taking into account the first relation in (3.21), we obtain

$$Q'_{33}(r, \theta, 0) = \frac{\sqrt{2}}{\pi\sqrt{r_1}} \sum_{n=0}^{\infty} \frac{\cos n\theta}{a^{n+1/2}} \int_0^a \frac{x^{n+1} \sigma_1^{(n)}(x)}{\sqrt{a^2 - x^2}} dx + O(r_1^0), \tag{3.22}$$

where $O(r_1^0)$ denotes terms that do not have singularities as $r_1 \to 0$.

Then from formulas (2.88), (3.22) and the second and third relations in (3.16), we obtain

$$K_I = \frac{2}{\sqrt{\pi}} \sum_{n=0}^{\infty} \frac{\cos n\theta}{a^{n+1/2}} \int_0^a \frac{x^{n+1} \sigma_1^{(n)}(x)}{\sqrt{a^2 - x^2}} dx, \quad K_{II} = 0, \quad K_{III} = 0, \tag{3.23}$$

where the Fourier coefficients $\sigma_1^{(n)}(x)$ $(n = 0, 1, 2, \ldots)$ are determined in terms of the normal load applied to the crack faces from the second and third relations in (3.4). The first, second, and third relations in (3.17) indicate that the SIFs in the case of equal roots are defined by (3.23).

Thus, the stress intensity factors in the nonaxisymmetric problem for a penny-shaped mode I crack in an unbounded prestressed body do not depend on the prestresses and coincide (up to notation) with those obtained by solving the nonaxisymmetric problem for a penny-shaped mode I crack in a linear elastic body without prestresses (see [135, formula (1.44)]).

If the load on the crack faces $\sigma(r, \theta)$ is an odd function in the coordinate θ, it is necessary to expand it into a Fourier series (3.5). Performing similar derivations, we obtain the following expression for the SIFs:

$$K_I = \frac{2}{\sqrt{\pi}} \sum_{n=1}^{\infty} \frac{\sin n\theta}{a^{n+1/2}} \int_0^a \frac{x^{n+1} \sigma_2^{(n)}(x)}{\sqrt{a^2 - x^2}} dx, \quad K_{II} = 0, \quad K_{III} = 0. \tag{3.24}$$

In the general case of an arbitrary normal load on the crack faces $\sigma(r, \theta)$, the SIFs are expressed as

$$K_I = \frac{2}{\sqrt{\pi a}} \sum_{n=0}^{\infty} \left[\frac{\cos n\theta}{a^n} \int_0^a \frac{x^{n+1} \sigma_1^{(n)}(x)}{\sqrt{a^2 - x^2}} dx + \frac{\sin n\theta}{a^n} \int_0^a \frac{x^{n+1} \sigma_2^{(n)}(x)}{\sqrt{a^2 - x^2}} dx \right], \quad K_{II} = 0, \quad K_{III} = 0. \tag{3.25}$$

Let us now determine the crack-tip opening displacement for $y_3 = 0$. With (3.18), (3.19), we have the following formulas in the case of unequal roots:

$$\delta = 2u_3(r_2, \theta, 0) = 2K^{(3)} u_3^{(0)} = 2\sqrt{\frac{r_2}{2\pi}} K_I \frac{\lambda + 2\mu}{2\mu(\lambda + \mu)} K^{(3)} = 2\sqrt{\frac{r_2}{2\pi}} K_I K, \tag{3.26}$$

$$\left(K = \frac{d_1 - d_2}{C_{44} d_1 d_2 (l_1\sqrt{n_1} - l_2\sqrt{n_2})} = \frac{m_1 - m_2}{C_{44}(1 + m_1)(1 + m_2)(l_1\sqrt{n_1} - l_2\sqrt{n_2})} \right). \tag{3.27}$$

Proceeding in a similar way in the case of equal roots, we obtain from (3.18) and (3.20) the crack-tip opening displacement for $y_3 = 0$ (3.26), where K characterizes the effect of the prestresses:

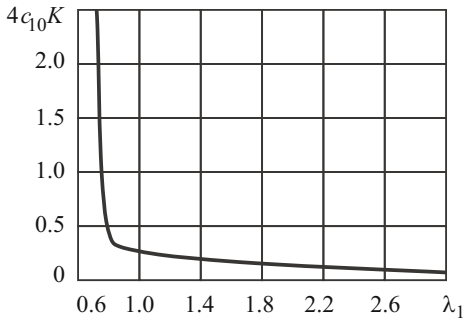

Fig. 11

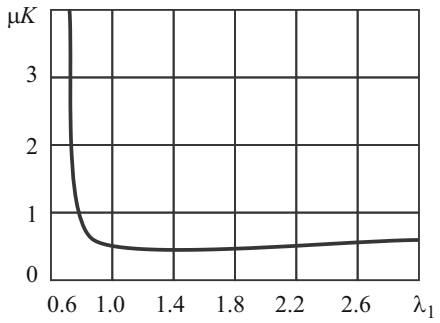

Fig. 12

$$K = \frac{2d_1 - d_2}{C_{44} d_1 d_2 \sqrt{n_1}\,(l_1 - l_2)} = \frac{1 + 2m_1 - m_2}{C_{44}(1+m_1)(1+m_2)\sqrt{n_1}\,(l_1 - l_2)}. \tag{3.28}$$

Thus, it follows from (3.26)–(3.28) that the opening displacement for a mode I crack in a prestressed material is strongly dependent on the prestresses, unlike the stress intensity factors. Let us analyze this relationship for hyperelastic materials with certain elastic potentials.

Material with Treloar potential (incompressible body; unequal roots) [146]. The parameters appearing in (3.27) for this potential are determined from (2.85). Substituting these parameters into (3.27), we get

$$K = \frac{\lambda_1^4(\lambda_1^3 + 1)}{2c_{10}(\lambda_1^9 + \lambda_1^6 + 3\lambda_1^3 - 1)}. \tag{3.29}$$

Figure 11 shows $4c_{10}K$ versus λ_1 for this material. It can be seen that the curve has a vertical asymptote as K tends to infinity (and the crack opening displacement $\delta = 2u_3(r_2, \pi, 0)$ increases abruptly, resonantly) when $\lambda_1^* = 0.666$ and the bracketed expression in the denominator of (3.29) vanishes, i.e., when

$$\lambda_1^9 + \lambda_1^6 + 3\lambda_1^3 - 1 = 0. \tag{3.30}$$

According to the approach described in Sec. 1.4, this resonant phenomenon is associated with the critical load λ_1 that causes local buckling (in a symmetric mode) in an unbounded elastic body with Treloar potential compressed along an isolated penny-shaped crack. Indeed, the critical value $\lambda_1^* = 0.666$ is in agreement with that obtained in [33] by solving the spatial nonaxisymmetric problem of the fracture of a Treloar material compressed along an internal penny-shaped crack. Note also that the value $\lambda_1^* = 0.666$ corresponds to surface instability of a body with Treloar potential [23, 24].

Material with Bartenev–Khazanovich potential (incompressible body; equal roots) [3]. The parameters appearing in (3.28) for this potential are determined from (2.84). Substituting these parameters into (3.28), we get

$$K = \frac{\lambda_1^{7/2}}{\mu(3\lambda_1^3 - 1)}. \tag{3.31}$$

Figure 12 shows μK versus λ_1 for this material. It follows from (3.31) that K tends to infinity as the initial shortening tends to the critical level

$$\lambda_1^* = \sqrt[3]{1/3} \approx 0.693, \tag{3.32}$$

that causes local buckling of the Bartenev–Khazanovich material compressed along an internal penny-shaped crack [33] and surface instability of this material.

3.1.2. General Nonaxisymmetric Problem for a Mode II or III Crack. Tangential loads are applied to a crack of radius a in the plane $y_3 = 0$ antisymmetrically about the crack plane (Fig. 4). In view of symmetry, we have the following boundary conditions on the boundary $y_3 = 0$ of the upper half-space $y_3 \geq 0$:

$$Q'_{33}(r,\theta,0) = 0, \quad Q'_{3r}(r,\theta,0) = q_1(r,\theta), \quad Q'_{3\theta}(r,\theta,0) = q_2(r,\theta) \quad (0 \leq r \leq a),$$

$$u_r(r,\theta,0) = u_\theta(r,\theta,0) = 0, \quad Q'_{33}(r,\theta,0) = 0 \quad (a < r < \infty), \quad 0 \leq \theta \leq 2\pi. \tag{3.33}$$

Assume that the right-hand sides in (3.33) can be expanded into Fourier series:

$$q_1(r,\theta) = \sum_{n=0}^{\infty} a^{(n)}(r)\cos n\theta,$$

$$q_2(r,\theta) = \sum_{n=1}^{\infty} b^{(n)}(r)\sin n\theta. \tag{3.34}$$

Using a procedure similar to that used in the previous subsection, we obtain the following expressions for the stress intensity factors at the crack tips [28]:

$$K_I = 0, \quad K_{II} = -\frac{2}{\sqrt{\pi a}}\frac{1}{a}\int_0^a a^{(0)}(r)\frac{r^2\,dr}{\sqrt{a^2 - r^2}} + \frac{2}{\sqrt{\pi a}}\mu_1\sqrt{\frac{2\pi}{a}}\sum_{n=1}^{\infty}[\Phi_1(a) - \Phi_2(a)]\cos n\theta,$$

$$K_{III} = -\frac{2}{\sqrt{\pi a}}\mu_1\sqrt{\frac{2\pi}{a}}\sum_{n=1}^{\infty}\left[(1-\nu_1)\Phi_1(a) + \Phi_2(a)\right]\sin n\theta, \tag{3.35}$$

where $\Phi_1(a)$ and $\Phi_2(a)$ are functions defined by

$$\Phi_1(t) = -\frac{t^{-n+3/2}}{(2-\nu_1)\mu_1\sqrt{2\pi}}\int_0^t [a^{(n)}(x) - b^{(n)}(x)]\frac{x^n\,dx}{\sqrt{t^2 - x^2}}, \tag{3.36}$$

$$\Phi_2(t) = \frac{\nu_1}{2}\Phi_1(t) + \frac{t^{-n-3/2}}{2\mu_1\sqrt{2\pi}}\left\{\frac{(1+2n)\nu_1}{2-\nu_1}\int_0^t x^n[a^{(n)}(x) - b^{(n)}(x)]\sqrt{t^2 - x^2}\,dx + \int_0^t [a^{(n)}(x) + b^{(n)}(x)]\frac{x^n\,dx}{\sqrt{t^2 - x^2}}\right\}.$$

The parameters μ_1 and ν_1 appearing in (3.35) and (3.36) depend on the prestresses:

$$2\mu_1 = C_{44}\frac{l_2\sqrt{n_2} - l_1\sqrt{n_1}}{l_1 l_2\sqrt{n_1 n_2}}, \quad \nu_1 = 1 - \sqrt{\frac{n_1 n_2}{n_3}}\frac{l_2(1+m_2) - l_1(1+m_1)}{(l_2\sqrt{n_2} - l_1\sqrt{n_1})(1+m_1)(1+m_2)}$$

for unequal roots and

$$2\mu_1 = C_{44}\frac{l_2 - l_1}{l_1 l_2\sqrt{n_1}}, \quad \nu_1 = 1 - \sqrt{\frac{n_1}{n_3}}\frac{l_2(1+m_2) - l_1(1+m_1)}{(l_2 - l_1)(1+m_1)(1+m_2)}$$

for equal roots.

Thus, the stress intensity factors K_{II} and K_{III} in the spatial nonaxisymmetric problem for a mode II or III crack depend on the prestresses. This is what differs the nonaxisymmetric problem for a mode II or III crack from the nonaxisymmetric problem for a mode I crack in which the SIFs do not depend on the prestresses.

Figure 5 shows the dependence of the SIFs on the prestresses in a compressible isotropic material with harmonic elastic potential (compressible body; equal roots) [132]. In Sec. 1.4, comments are also made on the observable resonant phenomena occurring as the prestresses tend to the level at which local buckling (in a flexural mode) occurs in a compressed unbounded body with a penny-shaped crack.

3.1.3. Axisymmetric Problem for a Mode I Crack. The boundary conditions are

$$Q'_{33}(r,0)=-\sigma(r), \quad Q'_{3r}(r,0)=0 \quad (0\le r\le a),$$
$$u_3(r,0)=0, \quad Q'_{3r}(r,0)=0 \quad (a<r<\infty). \tag{3.37}$$

The solution of this problem can be found as a special case of the solution of the nonaxisymmetric problem for a mode I crack (Sec. 3.1.1) for $n=0$. For example, substituting the second relation in (3.4) into (3.25), we obtain the expressions for the stress intensity factors:

$$K_I=\frac{2}{\sqrt{\pi a}}\int_0^a \frac{x\sigma(x)}{\sqrt{a^2-x^2}}\,dx, \quad K_{II}=0, \quad K_{III}=0, \tag{3.38}$$

which are the same as the stress intensity factors for a body without prestresses [135]. It follows from (3.38) that, as in the nonaxisymmetric problem for a mode I crack in a prestressed body, the stress distribution near the tip of the crack in its plane $y_3=0$ in the axisymmetric problem does not depend on the prestresses and coincides with the stress distribution in a linear elastic body without prestresses.

The components of the displacement vector for $y_3=0$ are represented as

$$u_3(r,0)=K^{(3)}u_3^{(0)}(r,0), \quad u_r(r,0)=K^{(r)}u_r^{(0)}(r,0), \tag{3.39}$$

where $u_3^{(0)}(r,0)$ and $u_r^{(0)}(r,0)$ are the components of the displacement vector in a linear elastic body without prestresses; the coefficients $K^{(3)}$ and $K^{(r)}$ characterizing the effect of the prestresses are defined by (3.19) for unequal roots and by (3.20) for equal roots. The crack-tip opening displacement for $y_3=0$, $r_2=a-r$ is given by

$$\delta=2\sqrt{\frac{r_2}{2\pi}}K_I K, \tag{3.40}$$

where K_I is defined by (3.38); K is defined by (3.27) for unequal roots and by (3.28) for equal roots.

The conclusions on the effect of the prestresses on the distribution of displacements at the crack tip and on the resonant phenomena occurring as the prestresses tend to the level causing local buckling of the material compressed along the crack in the axisymmetric problem are the same as those in the nonaxisymmetric problem for a mode I crack (Sec. 3.1.1).

3.1.4. Axisymmetric Problem for a Mode II Crack. As in the mechanics of brittle fracture of materials without prestresses [53, 135], a mode II crack is meant a crack to which a radial tangential load is applied antisymmetrically about the crack plane. In view of symmetry, we have the following boundary conditions on the boundary $y_3=0$ of the upper half-space $y_3\ge 0$:

$$Q'_{33}(r,0)=0, \quad Q'_{3r}(r,0)=-\tau(r) \quad (0\le r\le a),$$
$$u_3(r,0)=0, \quad Q'_{3r}(r,0)=0 \quad (a<r<\infty). \tag{3.41}$$

The solution of this problem is detailed in [23, 28]. The stress intensity factors in this problem are expressed as

$$K_I=0, \quad K_{II}=\frac{2}{\sqrt{\pi}a^{3/2}}\int_0^a \frac{x^2\tau(x)}{\sqrt{a^2-x^2}}\,dx, \quad K_{III}=0 \tag{3.42}$$

which are the same as the stress intensity factors for a body without prestresses [135]. It follows from (3.42) that the stress distribution near the tip of a mode II crack in its plane in a prestressed material does not depend on the prestresses and coincides with that in a linear elastic body without prestresses.

The components of the displacement vector for $y_3=0$ are represented as

$$u_3(r,0)=K^{(3)}u_3^{(0)}(r,0), \quad u_r(r,0)=K^{(r)}u_r^{(0)}(r,0), \tag{3.43}$$

where $u_3^{(0)}(r,0)$ and $u_r^{(0)}(r,0)$ are the components of the displacement vector in a linear elastic body without prestresses; $K^{(3)}$ and $K^{(r)}$ are coefficients describing the effect of the prestresses,

$$K^{(3)} = 2(\lambda+\mu)\frac{m_1\sqrt{n_2}\,l_2 d_2 - m_2\sqrt{n_1}\,l_1 d_1}{C_{44} d_1 d_2 (l_1\sqrt{n_1} - l_2\sqrt{n_2})}, \qquad K^{(r)} = 2\mu\,\frac{\lambda+\mu}{\lambda+2\mu}\,\frac{\sqrt{n_1 n_2}\,(d_1 l_1 - d_2 l_2)}{C_{44} d_1 d_2 (l_1\sqrt{n_1} - l_2\sqrt{n_2})} \tag{3.44}$$

for unequal roots and

$$K^{(3)} = 2(\lambda+\mu)\frac{m_1 l_2 d_2 - (m_1 - 1) l_1 d_1}{C_{44} d_1 d_2 \sqrt{n_1}\,(l_1 - l_2)}, \qquad K^{(r)} = 2\mu\,\frac{\lambda+\mu}{\lambda+2\mu}\,\frac{(d_1 l_1 - d_2 l_2)\sqrt{n_1}}{C_{44} d_1 d_2 (l_1 - l_2)} \tag{3.45}$$

for equal roots.

Material with Treloar Potential. For this material, we have

$$K^{(3)} = \frac{\lambda+\mu}{c_{10}}\,\frac{\lambda_1^4(1-\lambda_1^3)}{\lambda_1^9 + \lambda_1^6 + 3\lambda_1^3 - 1}, \qquad K^{(r)} = \frac{\mu(\lambda+\mu)}{c_{10}(\lambda+2\mu)}\,\frac{\lambda_1^4(1+\lambda_1^3)}{\lambda_1^9 + \lambda_1^6 + 3\lambda_1^3 - 1}. \tag{3.46}$$

It follows from (3.46) that $K^{(3)}$ and $K^{(r)}$ tend to infinity and, consequently, the displacements increase resonantly as the initial shortening reaches the critical value $\lambda_1^* = 0.666$ at which condition (3.30) is satisfied. As indicated in Sec. 3.1.1, at this value of λ_1, local buckling of the material around an internal penny-shaped crack occurs under compression along the crack.

Material with Bartenev–Khazanovich Potential. For this material, we have

$$K^{(3)} = \frac{\lambda+\mu}{\mu}\,\frac{\lambda_1^2(1-\lambda_1^3)}{3\lambda_1^3 - 1}, \qquad K^{(r)} = 2\,\frac{\lambda+\mu}{\lambda+2\mu}\,\frac{\lambda_1^{13/2}}{3\lambda_1^3 - 1}. \tag{3.47}$$

It follows from (3.47) that $K^{(3)}$ and $K^{(r)}$ tend to infinity and, consequently, the displacements increase resonantly when the initial shortening reaches the critical level (3.32) which causes local buckling of a material with Bartenev–Khazanovich potential compressed along an internal penny-shaped crack and surface instability of this material.

The conclusions on the effect of the prestresses on the distribution of displacements at the crack tip and on the resonant phenomena occurring as the prestresses tend to the level causing local buckling of the material compressed along the crack in the problem for a mode II crack are the same as those in the problem for a mode I crack.

3.1.5. Torsion Problem. Consider a crack to which a tangential circumferential load is applied antisymmetrically about the crack plane. The boundary conditions on the boundary $y_3 = 0$ of the upper half-space $y_3 \geq 0$ are the following:

$$Q'_{3\theta}(r,0) = -\tau_\theta(r) \quad (0 \leq r \leq a),$$
$$u_\theta(r,0) = 0 \quad (a < r < \infty). \tag{3.48}$$

The solution of this problem was found in [23, 28]. The stress intensity factors in this problem are expressed as

$$K_I = 0, \qquad K_{II} = 0, \qquad K_{III} = \frac{2}{\sqrt{\pi}\,a^{3/2}} \int_0^a \frac{x^2 \tau_\theta(x)}{\sqrt{a^2 - x^2}}\,dx \tag{3.49}$$

which are the same as the stress intensity factors for a body without prestresses [135]. It follows from (3.49) that the stress distribution in the crack plane in a prestressed material under torsion does not depend on the prestresses and coincides with that in a linear elastic body without prestresses.

The displacement for $y_3 = 0$ is expressed as

$$u_\theta(r,0) = K^{(\theta)} u_\theta^{(0)}(r,0), \qquad K^{(\theta)} = \mu\,\frac{\sqrt{n_3}}{C_{44}}. \tag{3.50}$$

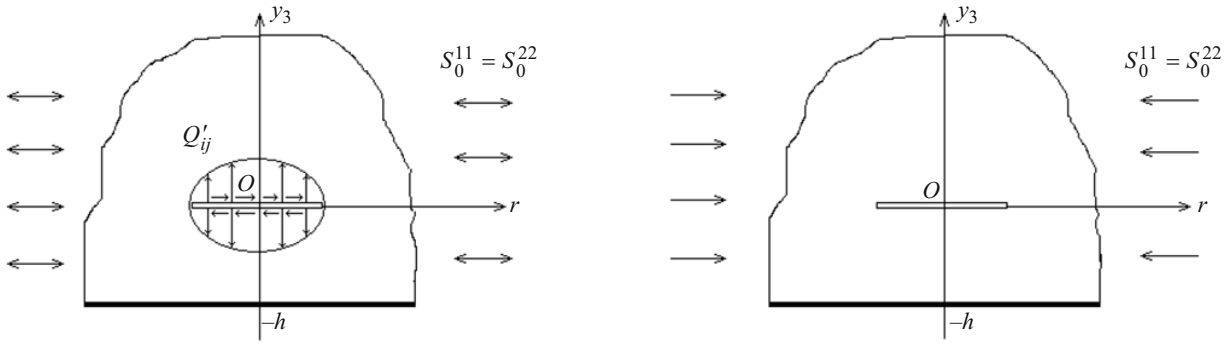

a *b*

Fig. 13

Considering (2.78) and (2.79), it is possible to show [23, 28] that $K^{(\theta)}$ defined by (3.50) cannot tend to infinity in the range of prestresses in which internal buckling of the material does not yet occur. Thus, no resonant phenomena are observed in the spatial problem for a mode III crack and, hence, no local buckling occurs in the material compressed along the crack.

3.1.6. Conclusions. The following conclusions can be drawn on problems for isolated cracks in an unbounded material with initial (residual) stresses.

In all problem formulations for free cracks (only stresses act on their faces), except for the general nonaxisymmetric problem for a mode II or III crack, the stress intensity factors do not depend on the prestresses and coincide with those in the classical mechanics of brittle fracture of materials without prestresses. The effect of the prestresses on the stress–strain state near cracks is manifested as strong dependence of the crack opening displacement on the prestresses.

The stress intensity factors K_{II} and K_{III} in the general nonaxisymmetric problem for a penny-shaped mode II or III crack depend on the prestresses even if the crack is "free."

As the initial compressive stresses tend to the level causing surface instability of the half-space, resonant phenomena occur: the stresses and displacements near the tip of a mode I or II crack change abruptly. Such resonant phenomena are absent in the problem for a mode III crack under torsion.

3.2. Near-Surface Penny-Shaped Crack in a Half-Space. Consider an elastic body occupying the half-space $y_3 \geq -h$ and having prestresses $S_0^{11} = S_0^{22}$ acting along a near-surface crack of radius a located in the plane $y_3 = 0$ and center on the Oy_3: $\{0 \leq r < a,\ 0 \leq \theta < 2\pi,\ y_3 = 0\}$ (Fig. 13).

We will discuss the results separately for the general nonaxisymmetric problem and for axisymmetric problems for mode I, II, and III cracks. The solutions of these problems were found in [2, 5, 38, 60 – 63, 66, 123, 139].

3.2.1. General Nonaxisymmetric Problem [63]. Let additional (to the prestresses) fields of normal tensile and shear stresses act on the crack faces, and the boundary of the half-space be free from loads (Fig. 13*a*). The boundary conditions are:

$$Q'_{33} = -\sigma(r,\theta), \quad Q'_{3r} = -\tau(r,\theta), \quad Q'_{3\theta} = -\tau_\theta(r,\theta) \quad (0 \leq r < a,\ y_3 = \pm 0),$$

$$Q'_{33} = 0, \quad Q'_{3r} = 0, \quad Q'_{3\theta} = 0 \quad (0 \leq r < \infty,\ y_3 = -h), \tag{3.51}$$

where $0 \leq \theta < 2\pi$.

If the half-space is compressed along a near-surface crack (Fig. 13*b*), the boundary conditions on the crack faces are the following (the first row in (3.51)):

$$Q'_{33} = 0, \quad Q'_{3r} = 0, \quad Q'_{3\theta} = 0 \quad (0 \leq r < a,\ y_3 = \pm 0).$$

Next, we will consider only the case of equal roots because the derivations for unequal roots are similar. The right-hand sides in (3.51) are expanded into Fourier series in θ:

$$\sigma(r,\theta) = \sum_{n=0}^{\infty} \sigma^{(n)}(r)\cos n\theta,$$

$$\tau(r,\theta)=\sum_{n=0}^{\infty}\tau^{(n)}(r)\cos n\theta,$$

$$\tau_{\theta}(r,\theta)=\sum_{n=1}^{\infty}\tau_{\theta}^{(n)}(r)\sin n\theta. \tag{3.52}$$

Representing the general solutions of the linearized equilibrium equations in terms of harmonious potential functions as in (2.80) and expanding these potential functions into Fourier series in the circumferential coordinate with coefficients in the form of Hankel transforms over the radial coordinate, we reduce the problem posed to six dual integral equations for each harmonic in θ (see [63] for more details):

$$\int_0^{\infty}\left\{n_1^{-1/2}d_1\left[\mu_1A_n^{(1)}+(k+\mu_1\coth\mu_1)A_n^{(2)}\right]-n_3^{-1/2}C_n^{(1)}\right\}J_{n+1}(\lambda r)\lambda d\lambda=-\frac{1}{C_{44}}[\tau^{(n)}(r)+\tau_{\theta}^{(n)}(r)],\quad r<a,$$

$$\int_0^{\infty}\left\{n_1^{-1/2}d_1\left[\mu_1A_n^{(1)}+(k+\mu_1\coth\mu_1)A_n^{(2)}\right]+n_3^{-1/2}C_n^{(1)}\right\}J_{n-1}(\lambda r)\lambda d\lambda=\frac{1}{C_{44}}[\tau^{(n)}(r)-\tau_{\theta}^{(n)}(r)],\quad r<a,$$

$$\int_0^{\infty}\left[(k-\mu_1 cth\mu_1)A_n^{(1)}-\mu_1A_n^{(2)}\right]J_n(\lambda r)\lambda d\lambda=-\frac{\sigma^{(n)}(r)}{C_{44}d_1l_1},\quad r<a,$$

$$\int_0^{\infty}X_1J_{n+1}(\lambda r)d\lambda=0,\quad r>a,$$

$$\int_0^{\infty}X_2J_{n-1}(\lambda r)d\lambda=0,\quad r>a,$$

$$\int_0^{\infty}X_3J_n(\lambda r)d\lambda=0,\quad r>a \tag{3.53}$$

$$\left(X_1=(1-(d_2l_2)/(d_1l_1))(1+\coth\mu_1)\left[(\mu_1/k)A_n^{(1)}+(1+\mu_1/k)A_n^{(2)}\right]-C_n^{(1)}\left(1+\coth\mu_3\right),\right.$$

$$X_2=(1-(d_2l_2)/(d_1l_1))(1+\coth\mu_1)\left[\mu_1/kA_n^{(1)}+(1+\mu_1/k)A_n^{(2)}\right]+C_n^{(1)}(1+\coth\mu_3),$$

$$X_3=2(1-(d_2l_2)/(d_1l_1))\left[(1-\mu_1/k)A_n^{(1)}-\mu_1/kA_n^{(2)}\right](1+\coth\mu_1),$$

$$\mu_1=\lambda n_1^{-1/2}h,\quad k=((l_1-l_2)d_2)/(d_1l_1)). \tag{3.54}$$

Hereafter we assume that $n\geq 1$ because the axisymmetric case $n=0$ is special (there are only four dual equations in this case) and addressed separately below.

Using the substitution method [50], we reduce the system of dual equations (3.53) to a governing system of Fredholm equations of the second kind:

$$\frac{1}{2}(sk+q)f_1(\xi)+\frac{1}{2}(sk-q)f_2(\xi)+\frac{2}{\pi}\int_0^1f_1(\eta)K_{11}(\xi,\eta)d\eta+\frac{2}{\pi}\int_0^1f_2(\eta)K_{12}(\xi,\eta)d\eta$$

$$+\frac{2}{\pi}\int_0^1f_3(\eta)K_{13}(\xi,\eta)d\eta=\frac{4}{\pi}\xi\int_0^{\pi/2}v_1'(\xi\sin\theta)d\theta,\quad 0\leq\xi,\eta\leq 1,$$

$$\frac{1}{2}(sk-q)f_1(\xi)+\frac{1}{2}(sk+q)f_2(\xi)+\frac{2}{\pi}\int_0^1 f_1(\eta)K_{21}(\xi,\mu)d\eta+\frac{2}{\pi}\int_0^1 f_2(\eta)K_{22}(\xi,\eta)d\eta$$

$$+\frac{2}{\pi}\int_0^1 f_3(\eta)K_{23}(\xi,\eta)d\eta=\frac{4}{\pi}\xi\int_0^{\pi/2} v_2'(\xi\sin\theta)d\theta,\qquad 0\le\xi,\eta\le 1, \tag{3.55}$$

$$\frac{1}{2}sk\,f_3(\xi)+\frac{2}{\pi}\int_0^1 f_1(\eta)K_{31}(\xi,\eta)d\eta+\frac{2}{\pi}\int_0^1 f_2(\eta)K_{32}(\xi,\eta)d\eta$$

$$+\frac{2}{\pi}\int_0^1 f_3(\eta)K_{33}(\xi,\eta)d\eta=-\frac{4}{\pi}\xi\int_0^{\pi/2} u'(\xi\sin\theta)d\theta,\qquad 0\le\xi,\eta\le 1$$

$$\left(v_1(\xi)=\frac{1}{C_{44}}\xi^{2n}\int_0^\xi \rho^{-n}\left[\tau^{(n)}(a\rho)+\tau_\theta^{(n)}(a\rho)\right]d\rho,\qquad v_2(\xi)=\frac{1}{C_{44}}\int_0^\xi \rho^n[\tau^{(n)}(a\rho)-\tau_\theta^{(n)}(a\rho)],\right.$$

$$\left.u(\xi)=\frac{n_1^{-1/2}}{C_{44}l_1}\xi^n\sigma^{(n)}(a\xi),\quad s=n_1^{-1/2}d_1(1-(d_2l_2)/(d_1l_1))^{-1},\quad q=n_3^{-1/2}\right). \tag{3.56}$$

The kernels in (3.55) have the form

$$K_{12}(\xi,\eta)=sk\,nb_1\frac{\xi^{n-1}}{\eta^{n+1}}S_n(z_{11})+\frac{s}{2k}nb_1^3\frac{\xi^{n-2}}{\eta^{n+2}(z_{11}^2-1)}\left\{\left[\left(\frac{8}{z_{11}^2-1}+n(n-1)+6\right)\frac{b_1^2}{\xi\eta}-6z_{11}\right]S_n(z_{11})\right.$$

$$\left.+(n-1)\left[3(z_{11}^2-1)-\frac{4b_1^2z_{11}}{\xi\eta}\right]P_n(z_{11})\right\}-sn\,b_1\frac{\xi^{n-2}}{\eta^{n+2}}\left[\left(\xi\eta-\frac{2b_1^2z_{11}}{z_{11}^2-1}\right)S_n(z_{11})+b_1^2(n-1)P_n(z_{11})\right]-qnb_3\frac{\xi^{n-1}}{\eta^{n+1}}S_n(z_{13})$$

$$+\sqrt{\pi}\xi^{2n}\frac{\Gamma(n+1)}{\Gamma(n+1/2)}\left\{skR_n(b_1,\eta)+\frac{s}{k}B(b_1,\eta)(n+1)\left[2(n+2)B(b_1,\eta)-3\right]R_n(b_1,\eta)\right.$$

$$\left.+s\left[1-2(n+1)B(b_1,\eta)\right]R_n(b_1,\eta)-qR_n(b_3,\eta)\right\},\ \text{etc.}$$

$$\left(b_j=2n_j^{-1/2}\beta\ (j=1,3),\ \beta=h/a,\ z_{11}=(b_1^2+\eta^2+\xi^2)/2\xi\eta,\ z_{21}=(b_1^2+1+\xi^2)/2\xi,\right.$$

$$\left.B(b,t)=b^2/(b^2+t^2),\quad R_n(b,t)=b/2(b^2+t^2)^{n+1},\ S_n(z)=(z^2-1)/4[Q_n(z)-zQ_{n-1}(z)],\right.$$

$P_n(z)=((z^2-1)^{-1}/4)Q_{n-1}(z), Q_n(z)$ are Legendre functions of the second kind).

Solving the system of integral equations (3.55), we can obtain expressions for the potential functions in (2.80) and, hence, describe the distribution of stresses and displacements in the material. Analyzing the asymptotic stress distribution in the crack plane $y_3=0$ and taking expressions (2.88) into account, we obtain the stress intensity factors for the nonaxisymmetric problem under consideration:

$$K_I=-\frac{1}{4}C_{44}l_1\sqrt{n_1}sk\sqrt{\pi a}\sum_{n=1}^{\infty}\cos n\theta\int_0^1 f_3(\eta)d\eta,$$

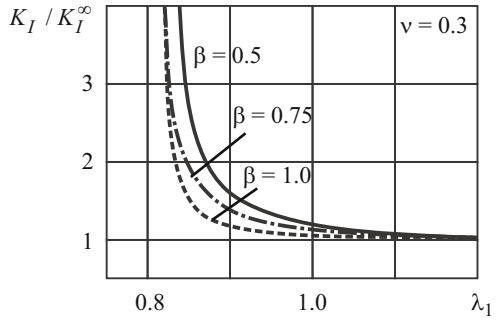

Fig. 14

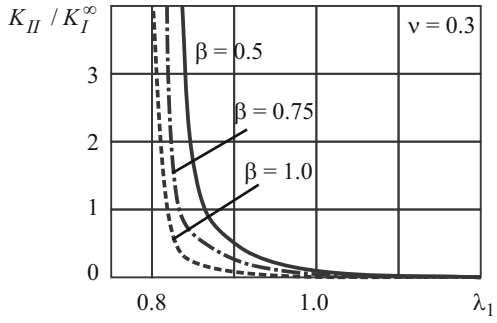

Fig. 15

$$K_{II} = \frac{1}{4} C_{44} sk\sqrt{\pi a} \sum_{n=1}^{\infty} \cos n\theta [f_1(1) + f_2(1)],$$

$$K_{III} = \frac{1}{4} C_{44} q\sqrt{\pi a} \sum_{n=1}^{\infty} \sin n\theta [f_1(1) - f_2(1)], \tag{3.57}$$

where the functions $f_1(\xi)$, $f_2(\xi)$, $f_3(\xi)$ are determined by solving Eqs. (3.55).

It follows from (3.57) that the crack and the free surface of the material qualitatively change the asymptotic stress distribution near the crack tip, compared with the case of an isolated crack in an unbounded material. Namely, this leads to nonzero stress intensity factors K_{II} and K_{III} if only normal tensile stresses act on the near-surface crack (i.e., $\sigma(r, \theta) \neq 0$, $\tau(r, \theta) = 0, \tau_\theta(r, \theta) = 0$) (recall that $K_I \neq 0, K_{II} = 0, K_{III} = 0$ for an isolated mode I crack in an unbounded body (see Sec. 3.1.1)) and nonzero stress intensity factor K_I if only tangential forces act on the crack faces ($\sigma(r, \theta) = 0$, $\tau(r, \theta) \neq 0$, $\tau_\theta(r, \theta) \neq 0$) ($K_I = 0, K_{II} \neq 0, K_{III} \neq 0$ for an isolated crack in an unbounded body (see Sec. 3.1.2)).

Moreover, all the three stress intensity factors depend on the prestresses because the parameters $C_{44}, s, q, k, k_i, l_i, n_i$, $i = 1, 2$, in (3.57) and (3.55) depend on the initial elongation (or shortening) λ_1 caused by the prestresses $S_0^{11} = S_0^{22}$.

Let us examine the limiting case where the distance between the crack and the boundary of the half-space tends to infinity: $h \to \infty$ ($\beta \to \infty$). An analysis of the expressions for the kernels of the Fredholm equations (3.55) reveals that $\lim\limits_{\beta \to \infty} K_{ij}(\xi, \eta) = 0$.

We will restrict ourselves to the case where the crack is loaded by normal stresses $\lambda_1 = 1 (\tau(r, \theta) = 0, \tau_\theta(r, \theta) = 0)$. Then from (3.55) we get

$$f_1^\infty(\xi) = f_2^\infty(\xi) = 0, \quad \frac{1}{2} sk\, f_3^\infty(\xi) = -\frac{4}{\pi} \xi \int_0^{\pi/2} u'(\xi \sin\theta) d\theta, \quad f_j^\infty(\xi) \equiv \lim_{\beta \to \infty} f_j(\xi).$$

If $\eta = \xi \sin\theta$, then

$$f_3^\infty(\xi) = -\frac{8}{\pi} \frac{1}{sk} \xi \int_0^{\pi/2} u'(\xi \sin\theta) d\theta = -\frac{8}{\pi} \frac{n_1^{-1/2}}{C_{44} l_1} \xi \int_0^{\xi} \frac{d}{d\eta} \left[\eta^n a_n(a\eta)\right] \frac{d\eta}{\sqrt{\xi^2 - \eta^2}} = -\frac{8}{\pi} \frac{1}{sk} \frac{n_1^{-1/2}}{C_{44} l_1} \frac{d}{d\xi} \int_0^{\xi} \frac{\eta^{n+1} a_n(a\eta)}{\sqrt{\xi^2 - \eta^2}} d\eta.$$

Then from (3.57) we get

$$K_I^\infty \equiv \lim_{\beta \to \infty} K_I = 2\sqrt{\frac{a}{\pi}} \sum_{n=0}^{\infty} \cos n\theta \int_0^1 \frac{\eta^{n+1} \sigma(a\eta)}{\sqrt{1 - \eta^2}} d\eta = \frac{2}{\sqrt{\pi a}} \sum_{n=0}^{\infty} \frac{\cos n\theta}{a^n} \int_0^a \frac{t^{n+1} \sigma(t)}{\sqrt{a^2 - t^2}} dt,$$

$$K_{II}^\infty = 0, \quad K_{III}^\infty = 0.$$

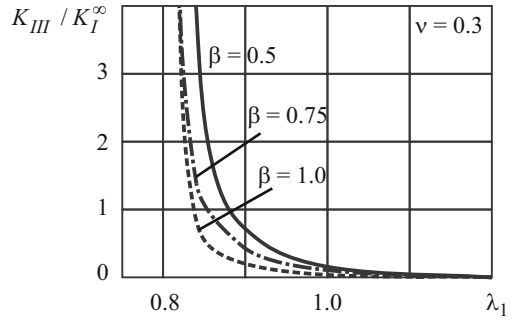

Fig. 16

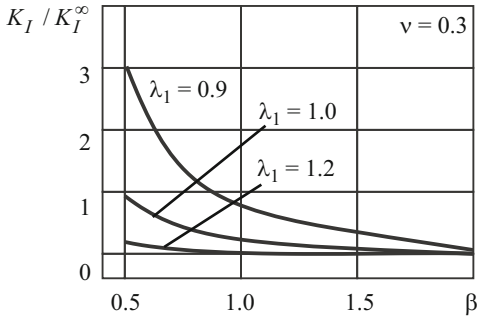

Fig. 17

Thus, if the distance between the crack and the free surface tends to infinity, the expressions for the SIFs are the same as those in the nonaxisymmetric problem of the fracture of a prestressed unbounded body with an isolated penny-shaped crack (Sec. 3.1.1, formulas (3.23)).

We will now discuss numerical results for some hyperelastic materials [63] with a crack subject to a normal tensile load defined by

$$\sigma(r, \theta) = \sigma_1 \cos \theta. \tag{3.58}$$

Material with Harmonic Potential. Figures 14, 15, and 16 show the variation in K_I / K_I^{∞}, K_{II} / K_I^{∞}, and K_{III} / K_I^{∞}, respectively, with λ_1 for Poisson's ratio $\nu = 0.3$ and different values of $\beta = h / a$. Here K_I^{∞} is the SIF in the nonaxisymmetric problem for a mode I crack in an unbounded body determined from (3.23), (3.58):

$$K_I^{\infty} = \frac{1}{2}\sqrt{\pi a}\sigma_1 \cos \theta.$$

It can be seen that the stress intensity factors are strongly dependent on the prestresses, the effect of the compressive prestresses being stronger than that of the tensile prestresses. The vertical asymptotes represent the resonant phenomena occurring when the initial compressive stresses reach the level at which the material near the near-surface crack loses stability (in a buckling mode symmetric about the crack plane).

For this material, Fig. 17 shows K_I / K_I^{∞} versus $\beta = h / a$ for $\nu = 0.3$ and for $\lambda_1 = 0.9$ (initial compression), $\lambda_1 = 1.2$ (initial tension), and $\lambda_1 = 1.0$ (no prestresses). It can be seen that the closer the distance between the crack and the free boundary of the body, the stronger the interaction between them. For example, if $\lambda_1 = 0.9$, then the value of K_I / K_I^{∞} for $\beta = 0.5$ is greater by a factor of 1.7 than the value of K_I / K_I^{∞} for $\beta = 2.0$. As the distance between the crack and the boundary of the half-space increases, the interaction between them weakens and the corresponding SIFs tend to those for an isolated crack in an unbounded body. The interaction between the crack and the free surface can be neglected, with accuracy sufficient for practical calculations, when the distance between them exceeds two crack radii.

Figure 18 illustrates the dependence K_I / K_I^{∞} on the prestresses λ_1 for $\beta = 0.5$ and different values of ν. It can be seen that the compressibility of a material with harmonic potential characterized by Poisson's ratio has a strong effect on the SIFs. For example, the value of K_I / K_I^{∞} for $\nu = 0.5$ exceeds the value of K_I / K_I^{∞} for $\nu = 0.1$ by 12% when $\lambda_1 = 0.95$, $\beta = 0.5$ and by a factor of 2.2 when $\lambda_1 = 0.9$, $\beta = 0.5$.

Material with Bartenev–Khazanovich Potential. For this material, Figs. 19, 20*a*, and 20*b* show the dependence of K_I / K_I^0, K_I / K_I^{∞}, and K_{III} / K_I^{∞}, respectively (K_I^0 is the stress intensity factor for a mode I crack in a material without prestresses) on λ_1 for different values of $\beta = h / a$. As can be seen, the stress intensity factors for this material are also strongly dependent on the prestresses and the geometrical parameters of the problem (the distance between the crack and the boundary and the crack radius). The vertical asymptotes indicate that the SIFs sharply increase as the initial compressive stresses tend to the level that causes local buckling of the material near a crack under compression along it.

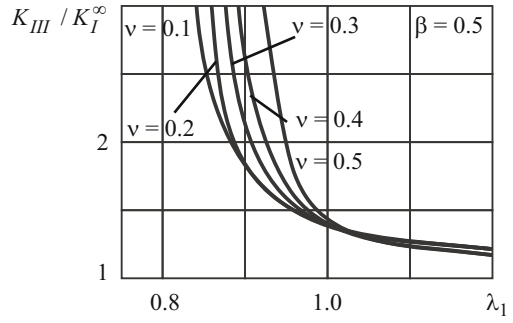

Fig. 18

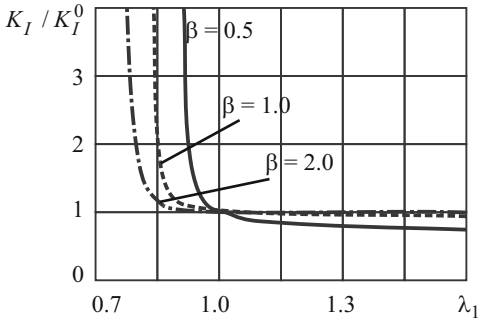

Fig. 19

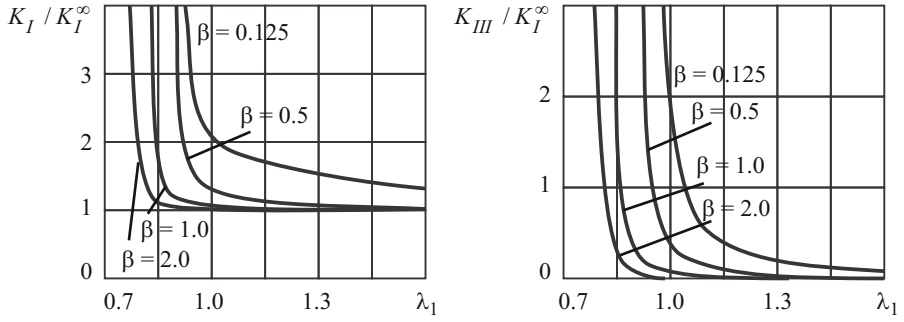

a *b*

Fig. 20

3.2.2. Axisymmetric Problem for a Mode I Crack [2, 5, 61, 123]. Let normal stresses of intensity $\sigma(r)$ symmetric about the crack plane $y_3 = 0$ be applied to the crack faces. In the case of equal roots, the stress intensity factors are defined by

$$K_I = -C_{44} d_1 l_1 \frac{k}{2}\sqrt{\pi a}\, f(1), \qquad K_{II} = -C_{44} n_1^{-1/2} d_1 \frac{k}{2}\sqrt{\pi a}\int_0^1 g(\xi)d\xi, \qquad K_{III} = 0, \tag{3.59}$$

where the functions f and g can be found by solving the system of Fredholm equations of the second kind

$$f(\xi) + \frac{4}{\pi k}\int_0^1 f(\eta)K_{11}(\xi,\eta)d\eta - \frac{4}{\pi k}\int_0^1 g(\eta)K_{12}(\xi,\eta)d\eta = -\frac{4}{\pi k}\int_0^{\pi/2} s(\xi\sin\theta)\,d\theta,$$

$$g(\xi) + \frac{4}{\pi k}\int_0^1 f(\eta)K_{21}(\xi,\eta)d\eta - \frac{4}{\pi k}\int_0^1 g(\eta)K_{22}(\xi,\eta)d\eta = 0, \qquad s(\xi) = \frac{\xi\sigma(a\xi)}{C_{44} d_1 l_1}. \tag{3.60}$$

The kernels in (3.60) have the form

$$K_{11}(\xi,\eta) = -\left[\frac{k}{2} I_1(2\beta_1,\eta) + \beta_1 I_2(2\beta_1,\eta) + \frac{\beta_1^2}{k} I_3(2\beta_1,\eta)\right],$$

$$K_{12}(\xi,\eta) = \frac{\beta_1^2}{k}\left[\eta^{-1} I_2(2\beta_1,\eta) - I_2(2\beta_1,1)\right], \qquad K_{21}(\xi,\eta) = -\frac{\beta_1^2}{k}\xi I_4(2\beta_1,\eta),$$

$$K_{22}(\xi,\eta) = \xi\left\{\frac{k}{2}\left[\eta^{-1} I_1(2\beta_1,\eta) - I_1(2\beta_1,1)\right] - \beta_1\left[\eta^{-1} I_2(2\beta_1,\eta) - I_2\left(2\beta_1,1\right)\right]\right.$$

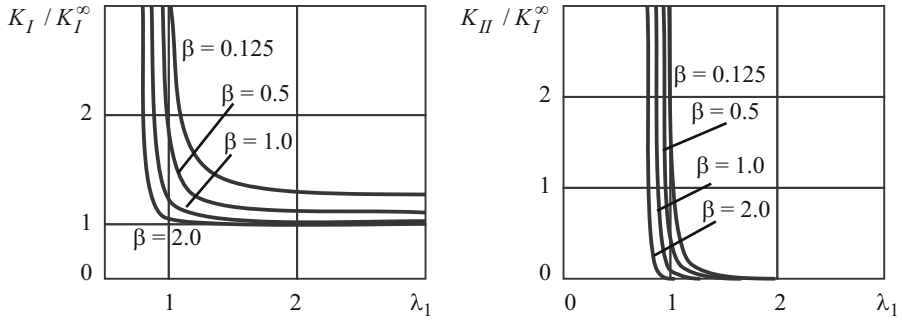

Fig. 21

TABLE 1

$\beta = h/a$	0.1	0.25	0.5	0.75	1.0	2.0	5.0	10.0
$\lambda_1 = 0.9$	—	—	—	3.0238	1.7378	1.1332	1.0115	1.0015
	—	—	—	1.5481	0.4526	0.0485	0.0018	0.0001
$\lambda_1 = 1.0$	8.4045	3.0817	1.7374	1.3770	1.2223	1.0482	1.0040	1.0005
	5.1692	1.2098	0.3609	0.1592	0.0816	0.0109	0.0004	0.0000
$\lambda_1 = 1.2$	2.2809	1.5696	1.2459	1.1288	1.0744	1.0146	1.0011	1.0001
	0.2219	0.1186	0.0523	0.0248	0.0125	0.0015	0.0001	0.0000

$$+\frac{\beta_1^2}{k}\left[\eta^{-1} I_3(2\beta_1,\eta) - I_3(2\beta_1,1)\right]\Bigg\}, \tag{3.61}$$

where

$$I_1(\beta,\eta) = \beta[2\xi\eta(\zeta^2-1)]^{-1}, \quad I_2(\beta,\eta) = I_1(\beta,\eta)\left[4\zeta I_1(\beta,\eta) - \beta^{-1}\right],$$

$$I_3(\beta,\eta) = 4I_1^2(\beta,\eta)\left[2(3\zeta^2+1)I_1(\beta,\eta) - 3\zeta\beta^{-1}\right],$$

$$I_4(\beta,\eta) = 12I_1^2(\beta,\eta)\left[16\zeta(\zeta^2+1)I_1^2(\beta,\eta) - \frac{4}{\beta}(3\zeta^2+1)I_1(\beta,\eta) + \zeta/\beta^2\right],$$

$$\zeta = (\beta^2+\xi^2+\eta^2)(2\xi\eta)^{-1}, \quad \beta_1 = n_1^{-1/2}\beta.$$

It can be seen from (3.60) that the value of K_{II} in the problem for a mode I crack is nonzero ($K_{II} = 0$ for an unbounded prestressed body with a mode I crack, according to (3.38)) because of the interaction between the crack and the free surface of the material. Note that a similar mechanical effect was discovered in the problem of the fracture of materials without prestresses [135]. Moreover, both K_I and K_{II} depend on the prestresses and the distance between the crack and the boundary of the half-space because the functions $f(\xi)$ and $g(\xi)$ following from (3.60) also depend on these parameters.

We will now discuss numerical results for specific materials with a crack under uniform normal load $\sigma(r) = \sigma = \text{const}$ applied to its faces.

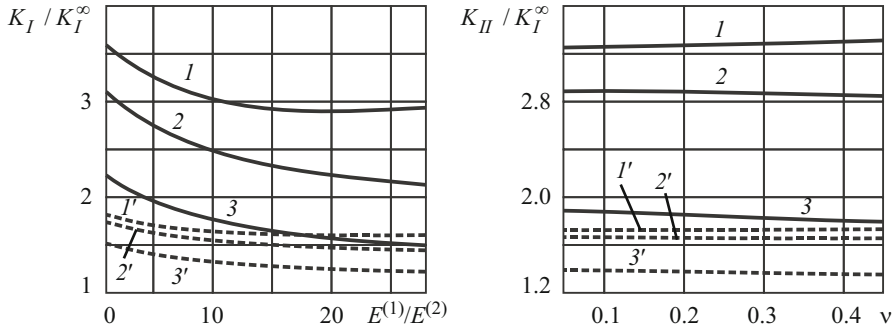

Fig. 22

Material with Treloar Potential. Figures 21*a* and 21*b* show the variation in K_I / K_I^∞ and K_{II} / K_I^∞, respectively (K_I^∞ is the SIF for a mode I crack in an unbounded body without prestresses) with λ_1 for different values of the dimensionless distance $\beta = h / a$ between the crack and the boundary of the body. It can be seen that K_I and K_{II} are strongly dependent on the prestresses. The vertical asymptotes in the range of compressive prestresses ($\lambda_1 < 1$) represent the resonant phenomenon occurring when the initial compressive stresses (and the parameter $\lambda_1 < 1$) reach the critical level at which local buckling occurs (in a mode symmetric about the crack plane) under compression. This phenomenon allows us to use the combined approach to determine the critical compressive stresses.

Table 1 summarizes the values of K_I / K_I^∞ (upper numbers) and K_{II} / K_I^∞ (lower numbers) for different values of the dimensionless distance between the crack and the boundary of the half-space normalized to the crack radius and for $\lambda_1 = 0.9$ (compressive prestresses), $\lambda_1 = 1.0$ (no prestresses), and $\lambda_1 = 1.2$ (tensile prestresses). As can be seen, the interaction between the crack and the free boundary increases the SIFs compared with that for a mode I crack in an unbounded body. As this distance increases, the interaction between the crack and the boundary of the body rapidly weakens and the SIFs tend to those for an isolated crack. Note that these curves are similar to those for a near-surface crack parallel to the free surface of a semibounded material without prestresses ([135, pp. 225–226]).

Laminated Two-Component Composite with Isotropic Plies. As indicated in Sec. 2.2, the continuum approach is to model such a composite by a transversely isotropic material with effective macrocharacteristics. Figure 22*a* shows the variation in K_I / K_I^∞ with the ratio $E^{(1)} / E^{(2)}$ of elastic moduli of the plies with equal Poisson's ratios $\nu^{(1)} = \nu^{(2)} = 0.3$, the volume fraction of the component with $E^{(1)}$ being $c_1 = 0.3$, for $\lambda_1 = 0.99$ (compressive prestresses; curves *1* and *1′*), $\lambda_1 = 1.0$ (no prestresses; curves *2* and *2′*), $\lambda_1 = 1.05$ (tensile prestresses; curves *3* and *3′*), for $\beta = 0.25$ (solid lines) and $\beta = 0.5$ (dashed lines). As the ratio $E^{(1)} / E^{(2)}$ increases, K_I / K_I^∞ decreases monotonically and quickly. For example, if the ratio of elastic moduli changes from 1 to 30 (for $\lambda_1 = 1.05$ and $\beta = 0.25$), the ratio K_I / K_I^∞ decreases by 34%. Moreover, the shorter the distance between the crack and the boundary, the greater the value of K_I / K_I^∞.

Figure 22*b* shows the dependence of K_I / K_I^∞ on ν for a composite with $\nu^{(1)} = \nu^{(2)} = \nu$, $E^{(1)} / E^{(2)} = 3$, and $c_1 = 0.3$. Solid lines *1*, *2*, and *3* correspond to $\beta = 0.25$, and dashed lines *1′*, *2′*, and *3′* to $\beta = 0.5$. Curves *1* and *1′* correspond to $\lambda_1 = 0.99$, curves *2* and *2′* to $\lambda_1 = 1.0$, and curves *3* and *3′* to $\lambda_1 = 1.1$.

3.2.3. Axisymmetric Problem for a Mode II Crack [60–62, 122, 123, 139]. Let tangential radial stresses of intensity $\tau(r)$ symmetric about the crack plane $y_3 = 0$ be applied to the crack faces. The stress intensity factors are defined by (3.59), and the functions f and g are determined by solving the system of integral equations

$$f(\xi) + \frac{4}{\pi k}\int_0^1 f(\eta) K_{11}(\xi, \eta)\, d\eta - \frac{4}{\pi k}\int_0^1 g(\eta) K_{12}(\xi, \eta)\, d\eta = 0,$$

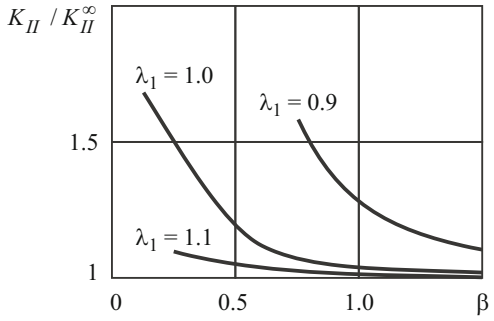

Fig. 23

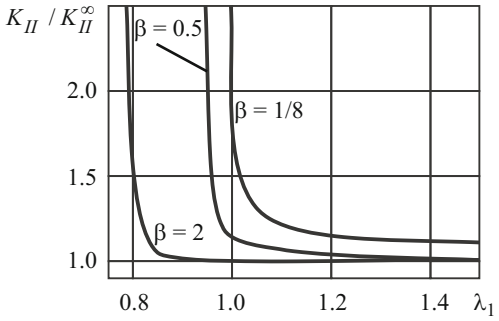

Fig. 24

$$g(\xi)+\frac{4}{\pi k}\int_0^1 f(\eta)K_{21}(\xi,\eta)\,d\eta-\frac{4}{\pi k}\int_0^1 g(\eta)K_{22}(\xi,\eta)\,d\eta=-\frac{4}{\pi k}\xi\int_0^{\pi/2} q'(\xi\sin\theta)d\theta, \tag{3.62}$$

where $q(\xi)=(\xi\tau(a\xi))/(C_{44}n_1^{-1/2}d_1)$, and the kernels are defined by (3.61).

In this problem, the interaction between the crack and the free surface is the cause of a new mechanical effect: nonzero stress intensity factor K_I ($K_I = 0$ in the problem for an isolated mode II crack in a prestressed unbounded body (3.42)).

We will discuss numerical results for some materials with a crack subject to a uniform shear load $\tau(r)=\tau=\text{const}$ on its faces. Note that the dependence (Fig. 6) of the stress intensity factors on the prestresses in a Treloar material for this problem was analyzed in Sec. 1.4. Figure 23 shows, for the same material, the ratio K_{II}/K_{II}^{∞} (where K_{II}^{∞} is the SIF (3.42) for an isolated mode II crack in a prestressed unbounded body) as a function of the normalized distance β between the crack and the boundary of the half-space for different values of λ_1. As can be seen, the free surface causes an increase in the SIFs compared with the case of a mode II crack in an unbounded material either with initial compressive ($\lambda_1 = 0.9$) and tensile ($\lambda_1 = 1.1$) stresses or without prestresses ($\lambda_1 = 1.0$).

Material with Bartenev–Khazanovich Potential. For this material, Fig. 24 shows the ratio K_{II}/K_{II}^{∞} as a function of λ_1 for different values of β. It can be seen that the prestresses have a strong effect on the asymptotic stress distribution near the crack. The vertical asymptotes represent the resonant phenomena occurring when the initial compressive stresses reach the level at which the material near the crack loses stability (in a buckling mode either flexural or antisymmetric symmetric about the crack plane). It is should be noted that for this material and a material with Treloar potential, the critical compressive loads that cause flexural buckling near a mode II crack are the same as the critical compressive loads that cause symmetric buckling near a mode I crack (see Sec. 3.2.2).

Composite Reinforced with Random Short Ellipsoidal Fibers in the Plane $y_3 = \text{const}$. The continuum approach models such a composite by a transversely isotropic body with effective macrocharacteristics (see Sec. 2.2). Figure 25 presents results for a composite reinforced with random elliptic carbon fibers with volume fraction $c_1 = 0.7$. It can be seen that the ratio K_{II}/K_{II}^{∞} strongly depends on the prestresses and asymptotically tends to infinity as the parameter λ_1 tends to the level causing local buckling of the half-space near a near-surface crack. Moreover, the value of the SIFs is also noticeably dependent on the distance between the crack and the free boundary. For example, for $\lambda_1 = 0.98$, the values of K_{II}/K_{II}^{∞} for $\beta = 0.25$ and $\beta = 1.0$ differ almost twofold.

3.2.4. Mode III Crack [38, 66, 123]. Consider a crack to which a tangential circumferential load of intensity $\tau_\theta(r)$ is applied antisymmetrically about the plane $y_3 = 0$. The stress intensity factors are defined by

$$K_I = 0, \quad K_{II} = 0, \quad K_{III} = \frac{1}{2}C_{44}n_3^{-1/2}\sqrt{\pi a}\int_0^1 f(\eta)d\eta, \tag{3.63}$$

where the function f is determined by solving the Fredholm equation of the second kind

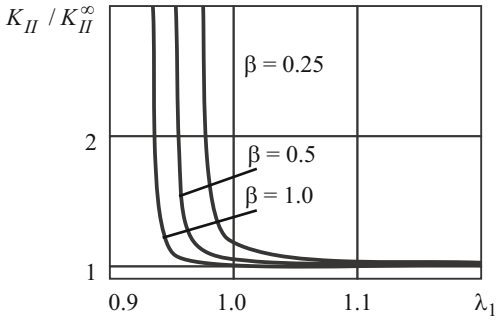

Fig. 25

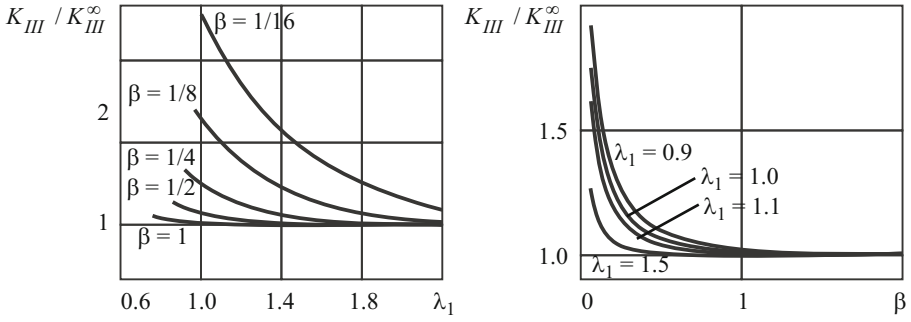

a *b*

Fig. 26

$$f(\xi)-\frac{1}{\pi}\int_0^1 f(\eta)K(\xi,\eta)d\eta=\frac{4}{\pi}\xi\int_0^{\pi/2}q'(\xi\sin\theta)d\theta,\qquad q(\xi)\equiv\frac{\xi\tau_\theta(a\xi)}{C_{44}n_3^{-1/2}} \tag{3.64}$$

with kernel $K(\xi,\eta)=2\xi[\eta^{-1}I_1(2\beta_3,\eta)-I_1(2\beta_3,1)]$; $\beta_3=n_3^{-1/2}\beta$, I_1 is defined by (3.61).

In the limiting case where the distance between the crack and the boundary of the half-space tends to infinity, the expression for K_{III} follows from (3.63), (3.64):

$$K_{III}^{\infty}=\frac{2}{a\sqrt{\pi a}}\int_0^a\frac{t^2\tau_\theta(t)dt}{\sqrt{a^2-t^2}}, \tag{3.65}$$

which is the same as the expression derived in [135] for a linear elastic body without prestresses.

We will discuss numerical results for some materials with a crack subject to a load $\tau_\theta(r)=\tau=\text{const}$ on its faces.

Material with Bartenev–Khazanovich Potential. Figures 26*a* and 26*b* show the ratio K_{III}/K_{III}^{∞} (where K_{III}^{∞} is defined by (3.65)) as a function of λ_1 and $\beta=h/a$, respectively.

It can be seen that the prestresses have a strong effect on K_{III}. Here, however, we do not observe resonant effects, unlike the cases of mode I and II cracks. This means that no local buckling occurs near a mode III crack in a compressed Bartenev–Khazanovich material. The close free boundary of the body increases the SIF compared with the case of an isolated crack. For example, if $\lambda_1=0.9$ and the distance between the crack and the boundary of the half-space is 1/16 of the crack radius, then KIII exceeds K_{III}^{∞} by a factor of 1.92. As the distance between the crack and the boundary of the half-space increases, this interaction rapidly weakens—it can be neglected for the purpose of engineering calculations if the distance is longer than two crack radii.

Laminated Two-Component Composite with Isotropic Plies. Figure 27*a* shows K_{III}/K_{III}^{∞} versus λ_1 for $E^{(1)}/E^{(2)}=4$, $\nu^{(1)}=\nu^{(2)}=0.3$, $c_1=0.3$, and different values of $\beta=h/a$. The curves are similar to those for the Bartenev–Khazanovich

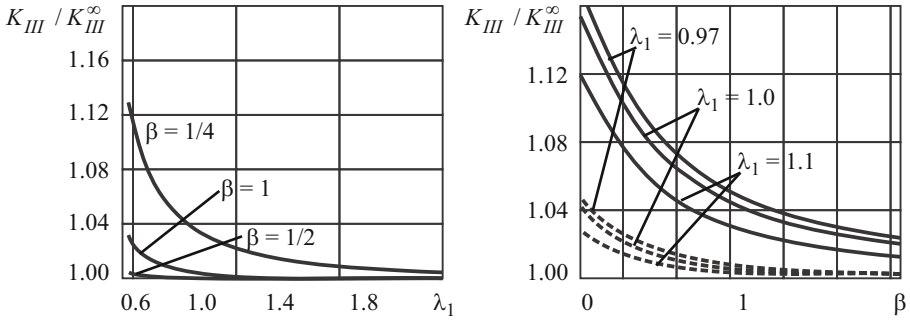

a *b*

Fig. 27

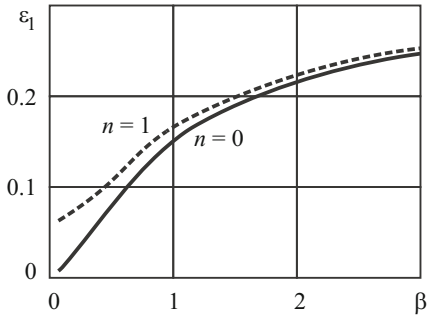

Fig. 28

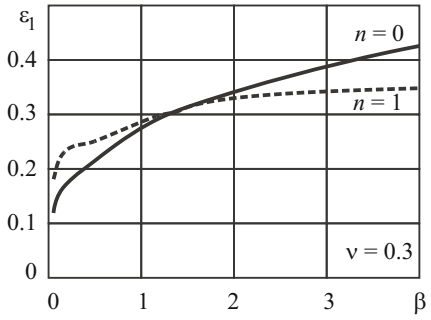

Fig. 29

material. Figure 27*b* shows K_{III}/K_{III}^{∞} as a function of $E^{(1)}/E^{(2)}$ for $\lambda_1 = 0.97$, $\lambda_1 = 1.0$, and $\lambda_1 = 1.1$. The solid lines correspond to $\beta = 0.25$, and the dashed lines to $\beta = 0.5$.

3.2.5. Critical Loads for Compression along a Near-Surface Crack. In Secs. 3.2.1–3.2.3, it was shown that as the initial compressive stresses in materials with various elastic potentials and in composites under nonaxisymmetric and axisymmetric loading along near-surface mode I and II cracks tend to a certain critical level, the stress distribution near the cracks displays asymptotic behavior—an abrupt increase in the stress intensity factors. The critical initial compressive stresses at which the SIFs increase resonantly are equal for K_I and K_{II}. According to the combined approach outlined in Sec. 1.4, this phenomenon allows us to determine the critical (limiting) compressive loads at which local buckling (in a nonaxisymmetric or axisymmetric mode) of the material occurs near a near-surface crack along which the material is compressed (Fig. 13*b*). Such a phenomenon was not observed in the problem of the torsion of a body with a near-surface crack, which suggests the absence of a buckling mode in a material compressed along a mode III crack.

Figures 28 and 29 show the relative critical (limiting) shortening $\varepsilon_1 = 1 - \lambda_1$ versus the relative distance β between the crack and the boundary of materials with Bartenev–Khazanovich and harmonic potentials, respectively.

The solid lines represent the axisymmetric buckling mode ($n = 0$), and the dashed the nonaxisymmetric buckling mode of the material near a near-surface crack (first circumferential harmonic, $n = 1$). It can be seen that the interaction of the crack and the boundary of the half-space substantially decreases the critical (limiting) shortening and, hence, the critical (limiting) compressive stresses, compared with the case of an isolated crack in an unbounded material (Sec. 3.1) (in this case, $\varepsilon_1^* = 0.307$ for the Bartenev–Khazanovich potential and formula $\varepsilon_1^* = 1/(2+\nu)$ (axisymmetric buckling mode) and $\varepsilon_1^* = (1-\nu)/2$ (nonaxisymmetric buckling mode) for the harmonic potential). As the distance between the crack and the boundary of the half-space increases, the interaction between them weakens and the critical loads tend to those for a crack in an unbounded material.

Figure 30 shows the influence of the volume fraction c_1 of glass on the critical compressive stress divided by the reduced elastic modulus E for a laminated two-component composite with isotropic plies (a composition of aluminoborosilicate glass and maleic epoxy resin) for $\beta = 0.25$. Figure 31 shows the variation in $\varepsilon_1 = 1 - \lambda_1$ with β for a composite reinforced with random short ellipsoidal carbon fibers in the isotropy plane, the volume fraction of fibers $c_1 = 0.7$.

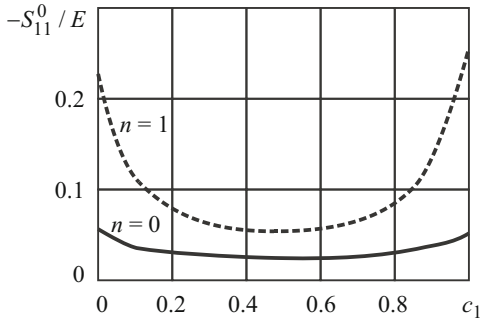

Fig. 30

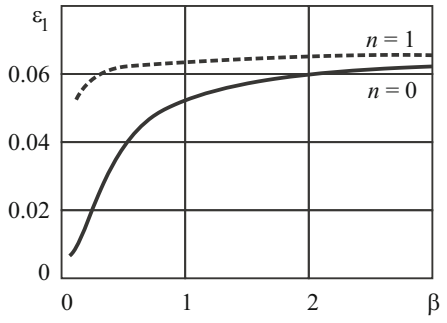

Fig. 31

The axisymmetric mode buckling ($n = 0$) is observed in all the materials, except for the material with harmonic potential. A nonaxisymmetric buckling mode is observed in a material with harmonic potential when $\beta > 1.5$, which is because, according to [24], nonaxisymmetric surface instability occurs in this material. At great values of β, the critical (limiting) compression loads in the problem for a near-surface become similar to those that cause surface buckling of a half-space without crack. Also, the numerical results indicate that the critical (limiting) compressive loads depend on the mechanical characteristics of the material and the geometrical parameters of the problem.

3.2.6. Conclusions. The interaction between the near-surface penny-shaped crack and the free surface of the prestressed material leads to some new mechanical effects. For example, the stress intensity factors are strongly dependent on the prestresses for all cracks considered (mode I, II, and III cracks) and for nonaxisymmetric and axisymmetric problem formulations. This is what differs the problem for a semibounded body with a near-surface crack and the problem for an unbounded body with an isolated crack (Sec. 3.1.1) where the stress intensity factors do not depend on the prestresses (except for the general nonaxisymmetric problem for a mode II or III crack), while the crack opening displacements depend on the prestresses.

When normal and radial shear loads act on the crack faces, the stress intensity factors change resonantly as the initial compressive loads tend to the critical level that causes local buckling of the material near the crack. However, when torsional loads act on the crack faces, no resonant phenomena occur, which suggests the absence of buckling modes in the torsion problem.

Moreover, the interaction between the crack and the boundary of the half-space results in nonzero values of K_{II} and K_I. It should be noted that this effect is similar to that in the problem for a half-space with a near-surface crack solved using the classical fracture mechanics of materials without prestresses [135].

If the distance between the crack and the boundary of the half-space is short, the interaction between the crack and the free boundary is quantitatively manifested as an increase in the stress intensity factors compared with the SIFs for an isolated crack in an unbounded body. As this distance increases, the interaction between the crack and the boundary of the body sharply weakens and the SIFs tend to those for an isolated crack. Note that these effects are also similar to those observed in problems for materials without prestresses [135].

By analyzing the resonant change in the stress intensity factors (obtained by solving problems of the fracture of prestressed materials with a mode I or II crack) occurring as the initial compressive loads tend to the level causing buckling of the material near the crack, we have determined the critical (limiting) compressive loads for a half-space compressed along a near-surface crack in certain materials. It has been shown that for all the materials considered, except for the material with elastic harmonic potential, the compressive buckling mode is axisymmetric.

3.3. Two Parallel Coaxial Penny-Shaped Cracks in an Unbounded Body. Consider a prestressed unbounded elastic body with two penny-shaped cracks of equal radius a located in parallel planes $y_3 = 0$ and $y_3 = -2h$ and centered on the Oy_3-axis (Fig. 32). The crack faces are loaded by additional (to the prestresses $S_0^{11} = S_0^{22}$) mutually balanced stresses (mode I, II, or III (Fig. 32*a*)) or are free from stresses (as in the problem of the compression of a material along cracks; Fig. 32*b*). Since the geometry and the system of forces are symmetric (antisymmetric) about the plane $y_3 = -h$ equidistant from the cracks, the problems can be reformulated for the half-space $y_3 \ge -h$ with one crack. However, unlike the problems addressed in Sec. 3.2, the boundary conditions on the boundary of the half-space are mixed.

Problems for two parallel coaxial cracks in prestressed bodies are solved in [4, 7, 8, 62, 72, 123].

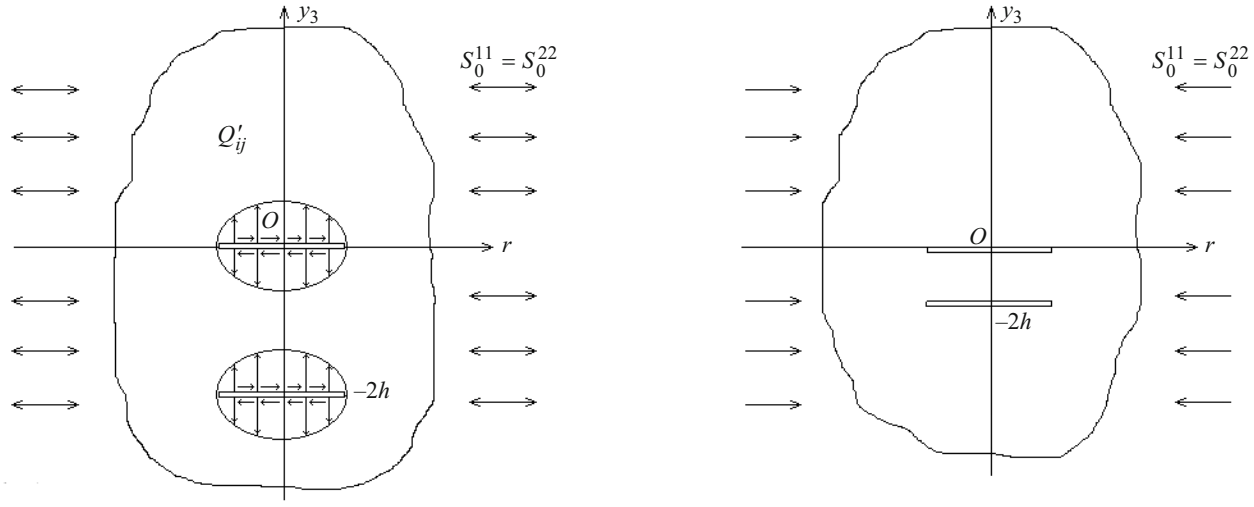

a *b*

Fig. 32

3.3.1. Nonaxisymmetric Problem [8]. Let normal tensile loads of equal intensity $\sigma(r, \theta)$ act on the crack faces. As indicated above, the problem can be reformulated for the half-space $y_3 = -h$ with a crack in the plane $y_3 = 0$. The mixed boundary conditions on the crack faces and on the boundary of the half-space are

$$Q'_{33} = -\sigma(r, \theta), \quad Q'_{3r} = 0, \quad Q'_{3\theta} = 0 \quad (0 \le r < a, \; y_3 = \pm 0),$$

$$u_3 = 0, \quad Q'_{3r} = 0, \quad Q'_{3\theta} = 0 \quad (0 \le r < \infty, \; y_3 = -h).$$

Representing the general solutions of the linearized equilibrium equations in terms of harmonious potential functions (2.77), (2.80) and expanding these potential functions into Fourier series in the circumferential coordinate with coefficients in the form of Hankel transforms over the radial coordinate and expanding the function $\sigma(r, \theta)$ into Fourier series (3.52), we reduce the problem to a system of dual integral equations for each harmonic in θ and then to a system of Fredholm equations of the second order (see [8] for more details), which have the following dimensionless form in the case of unequal roots (all variables are divided by the crack radius *a*):

$$\frac{1}{2}(sk/k_1 + q) f_1(\xi) + \frac{1}{2}(sk/k_1 - q) f_2(\xi) + \frac{2}{\pi}\int_0^1 f_1(\eta) K_{11}(\xi, \eta) d\eta$$

$$+ \frac{2}{\pi}\int_0^1 f_2(\eta) K_{12}(\xi, \eta) d\eta + \frac{2}{\pi}\int_0^1 f_3(\eta) K_{13}(\xi, \eta) d\eta = 0,$$

$$\frac{1}{2}(sk/k_1 - q) f_1(\xi) + \frac{1}{2}(sk/k_1 + q) f_2(\xi)$$

$$+ \frac{2}{\pi}\int_0^1 f_1(\eta) K_{21}(\xi, \eta) d\eta + \frac{2}{\pi}\int_0^1 f_2(\eta) K_{22}(\xi, \eta) d\eta + \frac{2}{\pi}\int_0^1 f_3(\eta) K_{23}(\xi, \eta) d\eta = 0,$$

$$\frac{1}{2} sk/k_2 f_3(\xi) + \frac{2}{\pi}\int_0^1 f_1(\eta) K_{31}(\xi, \eta) d\eta$$

$$+ \frac{2}{\pi}\int_0^1 f_2(\eta) K_{32}(\xi, \eta) d\eta + \frac{2}{\pi}\int_0^1 f_3(\eta) K_{33}(\xi, \eta) d\eta = \frac{4}{\pi}\xi \int_0^{\pi/2} u'(\xi \sin\theta) d\theta$$

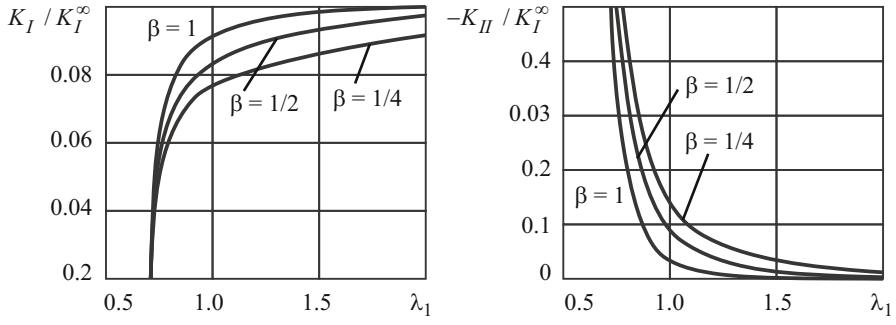

a *b*

Fig. 33

where $u(\xi) = (k_1 / C_{44} k_2)\,\xi^n \sigma^{(n)}(a\xi)$, $s = n_2^{-1/2} d_2 (1 - (d_2 l_2)/(d_1 l_1))^{-1}$, $q = n_3^{-1/2}$; k_1, k_2, and k are determined from (3.9).

The stress intensity factors are defined by

$$K_I = \frac{1}{4} C_{44} s \frac{k}{k_1} \sqrt{\pi a} \sum_{n=0}^{\infty} \cos n\theta \int_0^1 f_3(\eta) d\eta,$$

$$K_{II} = \frac{1}{4} C_{44} s \frac{k}{k_1} \sqrt{\pi a} \sum_{n=0}^{\infty} \cos n\theta [f_1(1) + f_2(1)],$$

$$K_{III} = \frac{1}{4} C_{44} q \sqrt{\pi a} \sum_{n=0}^{\infty} \sin n\theta [f_1(1) - f_2(1)], \tag{3.66}$$

whence follows that the interaction of two parallel cracks leads to qualitative changes in the asymptotic stress distribution near the crack tip compared with an isolated crack in an unbounded material, namely, to nonzero values of the stress intensity factors K_{II} and K_{III} for a near-surface crack loaded by normal tensile forces. Moreover, all the three SIFs depend on the prestresses since the parameters appearing in (3.66) and in the Fredholm equations depend on the initial elongation (or shortening) λ_1 caused by the prestresses $S_0^{11} = S_0^{22}$.

3.3.2. Axisymmetric Problem for Mode I Cracks [4, 62, 72, 123]. Let normal stresses of intensity $\sigma(r)$ symmetric about the crack plane be applied to the crack faces. In the case of unequal roots, the stress intensity factors are defined by

$$K_I = -\frac{1}{2} C_{44} d_2 l_2 \sqrt{\pi a} f(1), \qquad K_{II} = \frac{1}{2} C_{44} d_2 n_2^{-1/2} \sqrt{\pi a} \int_0^1 g(\xi) d\xi, \qquad K_{III} = 0, \tag{3.67}$$

where the functions f and g can be found by solving the system of Fredholm equations of the second order

$$f(\xi) + \frac{2}{\pi k} \int_0^1 f(\eta) K_{11}(\xi, \eta) d\eta + \frac{2}{\pi k} \int_0^1 g(\eta) K_{12}(\xi, \eta) d\eta = \frac{4}{\pi} \int_0^{\pi/2} s(\xi \sin\theta) d\theta,$$

$$g(\xi) + \frac{2}{\pi k} \int_0^1 f(\eta) K_{21}(\xi, \eta) d\eta + \frac{2}{\pi k} \int_0^1 g(\eta) K_{22}(\xi, \eta) d\eta = 0,$$

$$s(\xi) = -\frac{\xi \sigma(a\xi)}{C_{44} d_2 l_2}, \tag{3.68}$$

with the following kernels:

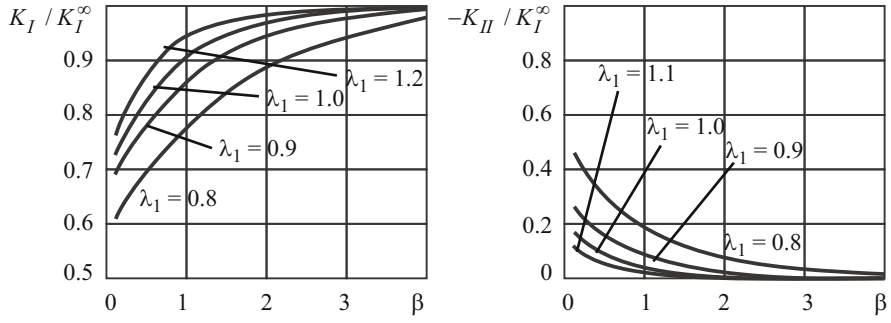

a *b*

Fig. 34

$$K_{11}(\xi,\eta) = k_1 I_1(2\beta_1,\eta) - k_2 I_1(2\beta_2,\eta),$$

$$K_{12}(\xi,\eta) = k_1\{[I_0(2\beta_1,1) - I_0(2\beta_2,1)] - \eta^{-1}[I_0(2\beta_1,\eta) - I_0(2\beta_2,\eta)]\},$$

$$K_{21}(\xi,\eta) = -k_2\xi\left[I_2(2\beta_1,\eta) - I_2(2\beta_2,\eta)\right],$$

$$K_{22}(\xi,\eta) = -\xi\{[k_2 I_1(2\beta_1,1) - k_1 I_1(2\beta_2,1)] - \eta^{-1}[k_2 I_1(2\beta_1,\eta) - k_1 I_1(2\beta_1,\eta)]\} \tag{3.69}$$

($\beta_i = n_i^{-1/2}\beta$ ($i = 1, 2$), $I_0 = 0.25\ln(\zeta+1)/(\zeta-1)$; ζ, I_1, and I_2 are defined by (3.61).

Formulas (3.67) indicate that the interaction of cracks with each other results in nonzero K_{II} in the problem for mode I cracks (it follows from (3.38) that $K_{II} = 0$ for a prestressed unbounded body with an isolated mode I crack). Note that a similar effect was discovered in solving the axisymmetric problem for two parallel coaxial mode I cracks in a body without prestresses [135]. Moreover, both K_I and K_{II} depend on the prestresses and the distance between the cracks because the functions $f(\xi)$ and $g(\xi)$ following from (3.68) also depend on these parameters.

We will now discuss numerical results for specific materials with cracks under uniform normal load $\sigma(r) = \sigma = \text{const}$ applied to their faces.

Material with Bartenev–Khazanovich Potential. Figures 33*a* and 33*b* show the variation in K_I / K_I^∞ and $-K_{II} / K_I^\infty$, respectively (K_I^∞ is the SIF for a mode I crack in an unbounded body without prestresses) with λ_1 for different values of the dimensionless distance $\beta = h / a$ between the cracks. It can be seen that K_I and K_{II} are strongly dependent on the prestresses. The vertical asymptotes in Fig. 33*b* represent a resonant phenomenon occurring when the initial compressive stresses (and, hence, the parameter $\lambda_1 < 1$) reach the critical level at which local buckling occurs (in a mode symmetric about the crack plane $y_3 = -h$) under compression along the cracks.

Material with Treloar Potential. Figure 34 illustrates the variation in the ratios K_I / K_I^∞ and $-K_{II} / K_I^\infty$ with the dimensionless semidistance between the cracks. It can be seen that the interaction of the cracks with each other leads to a considerable decrease in the SIFs compared with the case of a mode I crack in an unbounded body either with compressive ($\lambda_1 = 0.8$, $\lambda_1 = 0.9$) or tensile ($\lambda_1 = 1.1$, $\lambda_1 = 1.2$) prestresses or without prestresses ($\lambda_1 = 1.0$). For example, if $\lambda_1 = 0.8$ and the distance between two parallel cracks is equal to quarter the crack radius, then K_I is less than K_I^∞ by 40%. As the distance between the cracks increases, their interaction sharply weakens. When $\beta > 4$ (i.e., the distance between the cracks is greater than eight crack radii), it can be neglected for the purpose of practical calculations because the values of K_I for all examined values of λ_1 differ from K_I^∞ by less than 2%, while K_{II} is almost zero. A similar effect was observed in problems for two parallel coaxial cracks in a material without prestresses [50].

Laminated Two-Component Composite with Isotropic Plies. For a composition of aluminoborosilicate-glass and maleic epoxy resin plies (see Sec. 2.2), Fig. 35 shows the graph of K_I / K_I^∞ versus the volume fraction c_1 of glass for different values of λ_1. It can be seen that the prestresses and the mechanical characteristics of the composite affect the values of the SIFs.

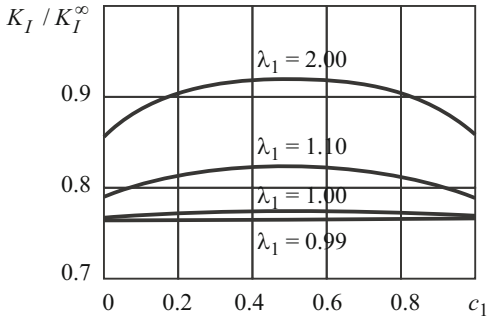

Fig. 35

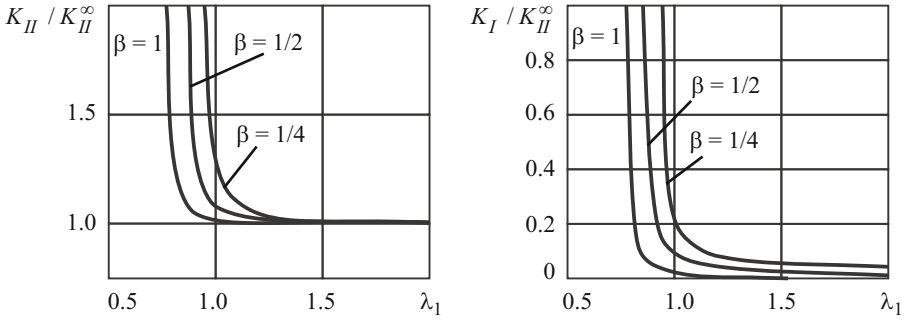

a *b*

Fig. 36

3.3.3. Axisymmetric Problem for Mode II Cracks [62, 123]. Let tangential radial stresses of intensity $\tau(r)$ antisymmetric about the crack planes $y_3 = 0$ and $y_3 = -2h$ be applied to the crack faces. The stress intensity factors are defined by (3.67), and the functions f and g are determined by solving the system of integral equations

$$f(\xi) - \frac{2}{\pi k}\int_0^1 f(\eta)K_{11}(\xi,\eta)d\eta - \frac{2}{\pi k}\int_0^1 g(\eta)K_{12}(\xi,\eta)d\eta = 0,$$

$$g(\xi) - \frac{2}{\pi k}\int_0^1 f(\eta)K_{21}(\xi,\eta)d\eta - \frac{2}{\pi k}\int_0^1 g(\eta)K_{22}(\xi,\eta)d\eta = -\frac{4}{\pi}\xi\int_0^{\pi/2} p'(\xi\sin\theta)d\theta,$$

$$p(\xi) \equiv -\frac{\xi\tau(a\xi)}{C_{44}n_2^{-1/2}d_2} \tag{3.70}$$

with kernels (3.69).

In this problem, the interaction between the cracks is the cause of a new mechanical effect: nonzero stress intensity factor K_I ($K_I = 0$ in the problem for an isolated mode II crack in a prestressed unbounded body, according to (3.42)).

We will discuss, as an example, numerical results for a Bartenev–Khazanovich material with cracks subject to a uniform shear load $\tau(r) = \tau = \text{const}$ on their faces. Figures 36*a* and 36*b* show the variation in K_{II} / K_{II}^∞ and K_I / K_{II}^∞, respectively (K_{II}^∞ is the SIF for a mode II crack in an unbounded body without prestresses) with λ_1 for different values of the dimensionless distance $\beta = h / a$ between the cracks. It can be seen that the prestresses have a strong effect on the SIFs. The vertical asymptotes in the range of compressive prestresses ($\lambda_1 < 0$) represent a resonant phenomenon occurring when the initial compressive stresses reach the critical level at which local buckling occurs (in a mode antisymmetric about the crack plane $y_3 = -h$ and a flexural mode) under compression along cracks. Note that the critical (limiting) compressive stresses $\lambda_1 < 1$ for an antisymmetric (flexural) buckling mode are higher (and the critical (limiting) tensile stresses are lower) than those obtained in Sec. 3.3.2 (see Fig. 33) for a symmetric buckling mode.

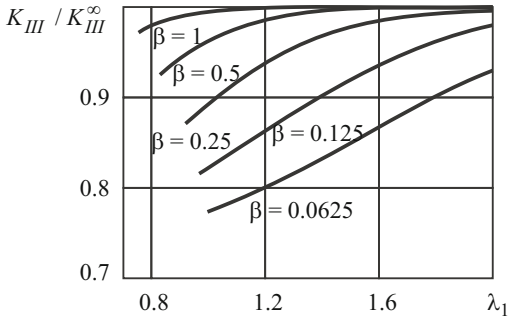

Fig. 37

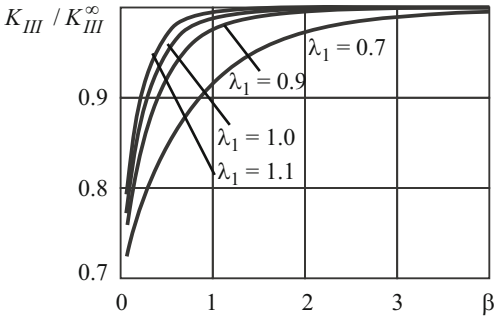

Fig. 38

Similar graphs of K_{II}/K_{II}^{∞} and K_I/K_{II}^{∞} versus λ_1 were obtained in [123] for a Treloar material.

3.3.4. Mode III Cracks [7, 123]. Let tangential torsional stresses of intensity $\tau_\theta(r)$ antisymmetric about the planes of the cracks be applied to their faces. The stress intensity factors are defined by

$$K_I = 0, \quad K_{II} = 0, \quad K_{III} = \frac{1}{2} C_{44} n_3^{-1/2} \sqrt{\pi a} \int_0^1 f(\eta) d\eta, \tag{3.71}$$

where the function f is determined by solving the Fredholm equation of the second kind

$$f(\xi) + \frac{1}{\pi} \int_0^1 f(\eta) K(\xi, \eta) d\eta = \frac{4}{\pi} \xi \int_0^{\pi/2} q'(\xi \sin\theta) d\theta, \tag{3.72}$$

where $q(\xi) = \dfrac{\xi \tau_\theta(a\xi)}{C_{44} n_3^{-1/2}}$, with kernel

$$K(\xi, \eta) = 8\beta_3 \xi^2 \left[\frac{1}{(4\beta_3^2 + \xi^2 + \eta^2)^2 - 4\xi^2\eta^2} - \frac{1}{(4\beta_3^2 + \xi^2 + 1)^2 - 4\xi^2} \right], \quad \beta_3 = n_3^{-1/2}\beta.$$

We will discuss numerical results for some materials with a crack subject to a load $\tau_\theta(r) = \tau = \text{const}$ on its faces.

Material with Bartenev–Khazanovich Potential. Figure 37 shows the variation in K_{III}/K_{III}^{∞} with λ_1 for different values of β. It can be seen that the prestresses have a strong effect on the stress intensity factor K_{III}. However, no resonant changes in the SIF are observed here, unlike the problems for mode I and II crack, because, obviously, when a material with two parallel cracks is compressed, no torsional buckling mode occurs.

Material with Treloar Potential. For this material, Fig. 38 illustrates the dependence of the SIFs on the relative semidistance between the cracks normalized to the crack radius. It can be seen that the interaction of two parallel coaxial mode III cracks decreases K_{III} compared with K_{III}^{∞} for a body with an isolated crack, i.e., somewhat "hardens" the body. Note that a similar behavior of two mode III cracks was observed in [142] in solving a similar problem for a material without prestresses. As the distance between the cracks increases, their interaction gradually weakens and can be neglected when this distance is greater than eight crack radii.

3.3.5. Critical Loads for Compression along Two Parallel Coaxial Cracks. According to the combined approach outlined in Sec. 1.4, the critical (limiting) compressive loads causing local buckling of a material compressed along two parallel coaxial cracks (Fig. 32*b*) are determined from the solution of the above inhomogeneous problems for a prestressed material with two parallel coaxial cracks as the initial compressive stresses at which stress intensity factors increase sharply.

For example, the critical compressive loads causing symmetric local buckling of the material near the cracks can be determined from the results obtained in Sec. 3.3.2 in solving the problem for a body with mode I cracks. Similarly, the critical

TABLE 2

β	0.0625	0.125	0.25	0.5	1.0	2.0	5.0	10.0
$\varepsilon_1^{(1)}$	0.2643	0.3035	0.3070	0.3074	0.3069	0.3076	0.3067	0.3066
$\varepsilon_1^{(2)}$	0.0080	0.0354	0.0894	0.1675	0.2420	0.2877	0.3048	0.3064

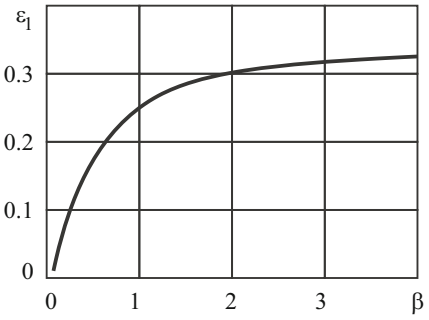

Fig. 39

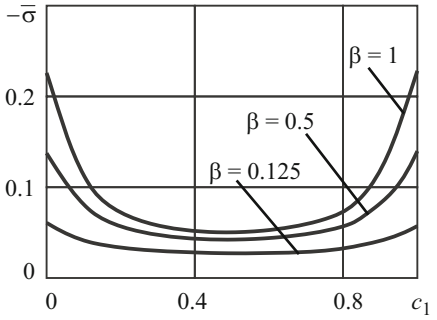

Fig. 40

compressive stresses that cause antisymmetric (flexural) local buckling of a material compressed along two parallel cracks can be found from the numerical results obtained in Sec. 3.3.3 in solving the problem for a body with mode II cracks. It was shown in Sec. 3.3.4 that no resonant effects occur in the problems for two mode III cracks, which suggests the absence of torsional buckling mode for such an arrangement of cracks.

For a Bartenev–Khazanovich material, Table 2 summarizes the values of relative critical (limiting) shortening $\varepsilon_1 = 1 - \lambda_1$ at which local buckling occurs in a material compressed along two parallel coaxial cracks for different values of β (the superscript "(1)" refers to a symmetric buckling mode, and the superscript "(2)" refers to an antisymmetric (flexural) buckling mode). It can be seen that $\varepsilon_1^{(2)} < \varepsilon_1^{(1)}$ in the entire range of variation in β, i.e., the material buckles in a flexural mode. When the spacing between cracks is small, they interact, thus considerably reducing the critical compressive loads. As the distance between cracks increases, the relative critical shortening tends to $\varepsilon_1^* = 0.307$ corresponding to the critical (limiting) compressive stresses for an isolated crack in an unbounded body with Bartenev–Khazanovich potential (see Sec. 3.1.1).

It follows from [4, 62, 123] that other hyperelastic materials (including those with Treloar potential) and composites buckle in a flexural mode. Therefore, we will omit below the superscript "(2)" for the flexural buckling mode.

Figure 39 shows the relative critical shortening $\varepsilon_1 = 1 - \lambda_1$ versus β for a Treloar material. The behavior of this graph is similar to that for the Bartenev–Khazanovich material.

For a laminated composite (composition of aluminoborosilicate glass and maleic epoxy resin), Fig. 40 shows the critical compressive stresses normalized to the reduced elastic modulus $\overline{\sigma} = S_0^{11} / E$ versus the volume fraction c_1 of glass for different values of β. As can be seen, the volume fractions of the components of the composite have a strong effect on the critical (limiting) compressive stresses.

Figure 41 shows the variation in ε_1 with the dimensionless semidistance β between the cracks in a composite reinforced with random short ellipsoidal carbon fibers in the planes $y_3 = \text{const}$. When the spacing between the cracks is small, they interact which considerably reduces the critical compressive loads. For example, when $\beta = 1/16$, ε_1 is less by a factor of almost 15 than that for a material compressed along an isolated crack.

3.3.6. Conclusions. Based on the above results on problems for two parallel coaxial circular cracks in a prestressed material, we may draw the following conclusions.

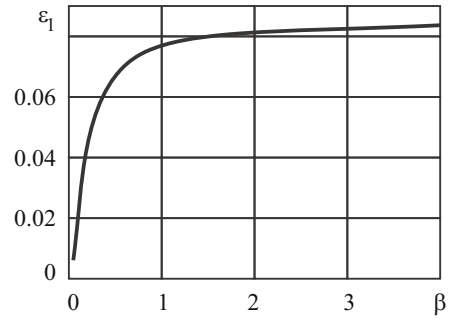

Fig. 41

The stress intensity factors are strongly dependent on the prestresses for all cracks considered (mode I, II, and III cracks) and for nonaxisymmetric and axisymmetric problem formulations. This is what differs the problems for two parallel coaxial cracks and the problem for an unbounded body with an isolated crack (Sec. 3.1.1) where the stress intensity factors do not depend on the prestresses (except for the general nonaxisymmetric problem for a mode II or III crack), while the crack opening displacements depend on the prestresses.

When normal and radial shear loads act on the crack faces, the stress intensity factors change resonantly as the initial compressive loads tend to the critical level that causes local buckling of the material near the cracks. However, when torsional loads act on the crack faces, no resonant phenomena occur, which suggests the absence of buckling modes under compression along two parallel cracks in the torsion problem.

Moreover, the interaction between the cracks results in nonzero values of K_{II} and K_I. It should be noted that this effect is similar to that in the problem for two parallel coaxial cracks solved using the classical fracture mechanics of materials without prestresses [135].

At short relative distances between the cracks, the interaction between them results in a decrease in K_I, an increase in K_{II}, and a decrease in K_{III} compared with the SIFs for an isolated mode I, II, and III cracks, respectively. These effects of interaction between the cracks in a prestressed material are similar to those revealed in solving the same problems using the classical fracture mechanics of materials without prestresses [50, 135, 142].

As the relative distance between the cracks increases, the interaction between them gradually weakens and the SIFs tend to those for an isolated crack. The interaction of two parallel cracks can be neglected for the purpose of practical calculations when the distance between them exceeds eight crack radii.

By analyzing the resonant change in the stress intensity factors (obtained by solving the problems for mode I and II cracks) occurring as the initial compressive loads tend to the level causing local buckling of the material near the crack, we have determined the critical (limiting) compressive loads for different materials compressed along two parallel coaxial cracks. It has been shown that buckling occurs in an antisymmetric (flexural) mode in all examined materials under compression.

The stress intensity factors and critical (limiting) compressive stresses are strongly dependent on the geometry of the problems (the distance between the cracks and crack radius) and the mechanical characteristics of the materials.

3.4. Periodic Array of Parallel Coaxial Penny-Shaped Cracks in a Space. Consider an unbounded elastic body with prestresses $S_0^{11} = S_0^{22}$ acting along an infinite array of coaxial penny-shaped cracks of radius a located in parallel planes $y_3 = \text{const}$: $\{r < a, 0 \le \theta < 2\pi, y_3 = 2hn, n = 0, \pm 1, \pm 2, \dots\}$ (Fig. 42). The crack faces are loaded by additional (to the prestresses $S_0^{11} = S_0^{22}$) mutually balanced stresses (mode I, II, or III (Fig. 42a)) or are free from stresses (as in the problem of the compression of a material along cracks; Fig. 42*b*).

Since the geometry and system of forces of the problem are symmetric about the plane $y_3 = 0$ and the components of the stress tensor and displacement vector are periodic (with period $2h$) in y_3, the original linearized problem for a body with a periodic array of parallel coaxial cracks can be reduced to a mixed boundary-value problem for the layer $0 \le y_3 \le h$.

Problems for a periodic array of parallel coaxial cracks in prestressed materials were addressed in [6, 64, 65, 68, 69, 123].

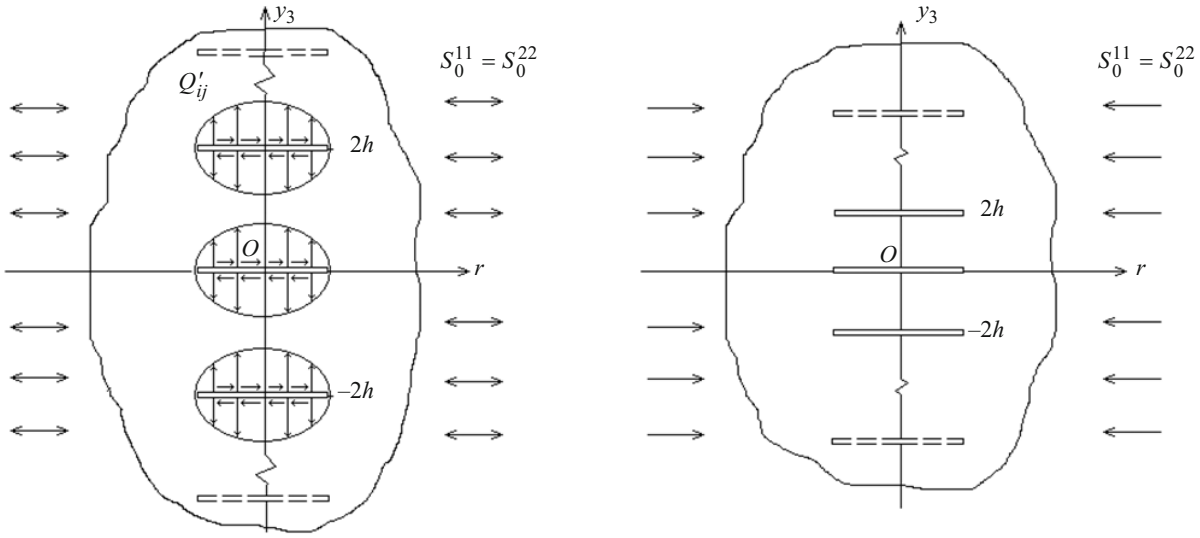

a *b*

Fig. 42

3.4.1. Nonaxisymmetric Problem [6]. Let normal tensile loads of equal intensity $\sigma(r,\theta)$ act on the crack faces. As indicated above, the problem can be reformulated for the layer $0 \le y_3 \le h$ with a crack in the plane $y_3 = 0$. The boundary conditions on the crack faces and the boundary of the half-space are the following (hereafter $0 \le \theta \le 2\pi$):

$$u_3 = 0 \quad (y_3 = 0,\ r > a),$$

$$Q'_{33} = -\sigma(r,\theta) \quad (y_3 = 0,\ r < a),$$

$$Q'_{3r} = 0, \quad Q'_{3\theta} = 0 \quad (y_3 = 0, 0 \le r < \infty),$$

$$u_3 = 0, \quad Q'_{3r} = 0, \quad Q'_{3\theta} = 0 \quad (y_3 = h, 0 \le r < \infty). \tag{3.73}$$

For the problem of the compression of a material along cracks (Fig. 42*b*), it is necessary to replace the second boundary condition in (3.73) by $Q'_{33} = 0\ (y_3 = 0,\ r < a)$.

Representing the general solutions of the linearized equilibrium equations in terms of harmonious potential functions (2.77), (2.80) and expanding these potential functions into Fourier series in the circumferential coordinate with coefficients in the form of Hankel transforms over the radial coordinate and expanding the function $\sigma(r,\theta)$ into Fourier series (3.52), we reduce the problem to a system of dual integral equations for each harmonic in θ and then to a Fredholm equation of the second order (see [6] for more details), which have the following form in the case of unequal roots:

$$\widetilde{\omega}_n(x) - \frac{2}{\pi}\int_0^a \widetilde{\omega}_n(t) K_n(x,t)\,dt = \frac{2}{\pi} x \int_0^{\pi/2} \Sigma'_n(x\sin\theta)\,d\theta, \quad 0 \le x \le a,\ n = 0, 1, 2, 3\ldots,$$

$$\Sigma_n(x) = -\frac{1}{C_{44} d_1 l_1} \frac{k_1}{k} x^n \sigma_n(x) \tag{3.74}$$

with kernel

$$K_n(x,t) = \frac{x^{n+1/2}}{k} \int_0^\infty \left[t^{-n+1/2} J_{n-1/2}(\lambda t) J_{n-1/2}(\lambda x) - a^{-n+1/2} J_{n-1/2}(\lambda a) J_{n-1/2}(\lambda x) \right] \left[k_1 \frac{e^{-\mu_1}}{\sinh \mu_1} - k_2 \frac{e^{-\mu_2}}{\sinh \mu_2} \right] \lambda\, d\lambda,$$

where $\mu_i = \lambda n_i^{-1/2} h$ $(i = 1, 2)$; k_1, k_2, and k are determined from (3.9).

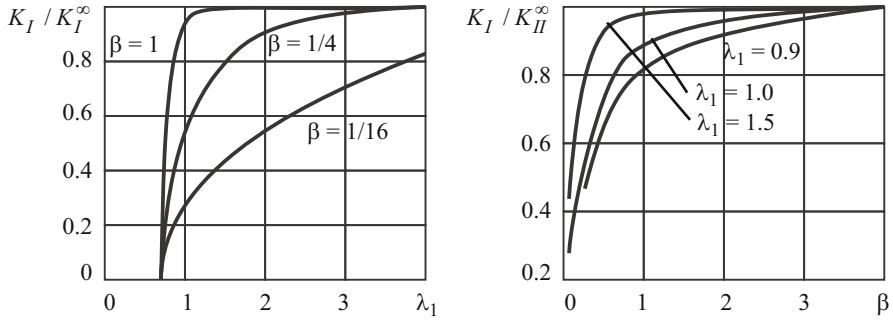

a *b*

Fig. 43

Analyzing the asymptotic stress distribution near the crack, we obtain the following expressions for the stress intensity factors:

$$K_I = -\sqrt{\pi} C_{44} d_1 l_1 \frac{k}{k_1} \sum_{n=1}^{\infty} \cos(n\theta) a^{-n-1/2} \int_0^a \tilde{\omega}_n(t)\,dt, \qquad K_{II} = 0, \qquad K_{III} = 0, \tag{3.75}$$

where $\tilde{\omega}_n(t)$ are determined from (3.74).

It is clear that K_I depends on the prestresses since the parameters appearing in (3.75) and in the Fredholm equation (3.74) depend on the initial elongation (or shortening) λ_1 caused by the prestresses $S_0^{11} = S_0^{22}$.

In the limiting case where the distance between the cracks tends to infinity, the expression for K_I follows from (3.75), (3.74):

$$K_I^\infty \equiv \lim_{h\to\infty} K_I = \frac{2}{\sqrt{\pi}} \sum_{n=1}^{\infty} \frac{\cos(n\theta)}{a^{n+1/2}} \int_0^a \frac{t^{n+1}}{\sqrt{a^2 - t^2}} \sigma_n(t)\,dt. \tag{3.76}$$

If the load on the crack faces is defined by $\sigma(r, \theta) = \sigma_1(r)\cos\theta$, we normalize the variables to the crack radius and introduce functions $\xi \equiv a^{-1}x$, $\eta \equiv a^{-1}t$, $f_1(\xi) \equiv a^{-1}\tilde{\omega}_1(a\xi) = a^{-1}\tilde{\omega}_1(x)$ to nondimensionalize the Fredholm equation:

$$f_1(\xi) - \frac{2}{\pi} \int_0^1 f_1(\eta) K_1(\xi, \eta)\,d\eta = \frac{2}{\pi} \xi \int_0^{\pi/2} \Sigma_1'(\xi \sin\theta)\,d\theta, \qquad 0 \le \xi \le 1, \tag{3.77}$$

with kernel $K_1(\xi, \eta) = \xi\{\eta^{-1}[R(\xi - \eta) - R(\xi + \eta)] - [R(\xi - 1) - R(\xi + 1)]\}$, where

$$R(z) = \frac{1}{k}\left[\frac{k_1}{\beta_1} \operatorname{Re}\psi\left(1 + \frac{iz}{2\beta_1}\right) - \frac{k_2}{\beta_2} \operatorname{Re}\psi\left(1 + \frac{iz}{2\beta_2}\right)\right], \tag{3.78}$$

$\operatorname{Re}\psi(1 + iz/2\beta_j)$, $j = 1, 2$, is the real part of the psi-function $\psi(z) = (d \ln \Gamma(z))/dz$ ($\Gamma(z)$ is the gamma function).

Then we have $K_I = -\sqrt{\pi a} C_{44} d_1 l_1 \frac{k}{k_1} \int_0^1 f_1(\eta)\,d\eta \cos\theta$.

We will discuss numerical results for some hyperelastic materials with a crack subject to a normal tensile force $\sigma(r, \theta) = \sigma_1(r)\cos\theta$, $\sigma_1(r) = \sigma = \text{const}$, on its faces.

For a Bartenev–Khazanovich material, Fig. 43*a* shows the variation in K_I / K_I^∞ (where K_I^∞ is the SIF for an isolated mode I crack determined from (3.76)) with λ_1 for different values of $\beta = h/a$. It can be seen that the prestresses have a strong effect on the SIF especially in the range where the prestresses are compressive.

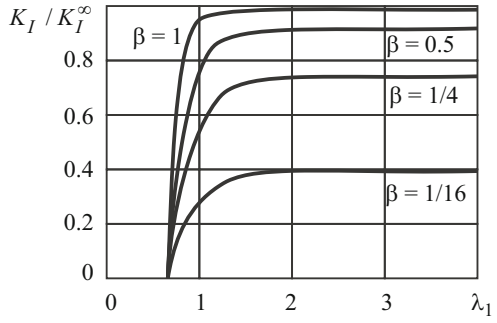

Fig. 44

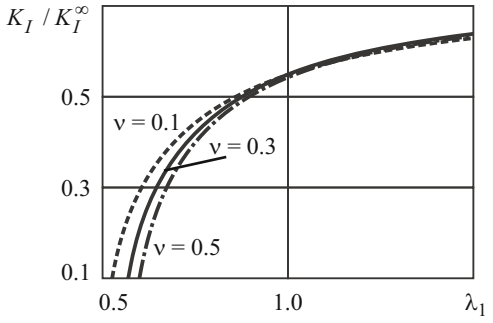

Fig. 45

Figure 43*b* shows, for the same material, the variation in K_I / K_I^∞ with β. It can be seen that the interaction of the cracks in a prestressed body leads to a decrease (especially at short distances between the cracks) in K_I compared with K_I^∞. For example, for $\lambda_1 = 0.9$ and $\beta = 0.25$, the K_I is less than K_I^∞ by a factor of 2.2. As the distance between the cracks increases, their interaction weakens and the corresponding SIFs tend to K_I^∞.

Figures 44 and 45 show the dependence of K_I / K_I^∞ on λ_1 for, respectively, a material with Treloar potential (for different values of β) and a material with harmonic potential (for $\beta = 0.25$ and different values of Poisson's ratio ν). It can be seen that the compressibility of the material considerably affects the stress intensity factors. For example, when $\lambda_1 = 0.7$, the value of K_I for the material with harmonic potential and Poisson's ratio $\nu = 0.1$ exceeds by 20% the value of K_I for the same material with $\nu = 0.5$.

3.4.2. Axisymmetric Problem for Mode I Cracks [64, 68, 123]. Let normal stresses of intensity $\sigma(r)$ symmetric about the crack plane be applied to the crack faces. The problem can be reformulated for the layer $0 \le y_3 \le h$ with a crack in the plane $y_3 = 0$ with boundary conditions similar to (3.73).

Applying the Hankel transform to the potential harmonic functions, we can reduce the problem to dual integral equations and then to the Fredholm equation of the second kind (see [68] for more details), which has the following dimensionless form in the case of unequal roots:

$$f(\xi) - \frac{1}{\pi}\int_0^1 f(\eta)K(\xi,\eta)d\eta = \frac{2}{\pi}\xi\int_0^{\pi/2} s(\xi\sin\theta)\sin\theta\, d\theta, \qquad s(\xi) \equiv -\frac{k_1\sigma(a\xi)}{kC_{44}d_1l_1} \tag{3.79}$$

with kernel $K(\xi,\eta) = R(\xi-\eta) - R(\xi+\eta)$, where $R(z)$ is defined by (3.78).

The SIFs are expressed by

$$K_I = -C_{44}d_1l_1\frac{k}{k_1}\sqrt{\pi a}\,f(1), \qquad K_{II} = 0, \qquad K_{III} = 0, \tag{3.80}$$

where f can be found by solving the integral equation (3.79).

It follows from (3.80) that the stress intensity factor K_I depends on the prestresses. We will now discuss numerical results for specific materials with cracks under uniform normal load $\sigma(r) = \sigma = \text{const}$ applied to their faces.

Material with Bartenev–Khazanovich Potential. Figure 46*a* shows the dependence of K_I / K_I^∞ on λ_1 for $\beta = 0.25$ and $\beta = 1.0$. Hereafter the solid lines represent a periodic array of parallel coaxial cracks, and the dashed lines represent, for comparison, two parallel coaxial cracks (Sec. 3.3). It can be seen that the stress intensity factors are strongly dependent on λ_1. Moreover, the values of K_I / K_I^∞ for a periodic array of cracks are lower than those for two parallel coaxial cracks (for the same values of β).

Figure 46*b* shows the variation in K_I / K_I^∞ with β for $\lambda_1 = 1.2$ (tensile prestresses), $\lambda_1 = 0.8$ (compressive prestresses), $\lambda_1 = 1.0$ (no prestresses). This demonstrates that the interaction among cracks in a periodic array of coaxial mode I cracks, as well

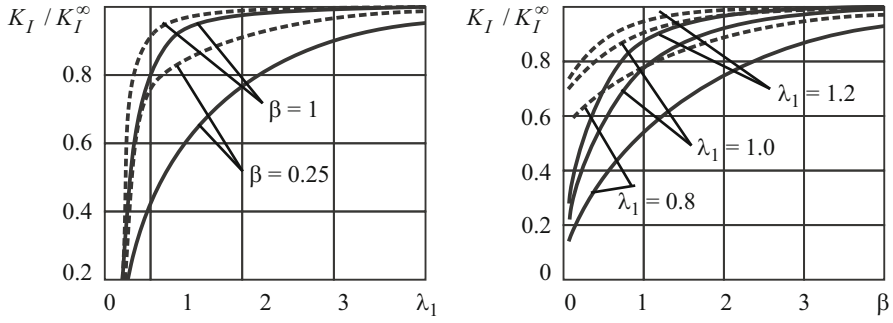

a *b*

Fig. 46

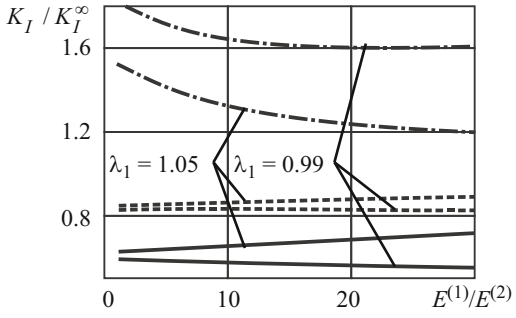

Fig. 47

as between two parallel coaxial mode I cracks, leads to a decrease in K_I compared with K_I^∞ for an isolated crack in an unbounded material. As the distance between the cracks increases, the interaction between them weakens and the corresponding SIFs tend to those for an isolated crack in an unbounded body.

Similar curves were drawn in [68] for materials with Treloar and harmonic potentials.

Laminated Two-Component Composite with Isotropic Plies. Figure 47 shows the substantial dependence of K_I / K_I^∞ on the ratio of elastic moduli of the plies for $\nu^{(1)} = \nu^{(2)} = 0.3, c_1 = 0.3, \lambda_1 = 1.05$ (tensile prestresses), and $\lambda_1 = 0.99$ (compressive prestresses). The results are presented for a periodic array of cracks (solid lines), two parallel cracks (dashed lines), and a near-surface crack (dash-and-dot lines) subject to a uniform normal load. The semidistance between the two parallel cracks is equal to that between cracks in the periodic array and the distance between the crack and the free boundary $\beta = 0.5$.

3.4.3. Axisymmetric Problem for Mode II Cracks [65, 69, 123]. Let tangential radial stresses of intensity $\tau(r)$ symmetric about the crack planes be applied to the crack faces. The equivalent boundary conditions for the layer $0 \le y_3 \le h$ with a crack in the plane $y_3 = 0$ are

$$Q'_{3r} = -\tau(r) \quad (y_3 = 0, 0 < r \le a),$$

$$u_r = 0, \quad Q'_{33} = 0 \quad (y_3 = h, \ 0 \le r < \infty),$$

$$u_r = 0 \quad (y_3 = 0, a < r < \infty),$$

$$Q'_{33} = 0 \quad (y_3 = 0, \ 0 \le r < \infty).$$

The problem posed is reduced to a Fredholm equation of the second kind [69], which has the following dimensionless form in the case of unequal roots:

$$f(\xi) - \frac{1}{\pi}\int_0^1 f(\eta)K(\xi,\eta)d\eta = \frac{2}{\pi}\xi\int_0^{\pi/2} p'(\xi\sin\theta)d\theta, \qquad p(\xi) = \frac{k_2\xi\tau(a\xi)}{kC_{44}n_1^{-1/2}d_1} \tag{3.81}$$

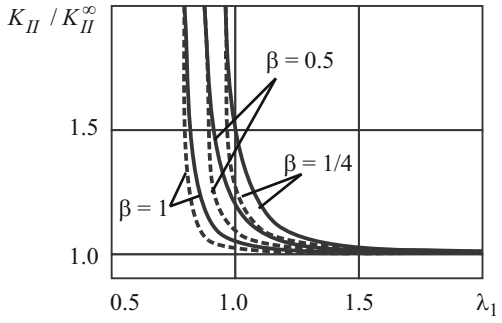

Fig. 48

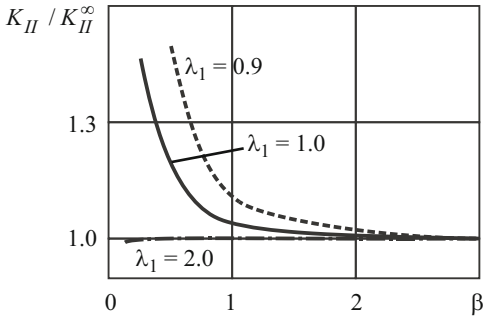

Fig. 49

with kernel $K(\xi,\eta)=\xi\eta^{-1}\left[R_1(\xi-\eta)-R_1(\xi+\eta)\right]-\xi\left[R_1(\xi-1)-R_1(\xi+1)\right]$, where

$$R_1(z)=\frac{1}{k}\left[\frac{k_1}{\beta_2}\operatorname{Re}\psi\left(1+\frac{iz}{2\beta_2}\right)-\frac{k_2}{\beta_1}\operatorname{Re}\psi\left(1+\frac{iz}{2\beta_1}\right)\right].$$

The SIFs are expressed by

$$K_I=0,\qquad K_{II}=C_{44}d_1n_1^{-1/2}\frac{k}{k_2}\sqrt{\pi a}\int_0^1 f(\eta)d\eta,\qquad K_{III}=0, \tag{3.82}$$

where f can be found by solving Eq. (3.81).

It follows from (3.82) that the stress intensity factor K_{II} depends on the prestresses. Numerical results are presented below for some materials with cracks subject to uniform shear forces $\tau(r)=\tau=\text{const}$ on their faces.

For a Bartenev–Khazanovich material, Fig. 48 shows the variation in K_{II}/K_{II}^{∞} with λ_1 for different values of β (as before, the solid lines correspond to a periodic array of cracks, and the dashed lines to two parallel cracks). It can be seen that the stress intensity factors are strongly dependent on λ_1. Moreover, the values of K_I/K_I^{∞} for a periodic array of cracks are greater than those for two parallel coaxial cracks (for the same values of β). The vertical asymptotes in the range of compressive prestresses ($\lambda_1<1$) represent a resonant phenomenon occurring when the initial compressive stresses reach the critical level at which the material locally buckles (in a flexural mode) near the cracks.

Similar graphs of SIFs versus prestresses for other hyperelastic materials (material with Treloar and harmonic potential) were obtained in [69, 123].

For a Treloar material, Fig. 49 shows the variation in K_{II}/K_{II}^{∞} with β for different values of λ_1. It can be seen that the interaction of mode II cracks increases the stress intensity factor K_{II} compared with an isolated crack in an unbounded body. As the spacing between cracks increases, K_{II} decreases, tending to K_{II}^{∞}. When $\beta>3$, the interaction of cracks can be neglected in practical calculations because the difference between the stress intensity factors for a periodic array of cracks and for one crack in an unbounded body is less than 3%.

3.4.4. Mode III Cracks [123]. Let tangential circumferential load $\tau_\theta(r)$ antisymmetric about the planes of the cracks be applied to their faces. The stress intensity factors are defined by

$$K_I=0,\qquad K_{II}=0,\qquad K_{III}=-C_{44}n_3^{-1/2}\sqrt{\pi a}\int_0^1 f(\eta)d\eta, \tag{3.83}$$

where f can be found by solving the Fredholm equation

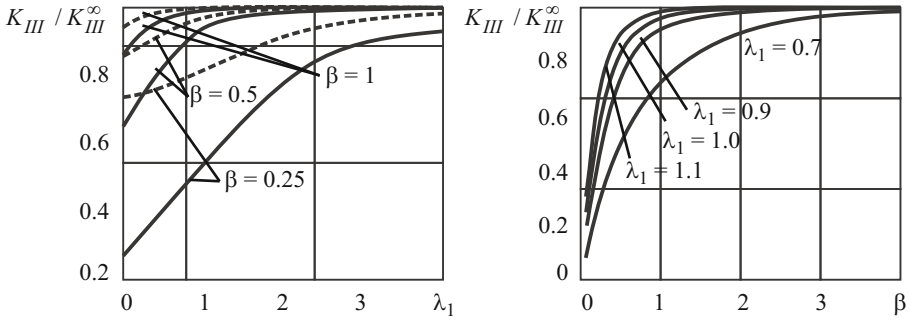

a *b*

Fig. 50

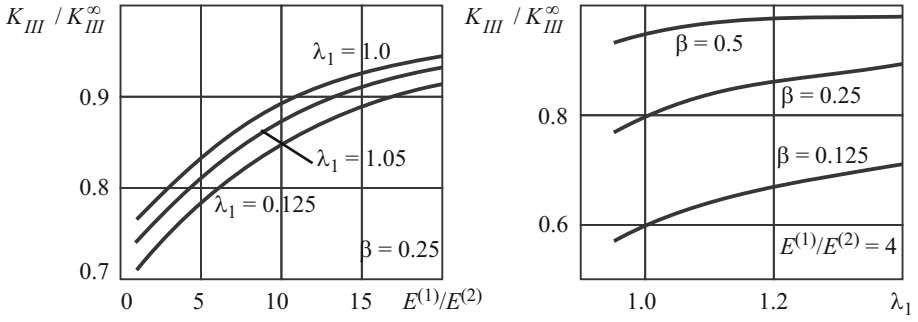

a *b*

Fig. 51

$$f(\xi)-\frac{1}{\pi}\int_0^1 f(\eta)K(\xi,\eta)d\eta=-\frac{2}{\pi}\xi\int_0^{\pi/2}q'(\xi\sin\theta)d\theta,\qquad q(\xi)=\frac{\xi\tau_\theta(a\xi)}{C_{44}n_3^{-1/2}}$$

with the following kernel:

$$K(\xi,\eta)=\frac{\xi}{\beta_3}\left\{\frac{1}{\eta}[R_3(\xi-\eta)-R_3(\xi+\eta)]-[R_3(\xi-1)-R_3(\xi+1)]\right\},$$

$$R_3(z)=\operatorname{Re}\psi(1+iz/(2\beta_3)).$$

We will discuss numerical results for some materials with a crack subject to a load $\tau_\theta(r)=\tau=\text{const}$ on its faces.

Material with Treloar Potential. Figures 50*a* and 50*b* show the dependence of K_{III}/K_{III}^{∞} on λ_1 and β, respectively (the solid lines correspond to a periodic array of cracks, and the dashed lines to two parallel cracks).

It can be seen that the prestresses have a strong effect on the stress intensity factors. However, unlike the problems for a prestressed body with a periodic array of mode I and II cracks, no resonant change in the SIF is observed here.

Figure 50*b* demonstrates that the interaction of the cracks leads to a decrease (especially at small values of β) in K_{III} compared with K_{III}^{∞} for an unbounded body with an isolated crack under a torsional load. As the distance between cracks increases, the value of K_{III} tends to the value of K_{III}^{∞}. When the distance between the cracks exceeds six crack radii, the difference between these SIFs is so small that can be neglected.

Laminated Two-Component Composite with Isotropic Plies. Figure 51*a* illustrates the dependence of K_{III}/K_{III}^{∞} on $E^{(1)}/E^{(2)}$ for $\beta=0.25$ and different values of λ_1. It can be seen that K_{III}/K_{III}^{∞} monotonically increases with $E^{(1)}/E^{(2)}$. Figure 51*b* shows the variation in K_{III}/K_{III}^{∞} with λ_1 for $E^{(1)}/E^{(2)}=4$ and different values of β. As can be seen, the SIF does not display resonant behavior because, obviously, there is no torsional buckling mode in a material with a periodic array of coaxial penny-shaped cracks in compression.

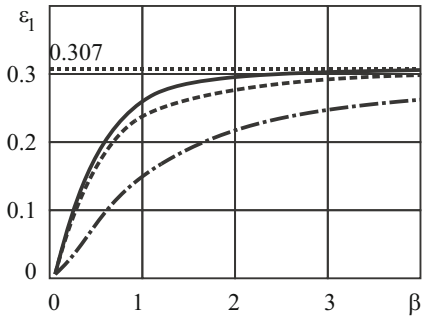

Fig. 52

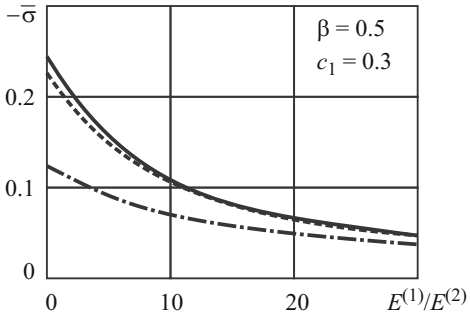

Fig. 53

3.4.5. Critical Loads for Compression along a Periodic Array of Parallel Coaxial Cracks. According to the combined approach outlined in Sec. 1.4, the critical (limiting) compressive loads causing local buckling of a material compressed along a periodic array of parallel coaxial cracks (Fig. 42*b*) are determined from the solution of the above inhomogeneous problems for a prestressed material with a periodic array of parallel coaxial cracks as the initial compressive stresses at which the stress intensity factors increase resonantly.

For example, the critical compressive stresses that cause antisymmetric (flexural) local buckling of a material compressed along a periodic array of parallel cracks can be found from the results obtained in Sec. 3.4.3 in solving the problem for a body with mode II cracks. It was shown in Sec. 3.4.4 that no resonant effects occur in the problems for a periodic array of mode III cracks, which suggests the absence of torsional buckling mode for such an arrangement of cracks.

Figure 52 presents the values of the critical (limiting) shortening $\varepsilon_1 = 1 - \lambda_1$ calculated using the above approach for a Bartenev–Khazanovich material. The figure illustrates dependence of ε_1 on $\beta = h / a$ for a periodic array of parallel cracks (Fig. 42*b*) (solid line), two parallel coaxial cracks (Fig. 32*b*) (dashed line), a near-surface crack parallel to the free surface of the material (Fig. 13*b*) (the dash-and-dot line), and an isolated crack (Fig. 10*b*) (dashed line). The parameter β is the semidistance between cracks divided by the crack radius for a periodic array of cracks and two cracks and is the distance between the crack and the boundary of the body divided by the crack radius for a near-surface crack. The results for a periodic array of cracks and two cracks are presented for the flexural buckling mode because the value of ε_1 for the symmetric mode is much greater than the value of ε_1 for the flexural mode [33, 68, 69]. In the case of a near-surface crack, the values of ε_1 for the flexural and symmetric modes coincide (Sec. 3.2).

It can be seen that the interaction of cracks with each other (for a periodic array of parallel cracks and two parallel cracks) or with the free boundary of the material (for a near-surface crack) leads to a substantial decrease in the critical (limiting) shortening ε_1 (and, hence, to a decrease in the critical compressive load) compared with the case of an isolated crack in an unbounded body ($\varepsilon_1^* = 0.307$). Moreover, in the entire range of variation in β, the values of ε_1 for a periodic array of cracks appear greater than those for two parallel cracks and a near-surface crack, but less than those for an isolated crack, which is physically consistent.

Similar graphs of ε_1 versus β for a Treloar material were drawn in [123].

Table 3 gives values of $\varepsilon_1 < 1$ (versus different values of β and ν) corresponding to the flexural buckling mode of a material with harmonic potential compressed along a periodic array of parallel coaxial cracks. When β is great, the value of ε_1 is equal to the critical value $\varepsilon_1^* = (2+\nu)^{-1}$ for an isolated crack in an unbounded material.

For a laminated two-component composite with isotropic plies, Fig. 53 shows the dimensionless critical compressive stresses $\bar{\sigma} = S_0^{11} / E$ (the stresses divided by the reduced elastic modulus) versus the ratio of the elastic moduli of the plies (the solid line represents a periodic array of cracks). For comparison, the figure also shows $\bar{\sigma}$ versus $E^{(1)} / E^{(2)}$ for two parallel cracks (dashed line) and a near-surface crack (dash-and-dot line). Note that the critical compressive stresses for a periodic array of cracks and for two parallel cracks correspond to the flexural buckling mode (determined from the solution for mode II cracks) because the values of $\bar{\sigma}$ corresponding to the symmetric buckling mode (determined from the solution for mode I cracks) appeared much higher than those for the flexural mode [33, 64, 65].

TABLE 3

ν	β								
	0.0625	0.125	0.25	0.50	0.75	1.00	2.00	5.00	10.00
0.1	0.0159	0.0529	0.1377	0.2631	0.338	0.3842	0.4565	0.4756	0.4762
0.2	0.0145	0.0481	0.1247	0.2399	0.3107	0.3562	0.4312	0.4538	0.4545
0.3	0.0133	0.0439	0.113	0.2182	0.2849	0.3291	0.4067	0.4337	0.4347
0.4	0.0123	0.0401	0.102	0.1974	0.2597	0.3023	0.3822	0.4151	0.4166
0.5	0.0114	0.0365	0.0916	0.1769	0.2343	0.2749	0.3567	0.3975	0.3999

3.4.6. Conclusions. Based on the above results on problems for a periodic array of parallel coaxial penny-shaped cracks in a prestressed material, we may draw the following conclusions.

The stress intensity factors are strongly dependent on the prestresses for all cracks considered (mode I, II, and III cracks) and for nonaxisymmetric and axisymmetric problem formulations.

When a radial shear load acts on the crack faces, the stress intensity factors change resonantly, tending to infinity as the initial compressive loads tend to the critical level that causes local buckling of the material near the cracks. However, when torsional loads act on the crack faces, no resonant phenomena occur, which suggests the absence of buckling modes under compression along a periodic array of parallel cracks in the torsion problem.

At short relative distances between the cracks, the interaction between them results in a decrease in K_I, an increase in K_{II}, and a decrease in K_{III} compared with the SIFs for an isolated mode I, II, and III cracks, respectively.

As the relative distance between the cracks increases, the interaction between them gradually weakens and the SIFs tend to those for an isolated crack. The interaction of cracks in an array of parallel cracks can be neglected for the purpose of practical calculations when the distance between them exceeds six crack radii.

By analyzing the resonant increase in the stress intensity factors (obtained by solving the problems for mode II cracks) occurring as the initial compressive stresses tend to the level causing local buckling (in a flexural mode) of the material near the cracks, we have determined the critical (limiting) compressive loads for different materials compressed along a periodic array of parallel coaxial cracks.

The stress intensity factors and critical (limiting) compressive stresses are strongly dependent on the geometry of the problems (the distance between the cracks and crack radius) and the mechanical characteristics of the materials.

4. Conclusions. We have reviewed studies on spatial problems of the brittle fracture of materials with prestresses acting in parallel to crack planes and the fracture of bodies compressed along cracks solved using a combined approach proposed by the authors of the present paper and based on three-dimensional linearized solid mechanics. The basic equations, problem formulations, and governing equations have a universal general form for compressible and incompressible isotropic elastic bodies with arbitrary elastic potential and composites modeled by transversely isotropic materials.

The approach was used to solve nonaxisymmetric and axisymmetric problems for isolated and interacting cracks in prestressed bodies and to analyze the effect of the prestresses, mechanical characteristics of materials, and geometry of problems on the stress–strain distribution around the cracks. Analyzing the resonant increase in the stress intensity factors and/or crack opening displacement (determined from linearized equations) as the initial compressive stresses tend to the critical level causing local buckling of the material near the cracks, we have determined the critical (limiting) shortening along the coordinate axes and the critical compressive stresses in problems of the compression of bodies along cracks.

Analyzing the results, we may draw the following conclusions.

1. In problems for isolated free cracks, the initial stress–strain state does not affect the stress intensity factors, but has a strong effect on the crack opening displacement for all systems of forces (except for the general nonaxisymmetric problem for a

penny-shaped mode II or III crack). In all the problems for prestressed bodies with interacting cracks, the prestresses acting along the cracks have a strong effect on the stress intensity factors at the crack tips.

2. In all the problems considered (except for the torsion problem), the stress and displacement fields change abruptly, resonantly as the initial compressive stresses tend to the levels at which the material undergoes local buckling near the cracks. This makes it possible to determine the critical (limiting) compressive loads directly by solving the corresponding inhomogeneous problems of the fracture of prestressed materials.

3. The interaction between cracks (periodic array of cracks, two parallel cracks) or between the crack and the free boundary of the half-space (near-surface crack) quantitatively changes (especially for small distances between cracks or between the crack and the half-space boundary) the stress intensity factors compared with those for an isolated crack in an unbounded material. At the distance between cracks (or between the crack and the half-space boundary) increases, this interaction gradually weakens and the stress intensity factors near the cracks tend to those for a crack in an unbounded material.

4. The interaction between two parallel coaxial cracks and between the near-surface crack and the free surface of the prestressed material introduces qualitative changes into the stress distribution near the crack such as nonzero values of K_{II} and K_I. These effects are similar to those in the problems of the fracture of bodies without prestresses with interacting cracks.

5. The stress intensity factors are strongly dependent on the mechanical characteristics of materials.

6. The critical (limiting) compressive loads that cause local buckling of the material near cracks depend on the geometrical parameters (crack radius, distance between cracks and between the crack and the boundary of the material) and the mechanical characteristics of the material.

Further studies on the brittle fracture of materials with prestresses acting in parallel to cracks and the fracture of bodies compressed along cracks using the combined approach may develop along the following lines:

– formulation and solution of problems for more complex arrangements of cracks in prestressed materials such as nonperiodic arrays of parallel cracks (by now, problems for prestressed bodies with isolated cracks, a near-surface crack, two cracks, and a periodic array of parallel coaxial internal cracks have been solved). Note that problems of the compression of composite laminates with cracks located at interfaces between plies and shifted relative to each other (see, e.g., [149]) have been solved recently;

– solution of problems of the fracture of prestressed materials with cracks and the fracture of bodies compressed along cracks that are noncircular in plan;

– formulation and solution of problems of the fracture of materials with prestresses using piecewise-homogeneous models of composites, which is important for a more detailed description of their structure;

– formulation and solution of spatial problems taking into account the asymmetry of the initial stress–strain state caused by the prestresses (by now, the cases of equal prestresses along the Oy_1- and Oy_2-axes (Fig. 8) have been studied);

formulation and solution of problems for inhomogeneous initial stress–strain states;

– analysis of the asymptotic behavior of the solutions to problems for prestressed bodies with cracks as the distance between parallel coaxial cracks or between the crack and the surface of the body tends to zero (the asymptotic behavior of the solutions to spatial problems of the compression of bodies with interacting cracks was studied in, e.g., [113]).

REFERENCES

1. V. M. Aleksandrov and B. V. Sobol', "Equilibrium of a prestressed elastic body weakened by a plane elliptical crack," *J. Appl. Math. Mech.*, **49**, No. 2, 268–272 (1985).
2. V. M. Babich, A. N. Guz, and V. M. Nazarenko, "Disk-shaped normal-rupture crack near the surface of a semiinfinite body with initial stresses," *Int. Appl. Mech.*, **27**, No. 7, 637–644 (1991).
3. G. M. Bartenev and T. N. Khazanovich, "Law of hyperelastic deformation of cross-linked polymers," *Vysokomolekul. Soed.*, **2**, No. 1, 21–28 (1960).
4. V. L. Bogdanov, "Axisymmetric problems of linearized fracture mechanics for a body with two parallel cracks," *Mat. Met. Fiz.-Mekh. Polya*, **49**, No. 1, 146–158 (2006).
5. V. L. Bogdanov, "Axisymmetric problem for a near-surface mode I crack in a composite material withy residual stresses," *Mat. Met. Fiz.-Mekh. Polya*, **50**, No. 2, 45–54 (2007).

6. V. L. Bogdanov, "Nonaxisymmetric problem for a periodic array of penny-shaped mode I cracks in a prestressed body," *Mat. Met. Fiz.-Mekh. Polya*, **50**, No. 4, 149–159 (2007).
7. V. L. Bogdanov, "Torsion of a prestressed material with two parallel coaxial cracks," *Dop. NAN Ukrainy*, No. 11, 59–66 (2008).
8. V. L. Bogdanov, "Nonaxisymmetric problem for two parallel coaxial mode I cracks in a prestressed material," *Dop. NAN Ukrainy*, No. 8, 49–59 (2010).
9. V. L. Bogdanov and V. M. Nazarenko, "Compression of a composite material along a macrocrack near the surface," *Mech. Comp. Mater.*, **30**, No. 3, 251–255 (1994).
10. V. V. Bolotin, "Damage and failure of composites by delamination," *Mech. Comp. Mater.*, **23**, No. 3, 291–298 (1987).
11. A. N. Guz, *Stability of Three-Dimensional Deformable Bodies* [in Russian], Naukova Dumka, Kyiv (1971).
12. A. N. Guz, *Stability of Elastic Bodies Subject to Finite Deformations* [in Russian], Naukova Dumka, Kyiv (1973).
13. A. N. Guz, "Linearized theory of fracture of prestressed brittle materials," *Dokl. AN SSSR*, **252**, No. 5, 1085–1088 (1980).
14. A. N. Guz, "Theory of cracks in elastic bodies with initial stresses—Formulation of problems, tear cracks," *Int. Appl. Mech.*, **16**, No. 12, 1015–1024 (1980).
15. A. N. Guz, "Theory of cracks in prestressed elastic. Shear cracks and limiting cases," *Int. Appl. Mech.*, **17**, No. 1, 1–9 (1981).
16. A. N. Guz, "Theory of cracks in prestressed highly elastic materials," *Int. Appl. Mech.*, **17**, No. 2, 110–118 (1981).
17. A. N. Guz, "Theory of cracks in elastic bodies with initial stresses (stiff materials)," *Int. Appl. Mech.*, **17**, No. 4, 311–316 (1981).
18. A. N. Guz, "Theory of cracks in elastic bodies with initial stresses (cleavage materials)," *Int. Appl. Mech.*, **17**, No. 5, 405–412 (1981).
19. A. N. Guz, "Theory of cracks in elastic bodies with initial stresses (three-dimensional static problems)," *Int. Appl. Mech.*, **17**, No. 6, 499–614 (1981).
20. A. N. Guz, "Three-dimensional problem for a disk-shaped crack in an elastic body with initial stress," *Int. Appl. Mech.*, **17**, No. 11, 963–970 (1981).
21. A. N. Guz, "General three-dimensional static problem for cracks in an elastic bode with initial stress," *Int. Appl. Mech.*, **17**, No. 12, 1043–1051 (1981).
22. A. N. Guz, "Mechanics of the brittle failure of materials with initial stress," *Int. Appl. Mech.*, **19**, No. 4, 293–308 (1983).
23. A. N. Guz, *Brittle Fracture Mechanics of Prestressed Materials* [in Russian], Naukova Dumka, Kyiv (1983).
24. A. N. Guz, *Fundamentals of the Three-Dimensional Theory of Stability of Deformable Bodies* [in Russian], Vyshcha Shkola, Kyiv (1986).
25. A. N. Guz, "Order of singularity at the crack tip in problems of brittle-fracture mechanics," *Fiz.-Khim. Mekh. Mater.*, **22**, No. 1, 24–29 (1986).
26. A. N. Guz, "The order of singularity at the crack tip in prestressed materials," *Dokl. AN SSSR*, **289**, No. 2, 310–312 (1986).
27. A. N. Guz, *Fracture Mechanics of Compressed Composite Materials* [in Russian], Naukova Dumka, Kyiv (1990).
28. A. N. Guz, *Brittle Fracture of Prestressed Materials*, Vol. 2 of the four-volume five-book series *Nonclassical Problems of Fracture Mechanics* [in Russian], Naukova Dumka, Kyiv (1991).
29. A. N. Guz, "Nonclassical problems of fracture mechanics," *Fiz.-Khim. Mekh. Mater.*, **29**, No. 3, 86–97 (1993).
30. A. N. Guz, *Funamentals of the Fracture Mechanics of Compressed Composites* [in Russian], in 2 vols., Litera, Kyiv (2008).
31. A. N. Guz and I. Yu. Babich, *Three-Dimensional Theory of Stability of Rods*, *Plates*, *and Shells* [in Russian], Naukova Dumka, Kyiv (1980).
32. A. N. Guz, M. Sh. Dyshel', G. G. Kuliev, and O. B. Milovanova, *Fracture and Stability of Thin Bodies with Cracks* [in Russian], Naukova Dumka, Kyiv (1981).
33. A. N. Guz, M. Sh. Dyshel', and V. M. Nazarenko, *Fracture and Stability of Materials with Cracks*, Vol. 4 Book 1 of the four-volume five-book series *Nonclassical Problems of Fracture Mechanics* [in Russian], Naukova Dumka, Kyiv (1992).

34. A. N. Guz, A. A. Kaminsky, V. M. Nazarenko, et al., *Fracture Mechanics*, Vol. 5 of the 12-volume series *Mechanics of Composite Materials* [in Russian], ASK, Kyiv (1996).
35. A. N. Guz and Yu. V. Klyuchnikov, "Three-dimensional static problem for an elliptical crack in an elastic body with initial stress," *Int. Appl. Mech.*, **20**, No. 10, 898–907 (1984).
36. A. N. Guz and V. M. Nazarenko, "Fracture mechanics of material in compression along cracks (review). Highly elastic materials," *Int. Appl. Mech.*, **25**, No. 9, 851–876 (1989).
37. A. N. Guz and V. M. Nazarenko, "Fracture mechanics of material under compression along cracks (survey). Structural materials," *Int. Appl. Mech.*, **25**, No. 10, 959–972 (1989).
38. A. N. Guz, V. M. Nazarenko, and V. A. Nikonov, "Torsion of a pre-stressed halfspace with a disk-shaped crack at the surface," *Int. Appl. Mech.*, **27**, No. 10, 948–954 (1991).
39. I. A. Guz, "Stability of a composite compressed along an interface crack," *DAN SSSR*, **325**, No. 3, 455–458 (1992).
40. Yu. V. Klyuchnikov, "Three-dimensional static problem for an external disk-shaped crack in an elastic body with initial stresses," *Int. Appl. Mech.*, **20**, No. 2, 118–123 (1984).
41. G. P. Sendeckyj (ed.), *Mechanics of Composite Materials*, Vol. 2 of the eight-volume series *Composite Materials*, Academic Press, New York (1974).
42. M. Ya. Leonov and V. V. Panasyuk, "Development of microcracks in a solid," *Prikl. Mekh.*, **5**, No. 4, 391–401 (1959).
43. V. I. Makhnenko, *Safe Operation Life of Welded Joints and Components of Modern Structures* [in Russian], Naukova Dumka, Kyiv (2006).
44. V. I. Makhnenko, V. M. Shekera, T. G. Kravtsov, and V. V. Sevryukov, "Influence of machining on the redistribution of residual stresses in built-up shafts," *Avtomat. Svarka*, No. 7, 3–6 (2001).
45. A. M. Mikhailov, "Generalization of the beam approach to problems of crack theory," *J. Appl. Mech. Tech. Phys.*, **10**, No. 3, 503–506 (1969).
46. A. N. Guz (ed.), *Nonclassical Problems of Fracture Mechanics* [in Russian], in four vols., five books, Naukova Dumka, Kyiv (1990–1993).
47. A. N. Polilov and Yu. N. Rabotnov, "Development of delamination in compressed composites," *Izv. AN SSSR*, No. 4, 166–171 (1983).
48. O. V. Primachenko and S. Yu. Babich, "The axisymmetric problem of a crack of normal tear in an initially stressed layer," *Int. Appl. Mech.*, **28**, No. 7, 421–426 (1992).
49. B. W. Rosen, "Mechanics of composite strengthening," in: *Fiber Composite Materials*, American Society of Metals, Metals Park, Ohio (1965), pp. 37–75.
50. Ya. S. Uflyand, *Integral Transforms in the Theory of Elasticity* [in Russian], Nauka, Leningrad (1967).
51. L. M. Filippova, "On the effect of initial stresses on the opening of a circular crack," *J. Appl. Math. Mech.*, **47**, No. 2, 240–243 (1983).
52. L. P. Khoroshun, B. P. Maslov, E. N. Shikula, and L. V. Nazarenko, *Statistical Mechanics and Effective Properties of Materials*, Vol. 3 of the 12-volume series *Mechanics of Composite Materials* [in Russian], Naukova Dumka, Kyiv (1993).
53. G. P. Cherepanov, *Mechanics of Brittle Fracture*, McGraw-Hill, New York (1979).
54. N. A. Shul'ga and V. T. Tomashevskii, *Process-Induced Stresses and Strains in Materials*, Vol. 6 of the 12-volume series *Mechanics of Composite Materials* [in Russian], ASK, Kyiv (1997).
55. R. A. Ainsworth, J. K. Sharples, and S. D. Smith, "Effects of residual stresses on fracture behaviour—experimental results and assessment methods," *J. Strain Analysis for Engineering Design*, **35**, No. 4, 307–316 (2000).
56. S. D. Akbarov, "Three-dimensional instability problems for viscoelastic composite materials and structural members," *Int. Appl. Mech.*, **43**, No. 10, 1069–1089 (2007).
57. S. D. Akbarov, *Stability Loss and Buckling Dela*min*ation*, Springer, Berlin (2012).
58. S. D. Akbarov and A. N. Guz, *Mechanics of Curved Composites*, Kluwer, Dordrecht (2000).
59. C. Atkinson and R. V. Craster, "Theoretical aspects of fracture mechanics," *Prog. Aerospace Sci.*, **31**, 1–83 (1995).
60. V. L. Bogdanov, "On a circular shear crack in a semi-infinite composite with initial stresses," *Material Science*, **43**, No. 3, 321–330 (2007).
61. V. L. Bogdanov, "Effect of residual stresses on fracture of semi – infinite composites with cracks," *Mech. Adv. Mater. Struct.*, **15**, No. 6, 453–460 (2008).

62. V. L. Bogdanov, “Influence of initial stresses on fracture of composite materials containing interacting cracks,” *J. Math. Sci.*, **165**, No. 3, 371–384 (2010).
63. V. L. Bogdanov, “Nonaxisymmetric problem of the stress–strain state of an elastic half-space with a near-surface circular crack under the action of loads along it,” *J. Math. Sci.*, **174**, No. 3, 341–366 (2011).
64. V. L. Bogdanov, “Influence of initial stresses on the stressed state of a composite with a periodic system of parallel coaxial normal tensile cracks,” *J. Math. Sci.*, **186**, No. 1, 1–13 (2012).
65. V. L. Bogdanov, “On the interaction of a periodic system of parallel coaxial radial-shear cracks in a prestressed composite,” *J. Math. Sci.*, **187**, No. 5, 606–618 (2012).
66. V. L. Bogdanov, “Influence of initial stresses on the fracture of a composite material with a near-surface mode III crack,” *J. Math. Sci.*, **174**, No. 3, 1–14 (2014).
67. V. L. Bogdanov, A. N. Guz, and V. M. Nazarenko, “Fracture of semi-infinite material with a circular surface crack in compression along the crack plane,” *Int. Appl. Mech.*, **28**, No. 11, 687–704 (1992).
68. V. L. Bogdanov, A. N. Guz, and V. M. Nazarenko, “Fracture of a body with a periodic set of coaxial cracks under forces directed along them: An axisymmetric problem,” *Int. Appl. Mech.*, **45**, No. 2, 111–124 (2009).
69. V. L. Bogdanov, A. N. Guz, and V. M. Nazarenko, “Stress–strain state of a material under forces acting along a periodic set of coaxial mode II penny-shaped cracks,” *Int. Appl. Mech.*, **46**, No. 12, 1339–1350 (2010).
70. V. L. Bogdanov, A. N. Guz, and V. M. Nazarenko, “Nonclassical problems in the fracture mechanics of composites with interacting cracks,” *Int. Appl. Mech.*, **51**, No. 1, 64–84 (2015).
71. V. L. Bogdanov and V. M. Nazarenko, “Study of the compressive failure of a semi-infinite elastic material with a harmonic potential,” *Int. Appl. Mech.*, **30**, No. 10, 760–765 (1994).
72. V. L. Bogdanov, “Mutual influence of two parallel coaxial cracks in a composite material with initial stresses,” *Materials Science*, **44**, No. 4, 530–540 (2008).
73. V. V. Bolotin, *Stability Problems in Fracture Mechanics*, John Wiley & Sons, New York (1994).
74. B. Cotterell, “The past, present, and future of fracture mechanics,” *Eng. Fract. Mech.*, **69**, 533–553 (2002).
75. R. S. Dhaliwal, B. M. Singh, and J.G. Rokne, “Axisymmetric contact and crack problems for an initially stressed neo-Hookean elastic layer,” *Int. J. Eng. Sci.*, **18**, No. 1, 169–179 (1980).
76. A. T. Dewald and M. R. Hill, “Eigenstrain-based model for prediction of laser peening residual stresses in arbitrary three-dimensional bodies. Part 1: model description,” *J. Strain Analysis*, **44**, 1–11 (2009).
77. G. J. Dvorak, “Composite materials: Inelastic behavior, damage, fatigue and fracture,” *Int. J. Solids Struct.*, **37**, No. 1–2, 155–170 (2000).
78. F. Erdogan, “Fracture mechanics,” *Int. J. Solids Struct.*, **37**, No. 1–2, 171–183 (2000).
79. J. D. Eshelby, “The force on the elastic singularity,” *Phil. Trans. Roy. Soc. London*, *Ser. A*, **244**, 87–112 (1951).
80. A. A. Griffith, “The phenomenon of rupture and flow in solids,” *Phil. Trans. Roy. Soc. London*, *Ser. A*, **221**, 163–198 (1920).
81. A. N. Guz, “Breakaway cracks in elastic bodies with initial stresses,” *Dokl. Akad. Nauk SSSR*, **254**, No. 3, 571–574 (1980).
82. A. N. Guz, “Spatial problem for shear cracks in elastic bodies with initial stresses,” *Dokl. Akad. Nauk SSSR*, **257**, No. 3, 562–565 (1981).
83. A. N. Guz, “A criterion of solid body destruction during compression along cracks (two-dimensional problem),” *Dokl. Akad. Nauk SSSR*, **259**, No. 6, 1315–1318 (1981).
84. A. N. Guz, “A criterion of solid body destruction under compression along cracks (a 3-dimensional problem),” *Dokl. Akad. Nauk SSSR*, **261**, No. 1, 42–45 (1981).
85. A. N. Guz, “Moving cracks in elastic bodies with initial stresses,” *Int. Appl. Mech.*, **18**, No. 2, 132–136 (1982).
86. A. N. Guz, “Fracture mechanics of composites in compression along cracks,” *Int. Appl. Mech.*, **18**, No. 6, 489–493 (1982).
87. A. N. Guz, “Energy criteria of the brittle fracture of materials with initial stresses,” *Int. Appl. Mech.*, **18**, No. 9, 771–775 (1982).
88. A. N. Guz, “On the criterion of brittle fracture of materials with initial stresses,” *Dokl. Akad. Nauk SSSR*, **262**, No. 2, 285–288 (1982).

89. A. N. Guz, “On the development of brittle-fracture mechanics of material with initial stresses,” *Int. Appl. Mech.*, **32**, No. 4, 316–323 (1996).
90. A. N. Guz, “On non-classical problems and mechanisms of fracture mechanics and its description,” *Int. Appl. Mech.*, **32**, No. 11, 827–844 (1996).
91. A. N. Guz, “Order of singularity in problems of mechanics of brittle fracture of materials with initial stresses,” *Int. Appl. Mech.*, **34**, No. 2, 103–107 (1998).
92. A. N. Guz, “Some modern problems of physical mechanics of fracture,” in: G. P. Cherepanov (ed.), *Fracture. A Topical Encyclopedia of Current Knowledge*, Krieger, Florida, USA (1998), pp. 709–720.
93. A. N. Guz, “Dynamic problems of the mechanics of the brittle fracture of materials with initial stresses for moving cracks. 1. Problem statement and general relationships,” *Int. Appl. Mech.*, **34**, No. 12, 1175–1186 (1998).
94. A. N. Guz, “Dynamic problems of the mechanics of brittle fracture of materials with initial stresses for moving cracks. 2. Cracks of normal separation (mode 1),” *Int. Appl. Mech.*, **35**, No. 1, 1–12 (1999).
95. A. N. Guz, “Dynamic problems of the mechanics of the brittle fracture of materials with initial stresses for moving cracks. 3. Transverse-shear (mode II) and longitudinal-shear (mode III) cracks,” *Int. Appl. Mech.*, **35**, No. 2, 109–119 (1999).
96. A. N. Guz, “Dynamic problems of the mechanics of the brittle fracture of materials with initial stresses for moving cracks. 4. Wedge problems,” *Int. Appl. Mech.*, **35**, No. 3, 225–232 (1999).
97. A. N. Guz, *Fundamentals of the Three-Dimensional Theory of Stability of Deformable Bodies*, Springer-Verlag, Berlin (1999).
98. A. N. Guz, “Description and study of some nonclassical problems of fracture mechanics and related mechanisms,” *Int. Appl. Mech.*, **36**, No. 12, 1537–1564 (2000).
99. A. N. Guz, “Constructing the three-dimensional theory of stability of deformable bodies,” *Int. Appl. Mech.*, **37**, No. 1, 1–37 (2001).
100. A. N. Guz, “Moving cracks in composite materials with initial stresses,” *Mech. Comp. Mater.*, **37**, No. 5/6, 695–708 (2001).
101. A. N. Guz, “Elastic waves in bodies with initial (residual) stresses,” *Int. Appl. Mech.*, **38**, No. 1, 23–59 (2002).
102. A. N. Guz, “Critical phenomena in cracking of the interface between two prestressed materials. 1. Problem formulation and basic relations,” *Int. Appl. Mech.*, **38**, No. 4, 423–431 (2002).
103. A. N. Guz, “Critical phenomena in cracking of the interface between two prestressed materials. 2. Exact solution. The case of unequal roots,” *Int. Appl. Mech.*, **38**, No. 5, 548–555 (2002).
104. A. N. Guz, “Critical phenomena in cracking of the interface between two prestressed materials. 3. Exact solution. The case of equal roots,” *Int. Appl. Mech.*, **38**, No. 6, 693–700 (2002).
105. A. N. Guz, “Critical phenomena in cracking of the interface between two prestressed materials. 4. Exact solution. The case of unequal and equal roots,” *Int. Appl. Mech.*, **38**, No. 7, 806–814 (2002).
106. A. N. Guz, “Comments on ‘Effects of prestresses on crack-tip fields in elastic incompressible solids’,” *Int. J. Solids Struct.*, **40**, No. 5, 1333–1334 (2003).
107. A. N. Guz, “On some nonclassical problems of fracture mechanics taking into account the stresses along cracks,” *Int. Appl. Mech.*, **40**, No. 8, 937–942 (2004).
108. A. N. Guz, “On study of nonclassical problems of fracture and failure mechanics and related mechanisms,” *ANNALS of the European Academy of Sciences*, 35–68 (2006–2007).
109. A. N. Guz, “On study of nonclassical problems of fracture and failure mechanics and related mechanisms,” *Int. Appl. Mech.*, **45**, No. 1, 3–40 (2009).
110. A. N. Guz, “Mechanics of crack propagation in materials with initial (residual) stresses (review),” *Int. Appl. Mech.*, **47**, No. 2, 121–169 (2011).
111. A. N. Guz, “Stability of elastic bodies under uniform compression (review),” *Int. Appl. Mech.*, **48**, No. 3, 241–293 (2012).
112. A. N. Guz, “Establishing the foundations of the mechanics of fracture of materials compressed along cracks (review),” *Int. Appl. Mech.*, **50**, No. 1, 1–57 (2014).
113. A. N. Guz, M. V. Dovzhik, and V. M. Nazarenko, “Fracture of a material compressed along a crack located at a short distance from the free surface,” *Int. Appl. Mech.*, **47**, No. 6, 627–635 (2011).

114. A. N. Guz, M. Sh. Dyshel', and V. M. Nazarenko, "Fracture and stability of materials and structural members with cracks: Approaches and results," *Int. Appl. Mech.*, **40**, No. 12, 1323–1359 (2004).
115. A. N. Guz and I. A. Guz, "Analytical solution of stability problem for two composite half-plane compressed along interacting cracks," *Composites*, *Part B*, **31**, No. 5, 405–411 (2000).
116. A. N. Guz and I. A. Guz, "On publications on the brittle fracture mechanics of prestressed materials," *Int. Appl. Mech.*, **29**, No. 7, 797–801 (2003).
117. A. N. Guz and I. A. Guz, "Mixed plane problems of linearized solid mechanics. Exact solutions," *Int. Appl. Mech.*, **40**, No. 1, 1–29 (2004).
118. A. N. Guz, I. A. Guz, A. V. Men'shikov, and V. A. Men'shikov, "Three-dimensional problems in the dynamic fracture mechanics of materials with interface cracks (review)," *Int. Appl. Mech.*, **49**, No. 1, 1–61 (2013).
119. A. N. Guz, V. I. Knukh, and V. M. Nazarenko, "Compressive failure of materials with two parallel cracks: Small and large deformation," *Theor. Appl. Fract. Mech.*, **11**, 213–223 (1989).
120. A. N. Guz and V. M. Nazarenko, "Symmetric failure of the half-space with penny-shaped cracks in compression," *Theor. Appl. Fract. Mech.*, **3**, No. 3, 233–245 (1985).
121. A. N. Guz, V. M. Nazarenko, and V. L. Bogdanov, "Nonaxisymmetric compressive failure of a circular crack parallel to a surface of halfspace," *Theor. Appl. Fract. Mech.*, **22**, 239–247 (1995).
122. A. N. Guz, V. M. Nazarenko, and V. L. Bogdanov, "Fracture under initial stresses acting along cracks: Approach, concept and results," *Theor. Appl. Fract. Mech.*, **48**, 285–303 (2007).
123. A. N. Guz, V. M. Nazarenko, and V. L. Bogdanov, "Combined analysis of fracture under stresses acting along cracks," *Arch. Appl. Mech.*, **83**, No. 9, 1273–1293 (2013).
124. A. N. Guz, V. M. Nazarenko, and I. P. Starodubtsev, "On problems of fracture of materials in compression along two internal parallel cracks," *Appl. Math. Mech.*, **18**, No. 6, 517–528 (1997).
125. I. A. Guz, "On modelling of a failure mechanism for layered composites with interfacial cracks," *ZAMM*, **78**, No. 1, 429–430 (1998).
126. I. A. Guz and A. N. Guz, "Stability of two different half-planes in compression along interfacial cracks: Analytical solution," *Int. Appl. Mech.*, **37**, No. 7, 906–912 (2001).
127. D. M. Haughton, "Penny-shaped cracks in a finitely deformed elastic solid," *Int. J. Solids Struct.*, **18**, No. 8, 699–704 (1982).
128. H. Horii and S. Nemat-Nasser, "Brittle failure in compression: splitting, faulting and brittle–ductile transition," *Phil. Trans. Roy. Soc. London*, **A3I9**, No. 1549, 337–374 (1986).
129. G. R. Irwin, "Fracture dynamics," in: *Fracturing of Metals*, Amer. Soc. for Metals, Cleveland (1948), pp. 147–166.
130. G. R. Irwin, "Onset of fast crack propagation in high strength steel and aluminium alloys," in: *Proc. 2nd Sagamore Ordinance Materials Conf.*, **2** (1956), pp. 289–305.
131. G. R. Irwin, "Analysis of stresses and strains near the end of a crack traversing a plate," *J. Appl. Mech.*, **24**, 361–364 (1957).
132. F. John, "Plane strain problems for a perfectly elastic material of harmonic type," *Commun. Pure Appl. Math.*, **13**, No. 2, 239–296 (1960).
133. A. A. Kaminsky, "Mechanics of the delayed fracture of viscoelastic bodies with cracks: Theory and experiment (review)," *Int. Appl. Mech.*, **50**, No. 5, 495–548 (2014).
134. B. Karihaloo and Q. Z. Xiao, "Linear and nonlinear fracture mechanics," in: Vol. 2 of the ten-volume series J. Milne, R. O. Ritchie, and B. Karihaloo, *Comprehensive Structural Integrity*, Elsevier Science, New York (2003), pp. 81–212.
135. M. K. Kassir and G. C. Sih, *Mechanics of Fracture*, Vol. 2. *Three-Dimensional Crack Problems*, Noordhoff, Leyden (1975).
136. M. Kurashige, "Circular crack problem for initially stressed neo-Hookean solid," *ZAMM*, **49**, No. 2, 671–678 (1969).
137. J. G. Murphy and M. Destade, "Surface waves and surface stability for pre – stretched, unconstrained, non-lineary elastic half-space," *Int. J. Non-Linear Mech.*, **44**, 545–551 (2009).
138. V. M. Nazarenko, "Fracture of plastic masses with translational strain-hardening in compression along near-surface cracks," *Int. Appl. Mech.*, **23**, No. 1, 61–64 (1987).
139. V. M. Nazarenko, V. L. Bogdanov, and H. Altenbach, "Influence of initial stress on fracture of a half-space containing a penny-shaped crack under radial shear," *Int. J. Fract.*, **104**, 275–289 (2000).

140. I. W. Obreimoff, “The splitting strength of mica,” *Proc. Roy. Soc. London*, **127A**, 290–297 (1930).
141. E. O. Orowan, “Fundamentals of brittle behavior of metals,” in: W. M. Murray (ed.), *Fatigue and Fracture of Metals*, Willey, London (1950), pp. 139–167.
142. M. L. Pasha, “Axially symmetric stress distributions in elastic solids containing penny-shaped cracks under torsion,” *J. Appl. Mech.*, **42**, No. 4, 896–897 (1975).
143. S. Rajit, R. S. Dhaliwal, R. M. Singh, and I. G. Rokhe, “Axisymmetric contact and crack problems for initially stressed Neo-Hookean layer,” *Int. J. Eng. Sci.*, **18**, No. 1, 169–179 (1980).
144. J. R. Rice, “A path independent integral and the approximate analysis of strain concentration by notches and cracks,” *J. Appl. Mech.*, **35**, No. 4, 379–386 (1968).
145. A. P. S. Selvadurai, “The penny-shaped crack problem for a finitely deformed incompressible elastic solid,” *Int. J. Fract.*, **16**, No. 4, 327–333 (1980).
146. L. R. G. Treloar, “Large elastic deformations in rubber-like materials,” *IUTAM Colloquium*, Madrid (1955), pp. 208–217.
147. E. Z. Wang and N. G. Shrive, “Brittle fracture in compression: Mechanisms, models and criteria,” *Eng. Fract. Mech.*, **52**, No. 6, 1107–1126 (1995).
148. A. A. Wells, “Application of fracture mechanics at and beyond general yielding,” *Brit. Weld. J.*, **10**, No. 11, 563–570 (1963).
149. B. Winiarsky and I. A. Guz, “The effect of cracks interaction in orthotropic layered materials under compressive loading,” *Phil. Trans. Roy. Soc.*, *Ser. A*, **366**, No. 1871, 1835–1839 (2008).